HOLOCENE PALEOHYDROLOGY IN THE NORTHEASTERN UNITED STATES: A HIGH RESOLUTION RECORD OF STORMS AND FLOODS

A Thesis Presented

by

Adam S. Parris

to

The Faculty of the Graduate College

of

The University of Vermont

In Partial Fulfillment of the Requirements
for the Degree of Master of Science
Specializing in Geology

October 2003

Accepted by the Faculty of the Graduate College, The University of Vermont, in partial fulfillment of the requirements for the degree of Master of Science specializing in Geology.

Thesis Examination Committee:

_____ Advisor
Paul R. Bierman, Ph.D.

_____
Andrea Lini, Ph.D.

_____ Chairperson
Beverly Wemple, Ph.D.

_____ Interim Dean,
David Dummit, Ph.D. Graduate College

Date: April 18, 2003

ABSTRACT

The frequency and timing of Holocene floods, and by inference storms, in steep basins in the hilly terrain of New England, specifically Vermont, New Hampshire, and Maine, can be identified clearly by high resolution (cm-by-cm) particle size analysis of sediment cores taken from post-glacial ponds and lakes (~ 0.1- 1.4 km^2). Eight sediment cores (4.5- 6 m in length) were taken from six of these lakes near the base of stream delta foreslopes. All of the cores were analyzed (cm-by-cm) for organic content (% loss-on-ignition (LOI)) and magnetic mineral content (Magnetic Susceptibility (MS)), and for siliclastic particle size. These analyses are paired with 80 ^{14}C dates (~8- 10 per core) to reconstruct a Holocene chronology of hydrologic events. In all cases, particle size analysis provides more direct, sensitive detection of terrestrial storm layers than other, proxy methods such as LOI and MS.

End-member modeling (EMM) of the particle size data from each core revealed three to five representative, end-member frequency distributions. Increases in the median particle size and in the relative abundance of the coarsest end-member frequency distributions indicate increases in the energy of sediment deposition by the streams feeding these deltas. More frequent floods (initiated by rainstorms, rain on snow, and/or snowmelt) cause increased deposition of coarse, clastic sediment into the lake. The EMM results show grading of some terrestrial flood layers, as well as a separate increase in coarse sediment associated with delta progradation.

The first of two cores from South Pond (Stark, NH) contains terrestrial flood layers defined by increases in coarse silt. The second core from South Pond, taken in a more proximal location (from the toeslope of a different delta), contains contemporaneous terrestrial flood layers defined by increases in the abundance of fine and medium sand. This disparity reveals the dominant influence of core location on the mode and the abundance of the coarsest sediments, and therefore on event detection.

Contemporaneous deposition of terrestrially-derived, storm layers in different cores retrieved from the base of different deltas in the same lake suggest large storms which cause flooding in a wide geographic area. Disparate ages for the storm layers in the same cores suggest the influence of local geomorphic characteristics on the extent of storm-induced, flood deposition in certain lakes. This finding illustrates the need to consider individual records together to examine Holocene trends in paleoflood frequency in New England.

An increase in the number of floods, inferred from grain size data, occurred ~4,000 cal yr B.P. The timing and cyclicity of flooding are similar to the timing and recurrence interval of hurricanes recorded in salt marshes along the north Atlantic coast and on the coast of the Gulf of Mexico. The agreement with hurricane records and the close proximity of the lakes to the north Atlantic coast suggest that the flood record in New Hampshire and Maine is influenced by large scale storms, like hurricanes, nor'easters, and tropical storms. Flooding in this region peaked around 800, 1,400, 2,100, 3,900, 6,800, 8,300, 11,500, and 13,300 years ago, and appears to be presently increasing toward another peak.

ACKNOWLEDGEMENTS

This thesis work was completed in a short period of time, particularly when considering the large volume of work that was completed. Of all the things that I've learned in the process of completing this work, the most important lesson was that my friends and family are the most important thing in my life. I never could have accomplished this work without them, and without the help of the many collaborators that I have been fortunate to have along the way.

Of those collaborators and friends, I am forever indebted to Anders Noren. His support, patience, guidance, and friendship on this project were invaluable. He repeatedly went beyond the call of duty by teaching me techniques both on the computer and in the field, while allowing me to figure things out for myself. Furthermore, he continued to make me smile, and listened patiently to all my whining at the toughest moments of the past two years.

I also would like to thank my advisor, Paul Bierman, for giving me the chance to work on this project, and for providing support throughout the project. This work was an investment of emotion, time, and considerable finance, during which many small, and sometimes big, things went wrong. Despite the fact that significant changes in his personal life were occurring during the period this work was completed, he remained patient and supportive.

Likewise, Andrea Lini provided constant support, guidance, and friendship through the toughest half of this research. Through the least glamorous aspect of the

research, the lab work, he constantly answered questions which inevitably arose, and he constantly provided comic relief for my Research Assistant, Andy Bosley, and I.

The completion of this work would not be possible without Andy Bosley's help. Andy was invaluable to me as a friend, and as an assistant in the lab. I relied on him heavily during the entire time the lab work was being completed, and he constantly came through with nothing but a smile, and often a supportive gesture. Andy is a great friend.

Andrea Lord was also an invaluable friend, who helped me settle in Burlington. I could never have accomplished this work without her, nor would I have wanted to do that. In the field, in the lab at Livermore, and in the office, it provided constant comfort and laughter to work alongside of Andi.

My field interpretations, and my relationship to the natural world were greatly enhanced by my relationship with Stephen Wright. I admire Stephen as the last of the true field geologists, and I also admire him as someone with the greatest sense of humor, kindness, and commitment to what is important in life. Stephen is an inspiration to everyone he meets, particularly in the Geology department at UVM, and I am certainly no small exception. I will carry his influence with me forever, and will always value his friendship.

Peter Ryan and the Middlebury College Geology Department were constantly accommodating and supportive of this research. Pete, in particular, provided a great deal of support, and grew to be a good friend. I will always look up to him as a geologist and teacher, and look forward to working with him in the future. The collaboration of Maarten Prins was absolutely crucial to this project, and I am forever grateful to him for

providing such support, as well as a place to see the “real” Netherlands from a local perspective.

My family means the entire world to me. I could never have finished, and indeed might not have inspired to start without them. My father, mother, and sister are all a part of me, and in that sense, have been with me every step of the way. Their love and support were constant and renewing. I will recognize forever Craig Kochel, Mary Evelyn Tucker, and John Grim as part of my family, and mean to extend all of my appreciation and love for my family to them.

During my time in Burlington, I was fortunate to have the best friends for which anyone could ask. They made Burlington my true home, and the best place to live since I left home. I love them as much as family. I want to thank: Joe Haun, Gregg Woolven, Brian DeVito, Lindsay White, Sarah Stopper, Katie Powers, Lindsey Vietor, Tim Baker, Mike Grunow, Will Kies, Evan Langfeldt, Mischa Hey, Jarett Emert, Leight Ault, Matt Capozi, Carolyn, Brooke, Jason Kellogg, Kelly Longfield, Vanessa Javor, Lela Hatfield, Stephanie Somers, Mindy, and Kirsten. I would like to thank especially Kristen Benchley for her love and support for so many late nights and early mornings through the toughest part of my thesis.

My fellow graduate students at UVM have put up with the various states I have been in for the past two years. They have been invaluable collaborators and friends, and I appreciate them greatly. Particularly, I’d like to thank Corey Simonson, Karen Jennings, Chris Lamon, Alex Claypool, Angelo Antignano, Kyle Nichols, Stephen Marcotte, Ken

Oldrid, Paula Mouser, Christina Cianfrani, A.J. Rossman, Luke Reusser, Eric Butler, Willy Amidon, Joanna Reuter, Rena Ford, and Robert Price.

For their support and/or friendship, I would also like to thank: Cully Hession, Beverly Wemple, Charlotte Mehrtens, Lyman Persico, Laura Mallard, Leah Morgan, Pat Frank, John Southon, Tom Guilderson, and the entire crew at Lawrence Livermore National Laboratory radiocarbon facility.

TABLE OF CONTENTS

LIST OF TABLES

LIST OF FIGURES

CHAPTER 1: INTRODUCTION

Floods caused by extreme precipitation events throughout the world present potentially devastating natural hazards due to their often unpredictable nature (Hupp, 1988; Komar, 1988; Baker, 1988). Extreme precipitation events in the hilly terrain of New England, specifically New Hampshire and Maine, caused floods in steep basins throughout the Holocene, leaving clear sedimentological signatures in post-glacial ponds and lakes (~ 0.1- 1.4 km^2; Brown et al., 2000; Noren et al., 2002). This study presents a careful examination of the natural archives of floods in 8 New England lake sediment records. It provides valuable information for land managers and is an important contribution to deciphering the record of climate in the North Atlantic region (Brown et al., 2000).

Background

Lake sediments from New England primarily consist of fine-grained, organic rich sediment (gyttja) formed by the accumulation of aquatic organisms, terrestrial plant detritus, and terrestrially-derived, fine grained inorganic sediment (Jackson and Whitehead, 1991; Spear et al., 1994). However, lake sediment also contains layers of terrestrially-derived, coarser grained inorganic sediment and coarse organic particles (leaves, twigs, pine needles, etc.) that are transported into the lake via inflowing streams and wind during exceptional hydrologic events (Brown et al., 2000; Noren et al., 2002; Brown et al., 2002). Many environmental variables determine the degree to which either of these two types of sediment accumulate in a record from an individual lake (Campbell, 1998; Brown et al., 2000; Noren et al., 2002). Climatic variables such as temperature and

moisture, and physical and chemical variables such as local soil composition and local bedrock type influence the aquatic and the terrestrial biologic assemblages which in turn influence the accumulation of gytta (Meyers and Ishiwatari, 1993).

A growing number of paleostorm chronologies assume that coarser-grained, terrestrially derived flood layers in lake sediments are the result of extreme precipitation events in lake basins (Bierman et al., 1997; Thorndycraft et al., 1998; Rodbell et al., 1999; Brown et al., 2000; Nesje et al., 2001). During extreme precipitation events, tributaries in the surrounding lake basins flood, and sediment transport capacity of the tributaries increases. This process causes the transport and eventual deposition of coarse, inorganic grains and organic debris, which noticeably interrupt the accumulation of gytta. After such storms, fine-grained gyttja begins to accumulate again, burying and preserving the flood deposits. Thus, identification of the terrestrially-derived, flood deposits through stratigraphic and dating analyses of sediment cores provides a chronology of paleostorms (Eden and Page, 1998; Rodbell et al., 1999; Brown et al., 2000; Lamoreaux, 2000; Nesje et al., 2001; Noren et al., 2002).

Many existing paleostorm chronologies were constructed by identifying flood layers in sediment cores from a single lake (Bierman et al., 1997; Thorndycraft et al., 1998; Rodbell et al., 1999; Brown et al., 2000; Nesje et al., 2001). So far, only one paleostorm chronology has been constructed using sediment cores from multiple lakes throughout a broad region, specifically Vermont and New York (Noren et al., 2002). All of these studies were aimed at elucidating regional storm records with the latter being the best representation of the frequency of storms over a broad region.

Previous studies (Page et al., 1994; Campbell, 1998; Eden and Page, 1998; Thorndycraft et al., 1998; Rodbell et al., 1999; Brown et al., 2000; Lamoreaux, 2000; Nesje et al., 2001; Ambers, 2001; Noren et al., 2002) have performed high resolution analyses on lake sediments, using proxy measurements for detecting flood layers. Analytical methods such as loss-ignition (LOI), magnetic susceptibility (MS), and X-radiography measure changes in the organic and in the inorganic content, as well as the color of lake sediment. Brown et al. (2000) used limited particle size analysis, only where the proxy measurements detected changes in organic and inorganic content. Consequently, this study, because it measures grain size, cm by cm in 8 sediment records, marks a major advance in the construction of paleostorm records from lake sediments.

Since paleostorm chronologies are derived from detection of physical changes in the transport capacity of tributaries in lake basins, high resolution (cm by cm) particle size analysis of lake sediment cores is a promising tool for direct measurement of these changes. Increased particle sizes of lake sediment in cores taken from locations proximal to inflowing tributaries directly reflect increases in the sediment transport capacity of those tributaries (Campbell, 1998).

Statement of Problem

To improve upon and to add to paleostorm records in the northeastern United States, my research aims to answer the following questions:

1. To what extent does particle size analysis of lake sediment cores reflect variations in streamflow and stream competency in lake basins in New England, through the Holocene?

2. How can grain size analysis of lake sediment be performed effectively and efficiently?
3. To what extent do the physical characteristics of terrestrial flood deposits in lake sediments from New Hampshire and Maine exhibit differences and uniformity throughout the Holocene?
4. Assuming that most storm events should be present in most cores, can we test dating techniques and the influence of core location on event detection, using separate cores taken from the base of two different lake deltas within the same lake?
5. In terms of the frequency and cyclicity of storms, does the paleostorm record for New Hampshire and Maine display similarities or differences with the best existing paleostorm record from Vermont and New York (Noren et al, 2002), as well as other paleoclimate records from the northeastern United States?

The Geography of my Thesis

This thesis contains five chapters, an overall list of references cited, and Appendices contained on paper and on CD-ROM. Chapter 2 is a comprehensive literature survey. Since the practice of paleostorm research spans different disciplines, the literature survey is divided into disciplinary sections including: studies containing significant paleoclimatic data, paleoflood and geomorphological data, methodological data for laboratory analyses, and studies detailing significant information about the deglacial history and geologic setting of New England.

Chapters 3 and 4 contain a paper submitted to the *Geological Society of America Bulletin*, with Chapter 3 being a Data Repository with a detailed description of the methods used in my study and Chapter 4 being the manuscript. Chapter 5 includes both a summary of findings and suggestions for future research followed by an overall list of References Cited. Because the volume of the Appendices (>4000 measurements with two files per measurement for one analytical method alone) is so large and in order to aid the use of such data in the future, this section includes a CD-ROM, divided into reconnaissance photos, and raw data (magnetic susceptibility, loss-on-ignition, radiocarbon, and grain size data). The CD-ROM is separated with individual folders for each studied lake. The first Appendix is included in the text and contains the Visual Log data.

CHAPTER 2: COMPREHENSIVE LITERATURE REVIEW

Lake sediment records in New England are exploited increasingly, as valuable climatic and land use data are being compiled from them (Bierman et al., 1997; Brown et al., 2000; Noren et al., 2002). However, the collection, processing, analysis, and interpretation of lake cores all span topics from a variety of disciplines. As such, I have tried to compile this chapter in such a fashion as to start broadly, with background information on the setting and discipline, and then to focus specifically on topics germane to my research.

2.1 De-Glacial History and Lake Establishment in New England

Much of the glacial geologic research focused in New England details the timing and extent of deglaciation of the Laurentide Ice sheet, which reached its maximum geographic extent in Long Island, NY approximately 18,000 ^{14}C years before present (21,000- 22,000 cal yr BP) (Benn and Evans, 1998; Ridge et al., 1999; Thompson, 1999). Further constraint on the age of ice proximal deposits, primarily through accurate method of dating macrofossils in lake sediments (Ridge et al., 1999) is needed to detail the patterns of the northern retreat of ice from New England to Canada.

The most comprehensive record of glacial retreat in the northeastern United States is based on the New England Varve Chronology (Antevs, 1922), basal ^{14}C dates from sediment cores taken from lakes and from ice proximal deposits, and paleomagnetic analysis of lake sediment cores (Ridge et al., 1999). Based on this chronology, deglaciation began in southern Vermont and New Hampshire about 12,600 ^{14}C yr BP (15,200- 15,500 cal yr BP), and continued until the ice sheet receded into southern

Quebec about 11,500 ^{14}C yr BP (13,700- 13,800 cal yr BP). In western Maine, timing of deglaciation was constrained further to 13,500 to 11,500 ^{14}C yr BP (16,400- 13,700 cal yr BP) (Thompson, 2001). Bulk sediment samples, used for ^{14}C analysis in these chronologies, have returned erroneous dates because bulk samples integrate a long core segment which contains progressively younger sediment from the bottom to the top (Ridge et al., 1999). The error associated with such a dating technique illustrates the importance of using the more accurate ages from macrofossils wherever possible (Ridge et al., 1999). However, macrofossils also can return erroneous dates, if they are significantly older than the time that they are eroded and deposited in the lake. All of the ^{14}C dates obtained in this study were obtained from macrofossils, and individual dates were rejected on the basis of stratigraphic inversion in relation to all other dates from that core.

Thompson (1999) and Ridge et al. (1999) also documented a re-advance of the ice sheet in the Littleton-Bethlehem area of northwestern New Hampshire, occurring approximately 12,000 ^{14}C yr BP (14,000- 14,100 cal yr BP). Five of the cores from New Hampshire (ST1, ST2, SU1, SU2, OG) are located in close proximity to the Littleton-Bethlehem readvance. However, the ice sheet retreated from the northwestern White Mountains in NH between 13,000 and 11,000 ^{14}C yr BP (13,000- 15,900 cal yr BP) (Thompson et al., 1999), and all of the basal dates from these cores postdate this retreat. The OG core is particularly close to the Littleton-Bethlehem area, but the lowest date in that core is only 4370 ^{14}C yr BP (4930 cal yr BP).

A worldwide cooling period occurred in the latest Pleistocene the Younger Dryas (YD) (Peteet et al., 1990). In the northeastern United States, the timing of the YD was approximately 11,000 to 10,000 ^{14}C yr BP (13,100- 11,500 cal yr BP). Vegetation changes associated with this period (Spear et al., 1994) likely reduced plant cover in New England, increasing the potential for runoff events recorded in lake sediments (Bierman et al., 1997; Brown et al., 2000; Noren et al., 2002). Five sediment records extend into the YD (CR, ST1, SU2, SY, WO).

Varves found in much of New England and the presence of sandy deltas found near valley walls allow glacial geologists to map the extent of numerous, large pro-glacial lakes (Ridge et al., 1999). The largest of such lakes were in the Champlain Valley, VT and Connecticut River Valley in VT and NH (Ridge et al., 1999). None of my study lakes is in one of these large, pro-glacial lake basins. However, some of my lakes were in close proximity to the ice front in the late Pleistocene, and multiple cores (ST1, ST2, SU1, SU2, WO) contained rhythmites with alternating layers of gray clay and sand or silt, similar to varves.

Ridge et al. (1999) noted varves with thick sand layers in some of their sediment cores, and suggested three mechanisms for the formation of such layers: 1. slumping of lake marginal deposits, 2. flood events, or 3. strong bottom currents associated with lake level lowering. The first two mechanisms can be suggested when varves or rhythmites are deposited on top of these sand layers, indicating a return to normal conditions after the deposition of the coarse material. In all of my cores, including the WO core, thick sand or silt layers are overlain by more rhythmites, and the rhythmites eventually are truncated,

either sharply or gradually, by organic rich mud (gytta) which represents the beginning of modern sedimentation. Although these sand and silt layers may represent flooding, they also can represent slumping of lake marginal sediments.

2.2 Sedimentological and Geomorphic basis for terrestrial layers as flood events

High gradient, inflowing streams in steep lake basins suspend and transport larger sediment as their velocity and discharge increase during floods (Boggs, 1995). As the muddy water of the stream enters the less dense freshwater in the lake, selective settling of the larger particles can occur (Boggs, 1995). If the residence time is short enough, as is the case in smaller lakes, and if the outflow is strong enough, the fine grains are transported out of the lake before they settle out (Campbell et al., 1994; Campbell, 1998). Thus, coarse grained layers in lake sediment have been interpreted as the result of terrestrial deposition related to flooding (Campbell, 1998).

Coarse sediment also can reflect other processes: wave erosion at the lake margin; slumping of lake marginal or delta foreset sediment to deeper water; or increased proximity to sediment source due to lake level lowering (Digerfeldt, 1986; Campbell, 1998). Wave erosion is considered a minimal influence on the amount of coarse particles in small, deep lakes with weak inlet streams, and therefore, less within-lake currents (Campbell, 1998). Slumping and subsequent deposition of coarse sediment from shallow to deep water produces clearly identifiable turbidites or coarse packages of sediment (Campbell, 1998). Examination of the visual stratigraphy in our cores did not reveal such clearly identifiable units in the sections dominated by organic rich mud, and lake level is considered a minimal influence in open lakes in humid climates where perimeter

bathymetry is steep and where the level is controlled by an outlet sill (Campbell et al., 1994; Campbell, 1998; Brown et al., 2000; Noren et al., 2002).

Earlier paleoflood investigations in New England discounted several other processes that could either directly or indirectly contribute to the formation of such coarse-grained, terrestrial sediment layers, including wildfires, vegetation blight, earthquakes, and snowmelt floods (Brown et al.; 2000, 2002; Noren et al., 2002). Wildfires, blight, and agriculture can clear hillslopes of vegetation increasing the likelihood of erosion and runoff during snowmelt or rainstorms. However, pollen and macrofossil investigations indicate that New England maintained continuous vegetative cover through the Holocene until European settlement (~250 cal yr BP; Davis and Jacobson, 1985; Jackson and Whitehead, 1991; Lin, 1996; Spear et al., 1994). Charcoal analyses of gyttja and terrestrial flood layers show no evidence for widespread fire in the Ritterbush Pond basin (Brown et al., 2000). Earthquakes likely were not a significant influence on the formation of terrestrial layers in lake sediment due to the relative tectonic stability in New England (Ouellet, 1997). Studies of lake sediment cores from the Canadian Arctic suggest that snowmelt floods do not transport enough sediment to produce such terrestrial sediment layers (Lamoreaux, 2000).

2.3 Flood-related, terrestrial deposition in lakes

Paleoflood research was pioneered using slackwater deposits as a means of measuring extreme flood events on rivers in the southwestern United States (Kochel and Baker, 1982). Since then, geomorphologists have deciphered paleohydrologic archives preserved in other depositional features including floodplain deposits, and alluvial,

debris, and overwash fans (Brakenridge, 1980; Bull, 1991; Liu and Fearn, 1993; Bierman et al., 1997; Knox, 1999; Nott et al., 2001; Jennings et al., 2003;). Such research extends the short-lived modern records of precipitation to longer temporal scales, providing a better indication of the natural patterns of extreme events prior to human impact on climate or the landscape. For instance, prehistoric paleoflood records from western North America detail the frequency of the observed El Nino Solar Oscillation (ENSO) before the modern record (Ely et al., 1993)

More recently, lake sediment cores were recognized as a means to identify and date Holocene floods (Page et al., 1994; Eden and Page, 1998; Thorndycraft et al., 1998; Rodbell et al., 1999; Bierman et al., 1997; Brown et al., 2000; Nesje et al., 2001; Noren et al., 2002; Brown et al., 2002). Coarse-grained, light-colored, inorganic sediment layers were linked temporally to major historical precipitation events (Page et al., 1994; Thorndycraft et al., 1998; Nesje et al., 2001; Ambers, 2001). Radiocarbon dating and age modeling of earlier Holocene flood layers established a record of extreme rainstorms (Eden and Page, 1998; Thorndycraft et al., 1998; Rodbell et al., 1999; Brown et al., 2000; Nesje et al., 2001; Noren et al., 2002).

The frequency and magnitude of these flood layers is a valuable means of extending the short, modern precipitation record, and of establishing trends in extreme precipitation throughout the Holocene. Paleostorm records from Laguna Pallcacocha in Ecuador marked the frequency of ENSO driven storms starting at 15 yrs from 15,000-7,000 cal BP and thereafter increasing to the modern frequency of 2.5- 8 yrs (Rodbell et al., 1999). In contrast, the paleostorm record taken from Lake Atnsjøen in eastern

Norway lacked a temporal connection to regionalized glacial fluctuations, snow avalanche, and debris flow records, suggesting that precipitation trends inferred from a single core may not reflect regional trends in precipitation or climate (Nesje et al., 2001). In the northwestern US, historic storms increased sediment yields in a flood-control reservoir fed by a large watershed (Ambers, 2001).

New England paleoflood and paleostorm records

The first paleoflood study was sparked by terrestrial flood layers identified in cores collected for pollen analysis from Ritterbush Pond, in northern VT (Lin, 1996). The isotopic ($\delta^{13}C$, ^{14}C) and elemental (loss-on-ignition (LOI), as a proxy for %C) analysis of these cores suggested that the inorganic sediment layers were deposited rapidly, were contemporaneous with periods of increased alluvial fan aggradation, and that the layers were the result of flooding associated with extreme rainstorms (Bierman et al., 1997). More cores from Ritterbush Pond were collected in proximal and distal locations near deltas at different parts of the lake margin (Brown et al., 2000, 2002; Brown, 2000). Detailed analysis of the stratigraphy of these cores revealed graded deposits and fine laminae in the flood layers, and also showed that the flood layers thinned from proximal to distal cores. Particle size analysis on individual terrestrial layers showed that the mean particle size was greater from the top of a layer to the bottom of a layer and that, in contemporaneous layers found in both proximal and distal cores, mean particle size of such a layer was greater in the proximal cores (Brown et al., 2000, 2002; Brown, 2000). Proxy measurements including X-radiography, LOI, and MS coupled with ^{14}C analysis revealed contemporaneous deposition of these flood layers in different locations

throughout the lake. Three periods of increased storminess (ca. 2.5, 6, and 9 cal kya) in New England were identified by terrestrial sediment layers in all 3 sediment cores taken from Ritterbush Pond (Brown et al., 2000).

A regional, paleostorm record was compiled from 13 lake sediment cores taken throughout Vermont and eastern New York (Noren et al., 2002). Frequency analysis of terrestrial flood layers in these cores revealed 3000 year cycles of storms in this region throughout the Holocene, correlating with the period and phase of the GISP2 time series of aerosol deposition (O'Brien et al., 1995). The millennial scale variability identified in both the GISP2 ice cores and New England lake records, as well as other paleoclimate records from northern Europe, may be indicative of significant, large scale climatic patterns, specifically different modes of the Artic Oscillation and their connection with or influence on the frequency of extreme storms in the northeastern United States.

Noren et al. (2002) suggested that the lake sediment record, inferred from LOI and other proxies, reflected periods of storm-induced erosion and deposition of terrestrial sediment, in part, because their record showed some correlation with periods of increased alluvial fan aggradation (Noren et al., 2002; Jennings et al., 2003).

The timing of the increased periods of storminess, measured by Noren et al. (2002), also corresponds to other geologic records of flooding and storminess in North America. Intense hurricane strikes in Florida and Alabama, recorded by overwash events, increased around 4 cal kyr BP, and peaked ca. 0.8, 1.4, 2.2, 2.6, and 3.0-3.2 kya (Liu and Fearn, 1993 and 2000). Peaks in storminess also correspond to an increase in the number

of floods in the north-central United States (Knox, 1999) and megafloods on the Mississippi river (Brown et al., 1999).

Liu and Fearn (2000) postulated that the increase in overwash events on the Gulf of Mexico coast was related to a shift in the jet stream ~ 3,000 ^{14}C yr BP, which altered the path of hurricanes to strike on the Gulf coast and move across the central United States. They cite the contemporaneous increase in the number of floods in the north central US and the Mississippi basin as evidence for this change in the path of the hurricanes. The predominant path of hurricanes prior to this shift, ca. 6,000 ^{14}C yr BP, was up the Atlantic coast (Liu and Fearn, 2000). Noren et al. (2002) cite convective thunderstorms as the mechanism for generating the terrestrial sediment layers in their record, suggesting that the regional influence of tropical cyclones, such as hurricanes, would cause centennial clustering of events and more contemporaneous deposition.

2.4 Proxy vs. Direct Methods

In almost all of the previous paleostorm studies using lake sediments, the primary analytical methods are proxies such as LOI, X-radiography, grayscale density, and magnetic susceptibility (MS) (Page et al., 1994; Eden and Page, 1998; Thorndycraft et al., 1998; Rodbell et al., 1999; Nesje et al., 2001; Brown et al., 2000; Bierman et al., 1997; Noren et al., 2002l; Brown et al., 2002). All of these methods distinguish lighter colored, inorganic sediments from darker-colored, organic-rich sediment. Visual stratigraphic analyses suggest that the light, inorganic sediments are coarser grained, and that the darker-colored sediments are fine grained. Proxy methods efficiently and economically distinguish these two types of sediment. However, the physical difference

in particle size between the two types of sediment is perhaps the characteristic most germane to paleoflood and paleostorm research as it directly reflects the transport capacity of the streams supplying the terrestrial, inorganic sediment.

Few previous paleostorm studies performed particle size analysis on lake sediments (Campbell, 1998; Campbell et al., 1998; Brown et al., 2000; Brierle, 2002), and only the terrestrial flood layers identified by proxy measurements were analyzed. As visual analysis suggested, the mean particle size of the terrestrial sediment layers was greater than the particle size of the surrounding organic-rich sediment. A subsequent study (Bosley et al., 2001) confirmed these data by performing high resolution (cm-by-cm) particle size analysis, LOI, and MS on two cores from Lake Morey in Vermont. In both cores, more terrestrial flood layers were identified by particle size analysis than by the proxy measurements (LOI or MS).

Paleo-oceangraphic and paleoclimatic studies widely employ particle size analysis to detect coarse-grained, terrestrial sediment layers in marine cores which indicate high energy depositional events indicative of flooding caused, in some cases, by increased precipitation (Brown et al., 1999; Prins et al., 2000; Nittrouer, 1999; Drake, 1999). In the study of terrestrial input by the Mississippi River, Brown et al. (1999) established increased terrestrial input by showing turnover in planktonic species and a coincident increase in coarse particles in the core. As part of the STRATAFORM project, Nittrouer (1999) concluded that flood and storm events, on the Eel River off the coast of northern California, combine to create normally stratified fine-grained layers with basal sand, and much terrestrial organic debris, such as the flood layer of 1995. Drake (1999) determined

an increase in the spatial extent of the 1995 flood layer through physical reworking over time, and determined a minimum layer thickness (4-5 cm) sufficient to survive the mixing process.

2.5 End Member Modelling

Changes in depositional conditions are usually inferred from general, down-core statistics such as mean and median particle size (Beierle, 2002). Folk and Ward (1957) illustrated the need to characterize particle-size distributions on the basis of depositional process, but noted the difficulty in achieving this goal due to mixing of different sizes during deposition. Particle size samples often produce polymodal size distributions with separate modes indicating a large volume of both fine and coarse particles. For instance, particle size analysis of a lake sediment core from Alberta, Canada, suggests that, at any given core depth, terrestrial sediment is a combination of many particle sizes, all of which indicate different depositional conditions (Campbell, 1998). A wide variety of statistical methods have been employed to "unmix" such samples into representative particle sizes or distributions so as to better define depositional processes (for summaries see Syvitski, 1991; Prins & Weltje, 1999).

Recently, end member modeling (EMM) was developed to interpret particle size distributions based on depositional processes (Weltje, 1997; Prins et al., 1999, 2002). EMM utilizes all the particle size distributions from a core to create discrete end-member, particle size frequency distributions (EMs) (Weltje, 1997; Prins et al., 1999, 2002). Each sample can then be defined as the weighted sum of multiple EMs. For instance, our cores are usually described by several EMs: a poorly-sorted fine silt EM, a poorly-sorted coarse

silt EM, and a well-sorted sand EM. Rather than describe an individual sample as dominantly silt, it can be described as containing less of the sand EM (~5%) and coarse silt EM (~10%) and more of the fine silt EM (~85%). Changes in the relative contribution of each EM down each core indicate changes in depositional conditions. For instance, sediment layers with a high percentage of the coarse EM can be interpreted as deposits formed during high-energy flooding of streams flowing into lakes.

The application of the EMM proved useful to help decipher controls on terrigenous sediment supply to the Arabian Sea for the last 20,000 years, where Prins et al. (2000) identified graded, turbidite layers which represent episodic events such as flash floods and earthquakes. Silt populations in north Atlantic marine cores were interpreted originally as high flow indicators during ice rafting events (McCave et al., 1995), but EMM of particle size data from the same region later demonstrated low flow during such events (Prins et al., 2002).

2.6 Laser Diffraction

Particle size analysis by laser diffraction began in the late 1970s (McCave and Syvitski, 1991), and has developed rapidly ever since. This method of particle measurement is based on the principle that particles of a given size diffract light through a given angle, which increases with decreasing particle size, a principle based on the Fraunhofer model of diffraction (Barth, 1984; Boggs, 1995; McCave and Syvitski, 1991). A parallel beam of light is passed through a chamber where the sample flows in suspension, and the diffracted light focuses onto a multielement ring detector (McCave and Syvitski, 1991). A lens is placed in between the detector and the chamber where the

sample is held in suspension, and with the detector at its focal point, the lens focuses undiffracted light to a point at the centre of the detector, leaving only the surrounding diffraction pattern (McCave and Syvitski, 1991). By using the measured intensity of the diffraction pattern, one is able to produce a size distribution (McCave and Syvitski, 1991).

Classical methods of counting and sieving are used still, although these techniques are employed primarily when samples are composed of gravel, sand, and silt sizes (McCave and Syvitski, 1991). Settling of particles for size measurement is primarily used for silt and clay sizes, and photon correlation spectroscopy is used almost entirely for clay sizes (McCave and Syvitski, 1991).

Laser diffraction is used primarily for silt- and sand-sized sediment, measuring these sizes with good precision; however, it sometimes produces less effective measurement of sub-micron sizes (Barth, 1984; McCave and Syvitski, 1991). Laser diffraction is used primarily for its efficiency, as it can measure a sample in under a few minutes without calibration (Barth, 1984; McCave and Syvitski, 1991). Given the large volume of samples in this study (n=3,451) and the fact that the Coulter LS 230 was the most readily available resource, laser diffraction served my purpose well.

However, consideration of sample preparation is an important precaution in the use of laser diffraction, particularly in light of the goals of the study and any lack of resolution by this technique. Mathews (1991) reported the importance of aggregates in pre-treatment of samples for size analysis, namely that one should consider whether or not aggregates are an important part of the sample and, if not, which technique to use in

their removal. Larger diameter, less dense aggregates could alter the interpretation of sediments in this study, as the aim is to determine transport and deposition patterns. Further, diagenetic processes can form post-depositional aggregates (Mathews, 1991) which also alters the interpretation of large particles as indicators of high-energy deposition. Mathews (1991) also noted that breaking size distribution profiles into individual components for statistical analysis and interpretation can be significantly altered by improper pre-treatment. End-member modeling of particle size data (see below) heavily relies on size distributions, and since I relied heavily on end-member modeling, I wanted precision (reproducibility of size distributions (McCave and Syvitski, 1991)) to be the foremost quality in my data set. Such precision also provided confirmation that the laser diffraction unit provided good results (Figure DR.13 and Figure DR.14, Chapter 3). Thus, I removed aggregates carefully by removing organic matter and using dispersant.

CHAPTER 3

Data Repository to accompany paper submitted to *Geological Society of America Bulletin* (Chapter 4)

Field Methods

Lake Selection

Potential lakes for coring were identified by reviewing every USGS 1:24,000 topographic map from New Hampshire and northwestern Maine. I selected candidate lakes on the basis of good access roads, steep basins, steep gradient, inflowing streams, and the presence (inferred or observed) of lake marginal alluvial fans or deltas. Reconnaissance trips were made to verify these criteria, particularly the presence of a sandy delta on at least one margin of the lake. The deltas are fed by steep, competent streams, originating at higher elevations in the basin (Chapter 4, Fig.2). I surveyed the bathymetry near the delta shore to find a coring location near the toeslope. Previous research suggested that proximal locations to the delta were best for event detection (Campbell, 1998; Conlan et al., 2001; Bosley et al., 2001; Parris et al., 2001), and our coring device requires at least ~7.5 m of water depth.

Lake Setting

South Pond (Stark, NH) is the northernmost lake in the study (Chapter 4, Fig. 1), and is located on White Mountain National Forest property. The main pond is part of a chain of smaller ponds that start just to the north and eventually flow to the east. South Pond sits in a saddle formed by two prominent bedrock ridges composed of granite which are covered by glacial till and mixed deciduous and coniferous forest. Two different cores

were taken adjacent to two different deltas (Chapter 4, Fig. 2). A stream originates south of Mill Mountain and empties into the lake on the southern end of the delta, adjacent to which SU1 was collected. An old channel runs directly across part of the delta, but the main channel empties well to the southern end of the delta on the western margin of the lake (Chapter 4, Fig. 2). Very coarse sand and cobbles were found along the entire western margin of the lake. The primary tributary, supplying the delta adjacent to which SU2 was collected, originates north of Mill Mountain, and winds down into the valley floor before emptying into the lake through a sandy shore on which park facilities are located. Many homes exist on or near the shore, but the influence of development does not affect terrestrial depositional signal for the Holocene, as it only represents the last ~250 years or less (Bierman et al., 1997; Meeks, 1986).

Worthley Pond (Rumney, NH) is the easternmost lake in the study (Chapter 4, Fig. 1, Fig. DR.1). Worthley Pond trends northeast/southwest, and has an outflow tributary on the northeastern margin. A ridgeline covered mostly with deciduous forest and composed of granitic bedrock stretches along the southeastern border. Multiple inflowing tributaries run down this ridgeline and empty into this developed margin of the lake with very sandy shores. The pond narrows in the middle where two broadly sloping surfaces extend into the lake. Thick surficial deposits cover the southeastern ridgeline bordering Worthley Pond, mostly in the form of glacial till.

Ogontz Lake (Lyman, NH) is within 30 km of the area which held the primary evidence for the established Littleton-Bethlehem Readvance of the Laruentide ice sheet (Ridge et al., 1999; Thompson, 2001), however, the OG core only reaches 4,930 cal yr

B.P. (Chapter 4, Fig. 1 and Table 2, Fig. DR.1). The Ogontz basin is covered with mixed coniferous and deciduous forest, thick glacial till, and reworked post-glacial deposits. The primary tributary supplying the delta adjacent to which we cored flows through surficial material, and has cut to bedrock in places. It has incised a narrow gully most of the length of the channel, and the banks of the gully contain abundant surficial material, in some places well sorted sand which suggests that some of the surficial deposits are fluvio-glacial. The lake marginal sediments are sandy. The lake is situated between two bedrock ridges composed of schist that bend from the south to the northeast. Vegetation in the Ogontz basin is a mixture of deciduous and coniferous forest. The Ogontz children's camp is the primary development on the southern shore of the lake since 1923, and historic photos of the lake can be found on the camp's website (http://www.campogontz.com/).

Crystal Lake (Eaton Center, NH) is within ~30 km of the eastern New Hampshire border (Chapter 4, Fig. 1, Fig. DR.3). It is pinched between two bedrock ridges to the east and west of the lake, and the landscape is more flat and open to the northeast and south, with one primary outflow tributary emptying the lake to north. The bedrock ridges are primarily composed of quartz pebble conglomerate, and covered by glacial till and mixed coniferous and deciduous vegetation. Most of the western margin of the lake marks the western extent of a large alluvial fan which progrades into the lake creating a delta. The stream which runs across the fan supplying the delta originates in the Rockhouse Mountain basin to the northwest. The portion of the channel flowing across the fan has

well developed banks and a well developed, transport limited channel with abundant amounts of sand, especially on the lake margin.

The Stinson Lake (Rumney, NH) basin is the largest of all the basins, and sits at the highest elevation (Chapter 4, Fig. 1 and Table 1, Fig. DR.4). It is located in the White Mountain National Forest, and is surrounded on all sides by prominent ridges composed mostly of granite. Vegetation in the Stinson basin is a mixture of deciduous and coniferous forest. On the southern margin of the lake, a large delta is supplied by two streams both of which become transport limited channels flowing through abundant coarse sand before emptying into the lake. On the southeastern margin, one stream flows across a fan-like surface, and becomes a transport limited channel with well developed banks and meander bends before emptying into the lake. The topset of this delta remains shallow (~20- 30 cm depth) while extending approximately 30 m into the lake. Both of these lake margins are comprised of abundant coarse sand, and are the coarsest cores defined by particle size analysis (see Results, Chap. 4). The outflow for Stinson Lake is located at the southwestern corner, which likely removed some fine grained material associated with terrestrial sediment deposition owing to its proximity to the two deltas (Campbell, 1998).

The Sandy Pond (Richmond, NH) basin is the smallest basin in the study (Chapter 4, Fig. 1, Fig. DR.5). Lower relief ridges surround the lake, however, the primary tributary supplying the only delta in this lake is a high order stream, which drains a very large area to the north of Sandy Pond. For a limited distance (~10 m) from the lake margin into the basin, the channel of this stream is transport limited and flows through

sand and silt. It quickly changes to a supply limited, step pool channel which cuts through surficial sediment to granitic bedrock in places. The basin is covered with mixed coniferous and deciduous forest. Extensive observations of the Sandy Pond basin were provided by two personal contacts (Hank Hallas and Shaun Bennett) which detailed hurricane and anthropogenic impact on Sandy Pond, as well as lake level changes. While diving in Sandy Pond, S. Bennett observed the delta extending into the lake and dropping off steeply. H. Hallas is a long time summer resident of Sandy Pond, and owns a farmhouse near the western edge of the pond. On at least two occasions (1938, 1955) hurricanes passed over the Sandy Pond basin causing erosion on the lake margin near the inflowing tributary (H. Hallas, personal communication).

As part of the fall 2001, University of Vermont Geomorphology class, the primary tributaries feeding the deltas in two basins, OG and SY, were examined in detail for channel morphology (Montgomery and Buffington, 1997) by Kristen Benchley. Observations of these streams indicate a progression from transport limited, plane bed channels to supply limited, step pool channels moving up gradient in the basin (http://geology.uvm.edu/morphwww/classes/morph/2001/projects/kristen.pdf). Significant sediment storage takes place along the banks and in the channels where woody debris, dams, and culverts occur. The transition from supply limited to transport limited channels occurs near the lake margin, suggesting that the terrestrial sediment on the lake margin is eroded and deposited during the floods which cause terrestrial deposition of terrestrially-derived sediment into the lake (Brown et al., 2000).

Core Collection

Six lakes were selected as part of the study (Chapter 4, Fig. 1). A total of 9 cores (~4.5-6 m long) were collected from these lakes, using the Reasoner percussion piston coring device without a core catcher (Reasoner, 1993; Noren, 2000). All of the cores were cut into 1.5 m sections in the field, and then stored at 4^{o}C. In one of the lakes (Crystal Lake, CR), we collected two cores from the same hole to extend the sediment record. Thus, these two cores were combined to form one sediment record (Fig. DR.6), making a total of 8 sediment records. In two other lakes (Stinson Lake, ST, and South Pond, SU), separate cores were taken at the base of two different deltas in the same lake to assess the local sediment variability and to compare the timing of deposition throughout the Holocene. The topmost 2-62 centimeters of the sediment record is not captured by the Reasoner device as well because the piston does not immediately begin to move up the core as it is pounded into the sediment and because it is difficult to judge accurately the depth of the sediment-water interface. Where sedimentation rates are faster, this unrecovered sediment represents little time. Where sedimentation rates are slower, as is the case with most of the lakes in this study, un-recovered core tops represent up to ~3,000 years of sediment accumulation (Chapter 4, Table 2).

Lab Methods

Magnetic Susceptibility, Core Processing, and Loss-on-ignition

Initial determination of core stratigraphy relied on magnetic susceptibility (MS), loss-on-ignition (LOI), and visual stratigraphic logs. MS provides a rapid assessment of

core stratigraphy, detecting terrestrial flood layers by measuring increases in the magnetic mineral content of unopened cores. Using a Bartington Magnetic Susceptibility Meter (model MS2) mounted on an automated track, we measured MS at 1 cm intervals soon after returning each core to the lab (Fig. DR.7). Thus, we were able to evaluate rapidly the utility of the cores taken from each lake by confirming the presence of terrestrial layers. However, the MS2 integrates measurements over ~5 cm intervals, and therefore the MS is a low resolution record.

We split the core sections, wrapping and sealing half of each section immediately to be stored in a 4^{o} C archive. The other half was photographed immediately with a high resolution digital camera. To construct a visual log, we examined the cores at 0.5 cm resolution for changes in color, texture, and the abundance and location of terrestrial macrofossils. We sampled the cores at 1 cm intervals, collecting macrofossils where we found them. All samples were freeze dried for at least 48 hours.

For LOI, ~250 mg of every sample was combusted at 450^{0}C. The samples are weighed before and after combustion, and the resulting ratio (mass lost (g)/original mass (g)) is a proxy for the amount of organic matter (Bengtsson and Enell, 1986).

Radiocarbon Dating

Macrofossils were selected for dating on the basis of their location immediately above, below, or in terrestrial flood layers, as defined by MS, LOI, and the visual stratigraphic log. Dates were obtained for 80 macrofossils using accelerator mass spectrometer (AMS) analysis of radiocarbon (^{14}C) at Lawrence Livermore National Laboratory (Chapter 4, Table 2). Samples were prepared under the instruction of John

Southon and calibrated using CALIB v4.2 (Stuiver and Reimer, 1993; Stuiver et al., 1998). Single calibrated ages were determined in the same fashion as Noren et al., 2002.

Grain Size Analysis

A total of just over 4000 sediment samples from all 8 cores were measured for grain size using a Coulter LS 230 Small Volume Module laser diffraction unit. My goal for preparation of sediments in this study was to have a thick, well mixed, and disaggregated slurry of inorganic sediments. None of the lake sediments obtained for this study contained secondary carbonates, and thus, HCl treatment of the sediments was unnecessary. NaOH treatment (see below) effectively removed any biogenic silica from the sediments. Organic matter (OM) removal proved to be the most critical step in sample preparation because the complete isolation of inorganic sediment from OM by H_2O_2 was particularly difficult, and the presence of OM impacted grain size results.

We tested two protocols for removing organic material from our samples. First, we weighed ~300 mg of sample into a 50 ml centrifuge tube. We then added 30 ml of 30% H_2O_2 and placed the sample on a Branson Ultrasound 8210 (70^0C) for 24 hours. The samples were lightly capped before being placed on the ultrasound so that most of the vapor resulting from the reaction could escape. Condensation of this vapor kept enough liquid in the tube so the sample did not dry out. Capping prevented strongly reacting samples from contaminating other samples.

We constructed a reaction time series to test the validity of this method. To construct the reaction time series, four separate samples from a 1 cm interval of one core (SY226A, SY226B, etc.) were weighed into centrifuge tubes, added to H_2O_2, and then

placed on the ultrasound. The initial amount of %C in the sample was calculated from the LOI value of that sample using the formula %TOC= 0.53* %LOI (Brown, 2000). We removed the samples, separately, at 6 hour increments (6, 12, 18, 24 hours). We then dried the samples in an oven set to 60^0C and weighed ~150 mg for measurement in the elemental analyzer measuring the %C with a CE NC2500 elemental analyzer (Fig. DR.8). This method produced a curve that gradually decreased in %C, until finally reaching 1.02 %C after 24 hours of reaction time (Fig. DR.8). Given this low value for %C, we initially thought this method sufficient for the OM combustion of our sample (Lavkulich and Weins, 1970).

Nevertheless, this first method produced very "noisy" results, where median and mean grain size varied significantly down core from our expected outcomes according to LOI and MS (Fig. DR.9). Therefore, we tried a different technique for OM digestion using a double treatment of H_2O_2. We weighed ~300 mg of sample into the centrifuge tube, and added 30 ml of 30% H_2O_2. We placed the sample on the ultrasound for 8 hours, and after 8 hours, we removed the sample, centrifuging and decanting the H_2O_2. We then added 30 ml of fresh 30% H_2O_2, placing the sample back on the ultrasound for another 12 hours.

To test this method, we constructed a similar peroxide reaction time series (Fig. DR.8). We weighed ~300 mg of sample from a 1 cm interval of a different core with very similar %C as the first test (18% & 19%, respectively) into four separate centrifuge tubes. We added 30 ml of 30% H_2O_2, and placed them on the ultrasound lightly capped. All of the samples were removed at 8 hours, and we added fresh H_2O_2 to three samples

replacing them on the ultrasound for 4, 8, and 12 more hours. This method produced a curve which reached a lower %C in one of the samples (CR371C=0.54%C) after a total of 16 hours on the ultrasound. Also, the % C in these samples remained much more constant over the last 12 hours (~1 %C) than the samples from the previous experiment (Fig. DR.8). However, aside from the sample which reached 0.54 %C, the two methods produced the similar results in that most samples ended with ~ 1 %C.

Despite only subtle differences in the H_2O_2 reaction time series, the two methods produced drastically different results in mean and median grain size down core (Fig. DR.9). The results from the two methods are expressed best by the size graphs (Fig. DR.10). These graphs illustrate an observed difference in both cores of a large volume of grains above 200 μm; such large grains are very rare when peroxide is changed mid-treatment.

For all the cores, inorganic grain size samples were prepared uniformly for laser diffraction by using a three treatment technique. The first treatment was for OM removal by H_2O_2. 300 mg of each sediment sample was weighed into a 50 mL centrifuge tube labeled with core ID and sample number on the cap and the tube, and 30 mL of 30% H_2O_2 was added to each sample. The initial reaction of OM with the H_2O_2 was the strongest. Thus, if sediment samples are very high in OM content, we let the reaction wane before adding samples to the ultrasound. Samples which threaten to boil over the centrifuge tube were doused with de-ionized water until the reaction stabilized. Adding generous amounts of DI dilutes the H_2O_2. The samples were lightly capped and placed in a sonicating hot bath at 70^{o} C for 8 hours, using a Branson Ultrasound 8210. Lucite sheets

(~2 cm thick) were selected to fit on top of the open part of the ultrasound, and were drilled with 50 holes specifically fit to the width of the centrifuge tube, thereby forming a centrifuge tube holder. The hole for each tube must be drilled so that the threads for the cap of the centrifuge tube will not pass through the hole. After 8 hours, the samples were removed, and fluid levels were evened out using de-ionized water. The samples were centrifuged at 2400 rpm for 6 minutes, decanted, and 30 mL of fresh H_2O_2 was added to them. We tightly capped and shook each sample to make sure the remaining sediment was disaggregated before loosening the cap and placing it back on the ultrasound for another 12 hours to react.

After OM was removed, the samples were centrifuged, decanted, and rinsed with 30 mL of de-ionized water twice. The second treatment of our technique was the removal of biogenic silica by NaOH. The samples were treated with 10 mL of 1M NaOH for 4 hours at 70^{o} C on the ultrasound. Again, the samples were tightly capped and shaken before loosening the caps and placing the samples on the ultrasound.

After biogenic silica was removed, the samples were centrifuged, decanted, and twice rinsed with 30 mL of de-ionized water. We added ~2 mL of Sodium Metaphosphate dispersant (25 g of sodium metaphosphate dissolved in 500 mL of de-ionized water) to each sample. Since the object is to have a thick slurry of sediment, the amount of dispersant added varied depending on the amount of sediment remaining after all the pre-treatment. Nevertheless, the amount did not significantly vary from 2 mL.

The Coulter LS 230 Small Volume Module calculated the grain sizes of each sample in this study using the Fraunhofer model. Under the Preferences menu, the Size

Statistics to be calculated by the machine were specified as Mean and Median diameter, D (3, 2), Mean/Median ratio, Mode, 95% Confidence Limits, Standard Deviation, Variance, Coefficient of Variation, Skewness, Kurtosis, and d90. Also under the Preferences menu, the Size Graph output was set to Differential Volume %. A separate folder on the desktop was created for each core, as well as the garnet standards, so that each run was directed to the corresponding folder by the Change Directory command under the File Menu.

The LS 230 was set to measure Offsets and Alignment of the laser beam every hour, and the background was measured for 60 seconds before each run. Also, the machine was set to measure loading and sample was added until 8-12% obscuration was achieved. A plastic 10 mL pipette with the tip cut to at least 1 mm for large grains was used to transfer samples into the chamber of the LS 230. Each sample was disaggregated with a mini-vortexer set to 2500 rpm for at least 30 seconds prior to running the sample, and the sample was held on the vortexer as it was pipetted from the centrifuge tube to ensure a well mixed sample. The Sample Info, Statistics, and Size Listing were exported to Microsoft Excel under the Run File menu in tab delimited format.

A 50 cm section of the Ogontz Lake core (OG) was replicated to test reproducibility in our preparation techniques (Fig. DR.11), and a 35 μm garnet powder standard obtained from Coulter was run before each use of the laser diffraction unit to test the accuracy of the LS 230 (Fig. DR12).

A

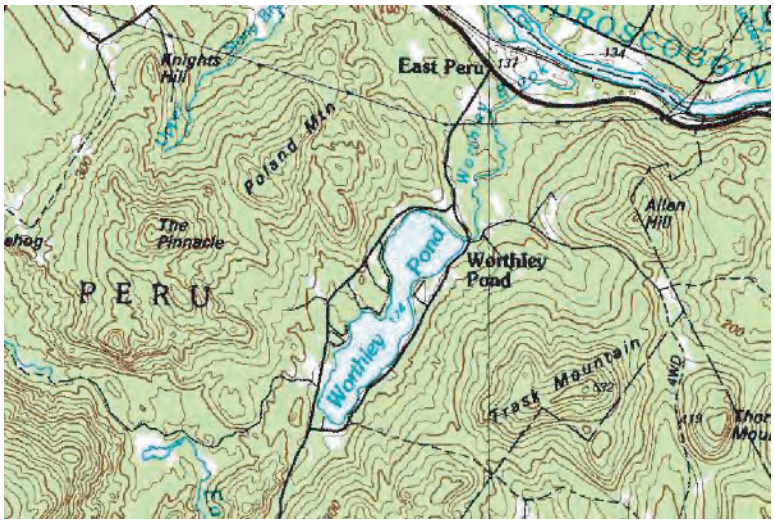

B

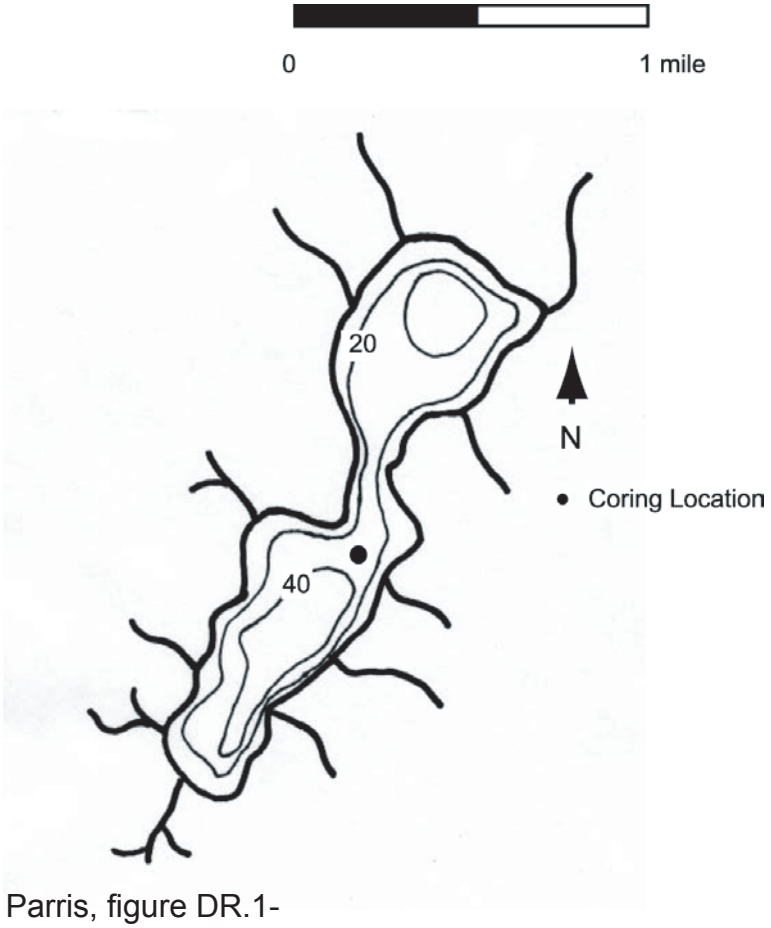

Parris, figure DR.1-
Worthley Pond (WO) watershed, Peru Maine. A. Adapted from U.S. Geological Survey quadrangle map, Peru, ME. B. Bathymetric map of WO; isobaths, 20 feet. Dot indicates core location. Bathymetric map provided by NH Department of Conservation.

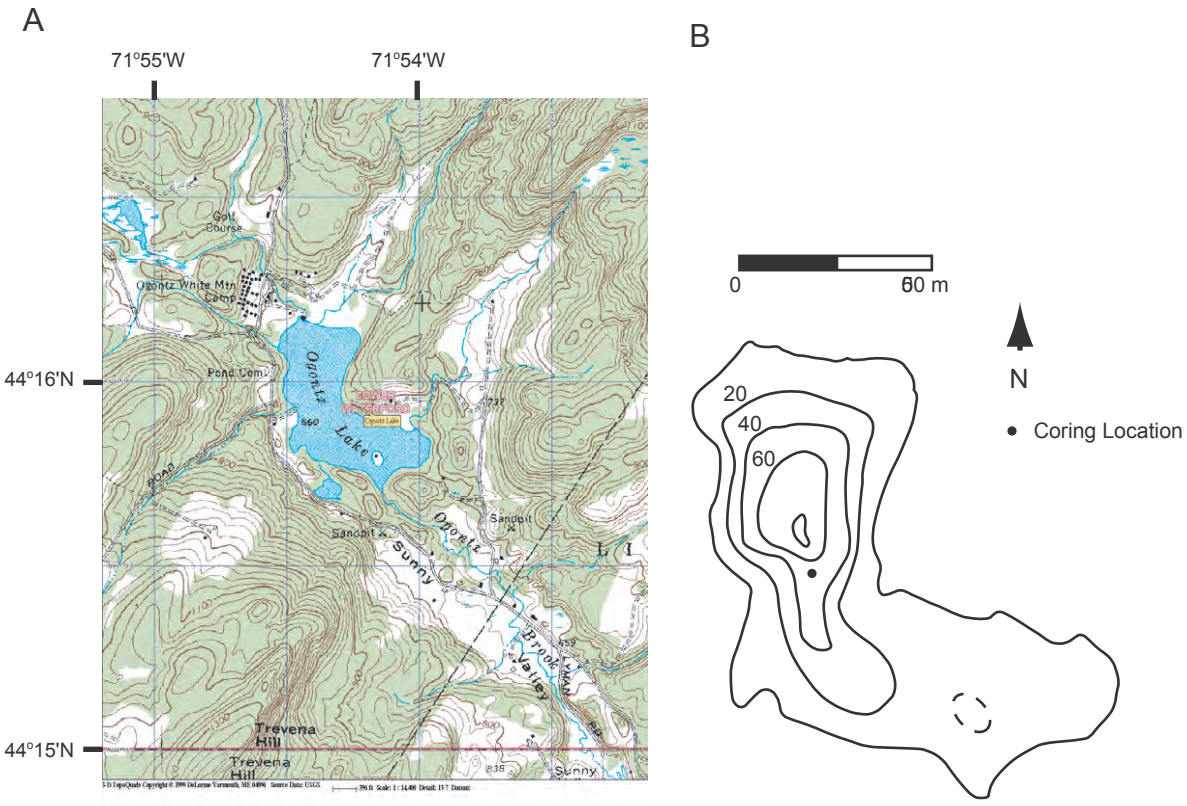

Parris, figure DR.2-
Ogontz Lake (OG) watershed, Lisbon, New Hampshire. A. Adapted from U.S. Geological Survey quadrangle map, Lower Waterford, NH. B. Bathymetric map of OG; isobaths, 20 feet. Dot indicates core location. Bathymetric map provided by NH Department of Conservation.

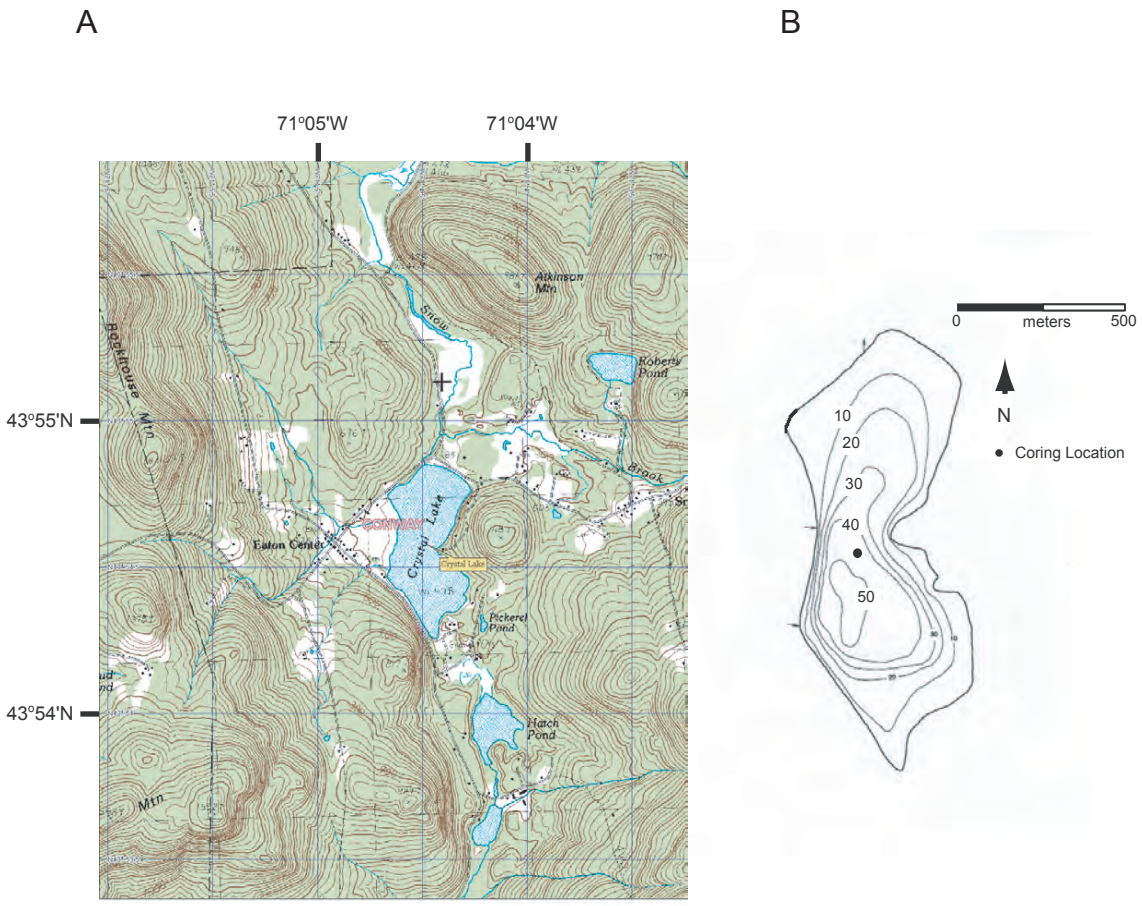

Parris, figure DR.3-
Crystal Lake (CR) watershed, Eaton Center, New Hampshire. A. Adapted from U.S. Geological Survey quadrangle map, Conway, NH. B. Bathymetric map of CR; isobaths, 10 feet. Dot indicates core location. Bathymetric map provided by NH Department of Conservation.

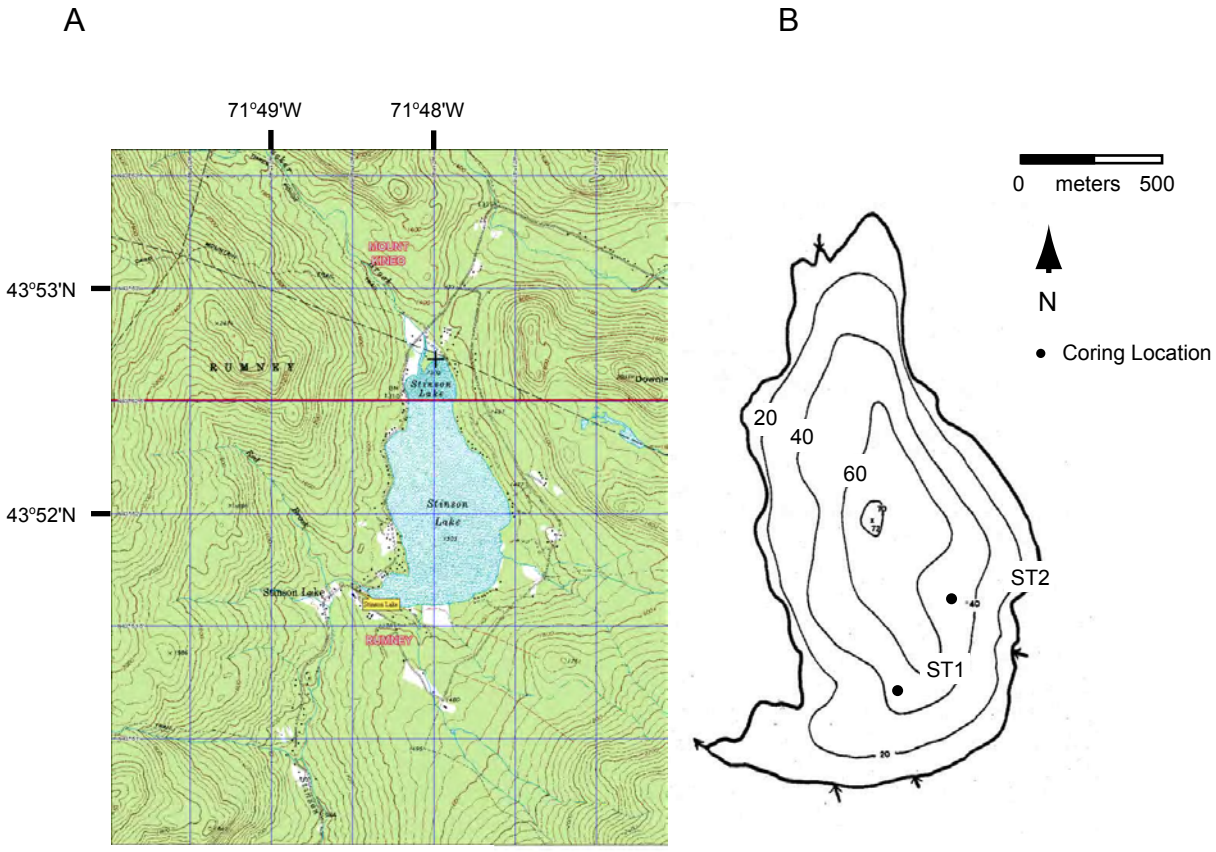

Parris, figure DR.4-
Stinson Lake (ST) watershed, Rumney, New Hampshire. A. Adapted from U.S. Geological Survey quadrangle maps, Mt. Kineo and Rumney, NH. B. Bathymetric map of ST; isobaths, 20 feet. Dots indicate core location. Bathymetric map provided by NH Department of Conservation.

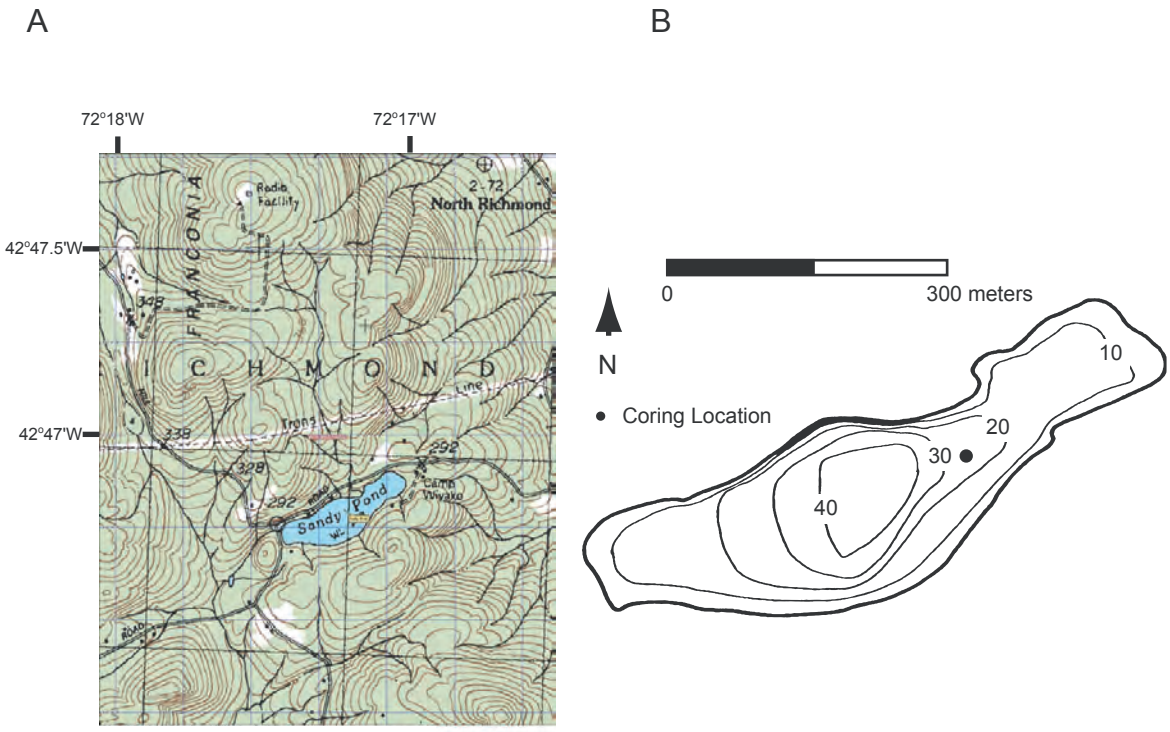

Parris, figure DR.5-
Sandy Pond (SY) watershed, Richmond, New Hampshire. A. Adapted from U.S. Geological Survey quadrangle map, Richmond. B. Bathymetric map of SY; isobaths, 10 feet. Dot indicates core location. Provided by NH Department of Conservation.

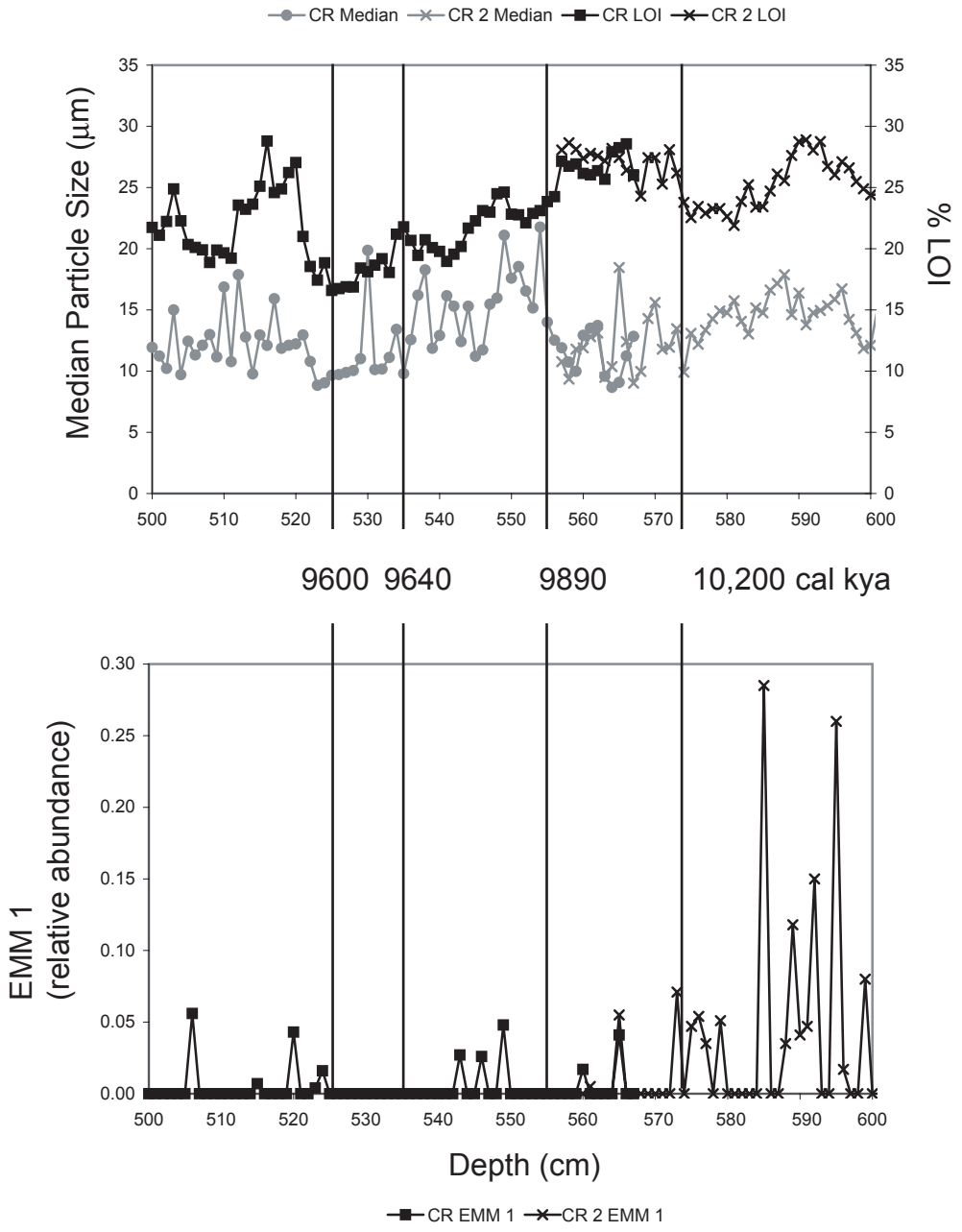

Parris, figure DR6-
The Crystal Lake (CR) sediment record was extended by retrieving more sediment from the same coring location. Overlap between the two records was recorded by % Loss-on-ignition, Median particle size, the proportion of the coarse EMD, and radiocarbon dates. CR is the first core, and CR2 is the second core taken from the same location. A depth of 110 cm in CR2 was set equal to 555 cm in CR. In this fashion, the CR sediment record was extended to 705 cm, from an original 567 cm.

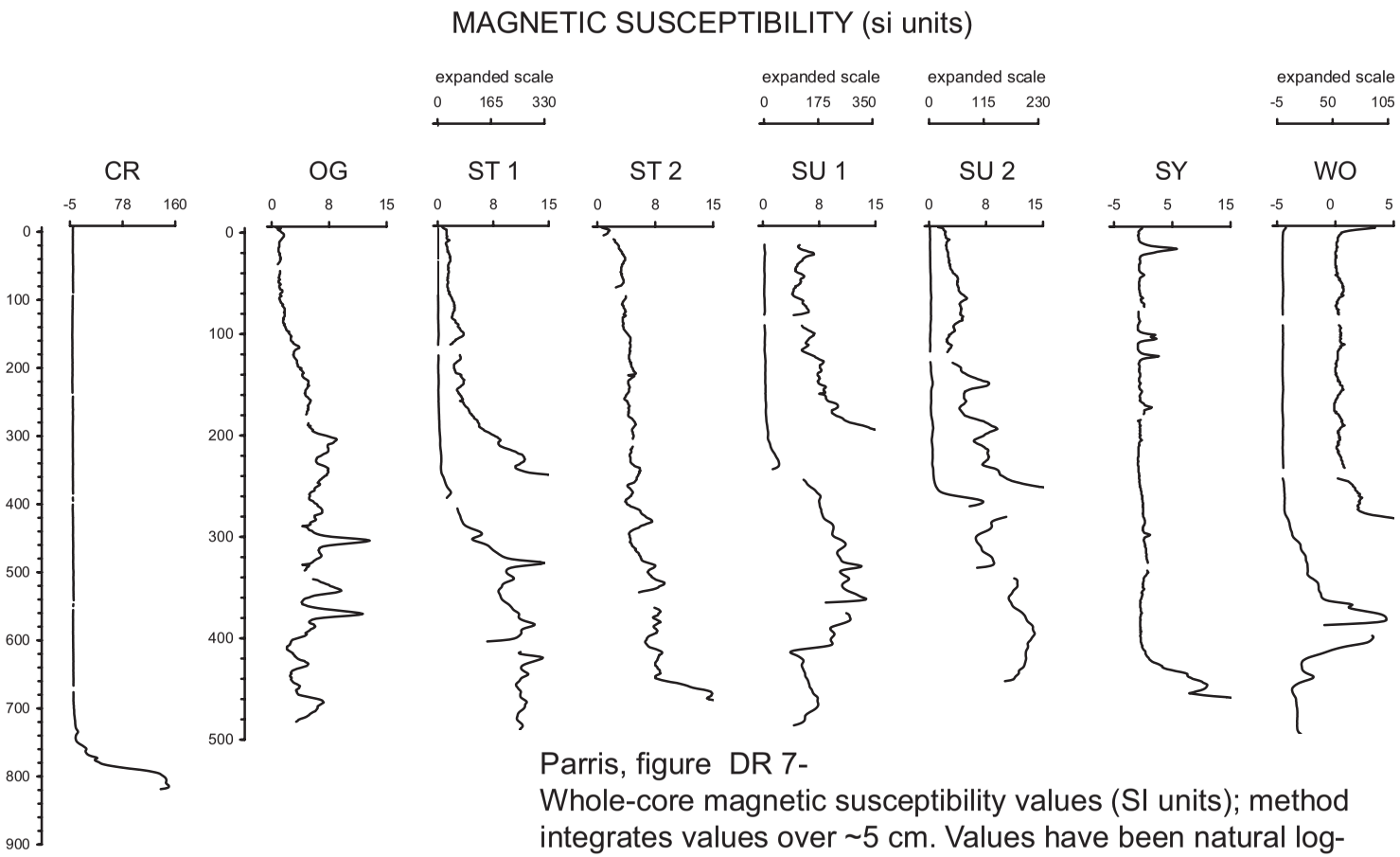

Parris, figure DR 7-
Whole-core magnetic susceptibility values (SI units); method integrates values over ~5 cm. Values have been natural log-transformed. Expanded scale (shown above core ID) corresponds to higher values found toward the bottom of the core, which correspond to to the stratigraphic boundary between inorganic rhythmitesogranic mud. Core ID letters correspond to lakes in Table 1 and Figure DR.2.

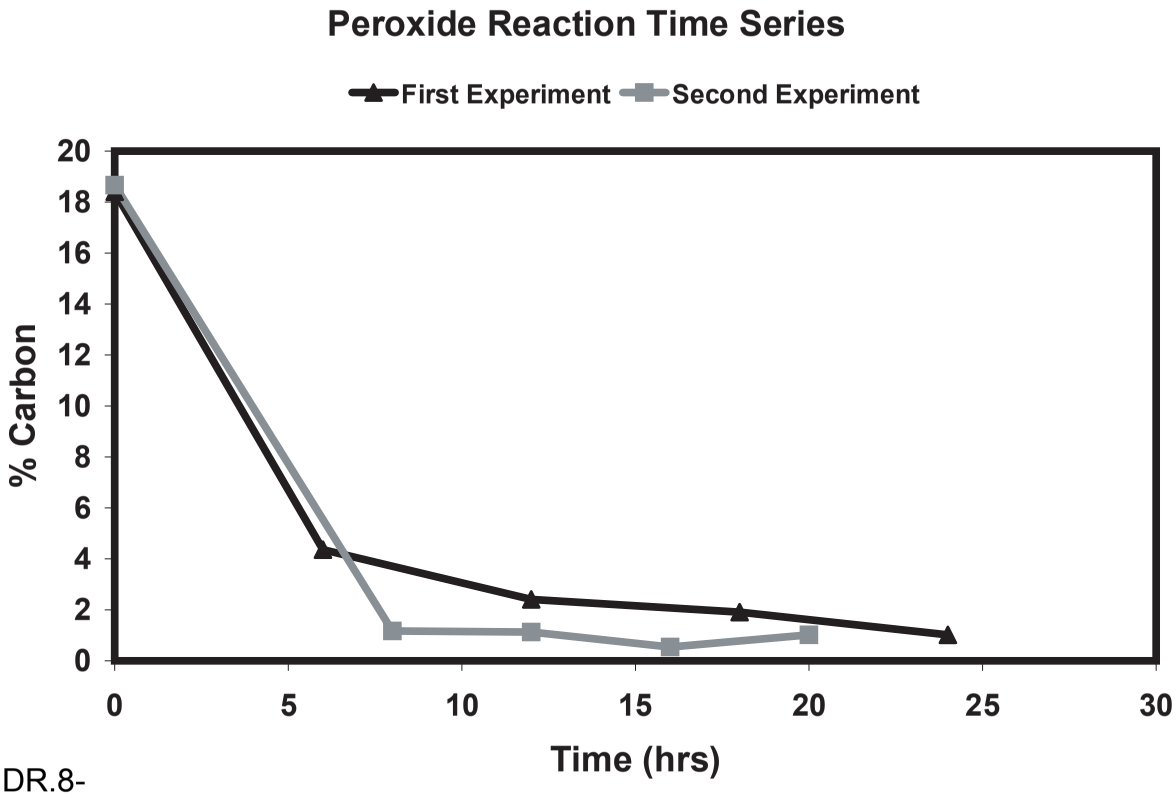

Parris, figure DR.8-
Comparison of organic matter removal by single and double treatment of 30% H_2O_2. Single treatment method shown in black, and double treatment in gray. % Carbon was calculated from LOI (%C=0.53*%LOI; Brown, 2000). Four separate samples, with similar LOI values, from the same depth in two different cores (SY, first experiment; CR, second experiment) were treated for each respective experiment. Samples were treated on a sonicating hot bath (70^{o}C) and pulled off at separate time intervals. A single treatment of peroxide was used for the first treatment, and a double treatment was used for the second experiment.

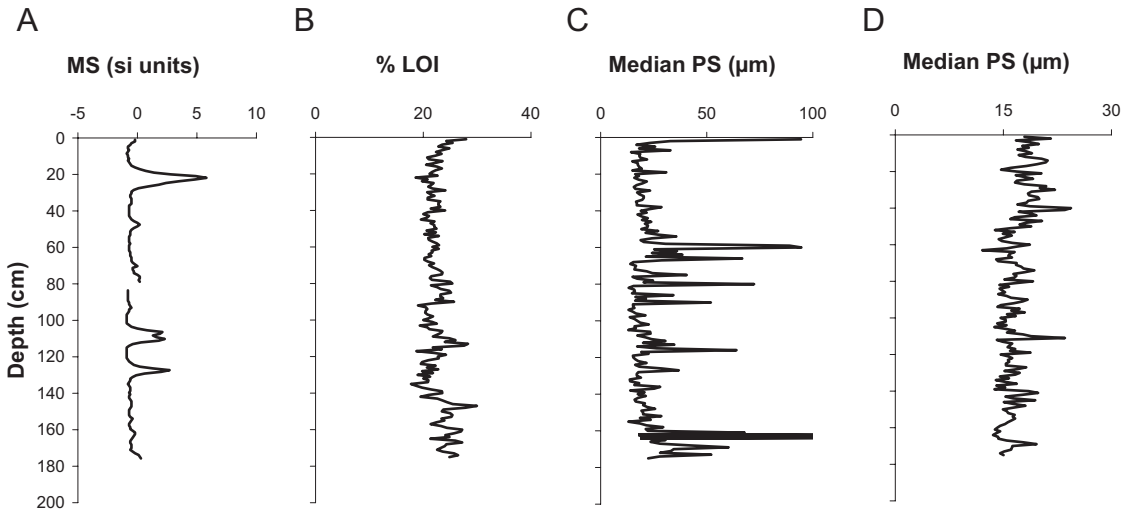

Parris, figure DR.9-
Magnetic Susceptibility (MS), % Loss-on-ignition, and Median particle size (PS) results from the top 200 cm of the Sandy Pond core (SY). A. Results from all three analyses using a single peroxide treatment in fig. DR. 10. B. Results from all three analyses using the second method of peroxide treatment in fig. DR.10. Results in A, compared to B, show the effect of organic matter on particle size results.

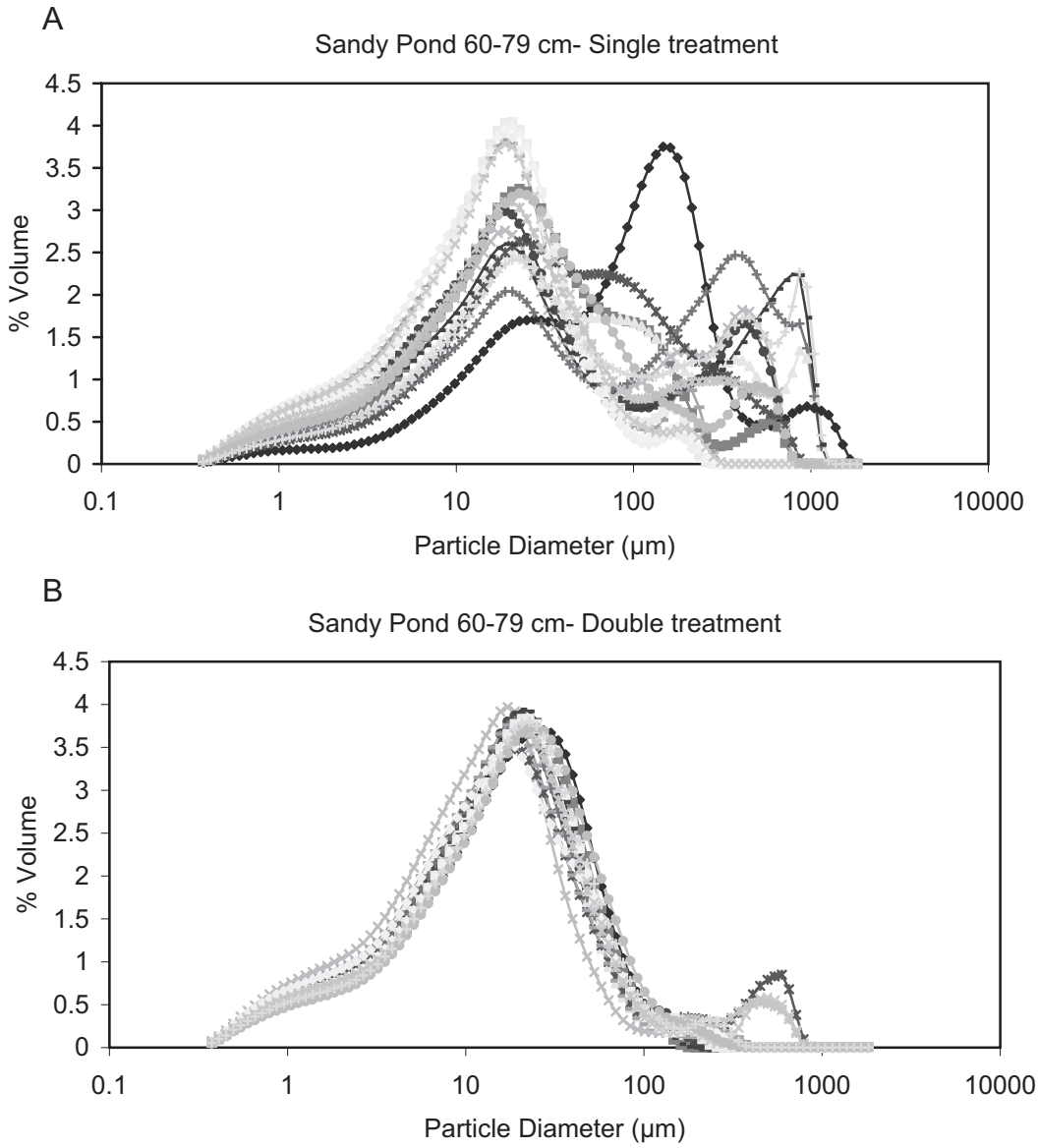

Parris, figure DR.10-
Particle size distributions from a 20 cm section of the Sandy Pond core (SY), using single and double peroxide treatment methods (fig. DR. 10). A. Size distribution results using single peroxide treatment method. B. Size distribution results using double peroxide treatment method.

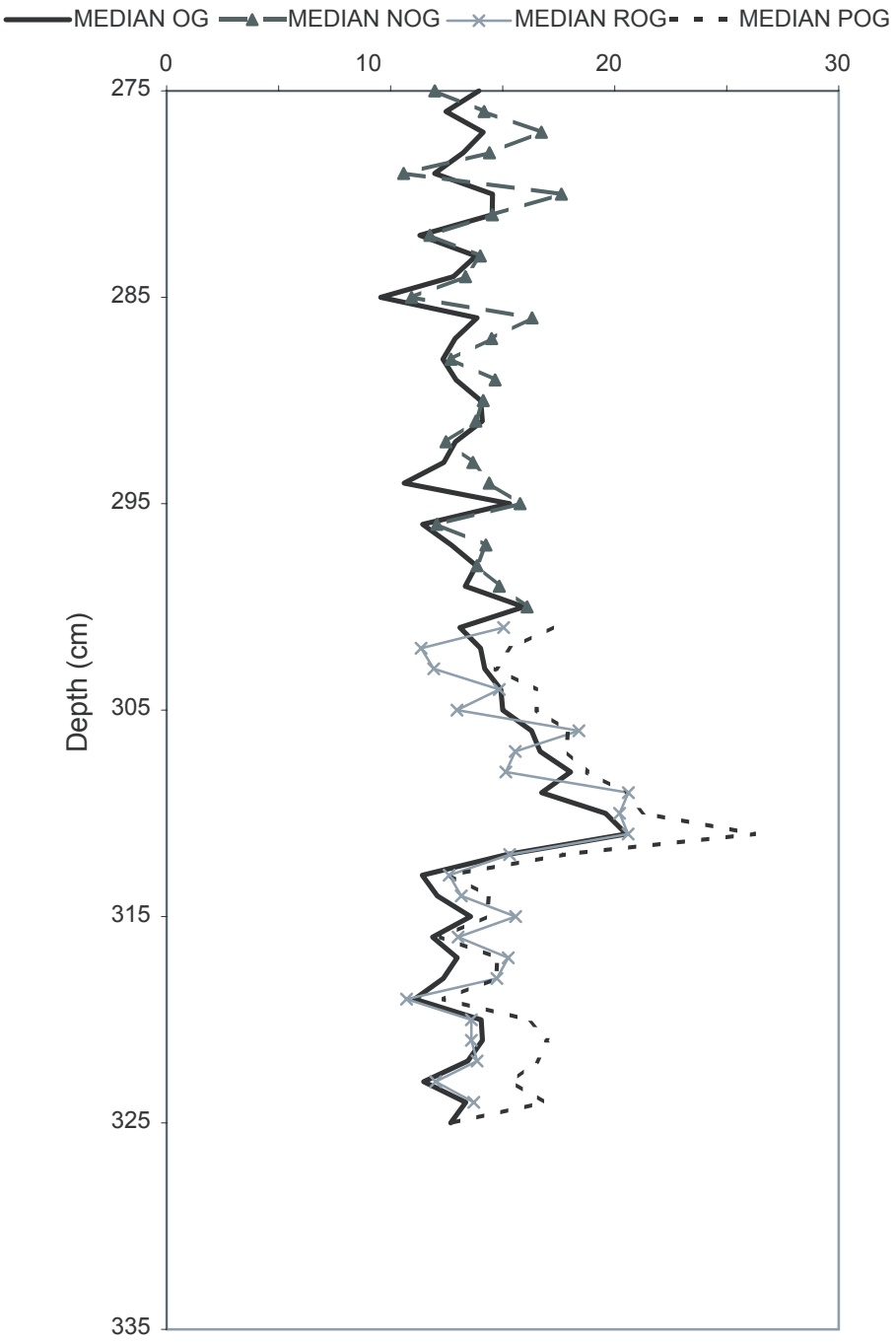

Parris, figure DR.11-
Replicate analyses on the Ogontz Lake core (OG) were used to test reproducibility of preparation technique. Median OG= Original median particle size results, using double treatment of hydrogen peroxide. Median NOG= Median particle results of samples 275- 300, after treating the original samples with a second treatment of 1 M NaOH. Median ROG= Median particle size results of replicated section of the original samples. Median POG= Median particle size results of samples 301- 325, after treating the original samples with a third treatment hydrogen peroxide.

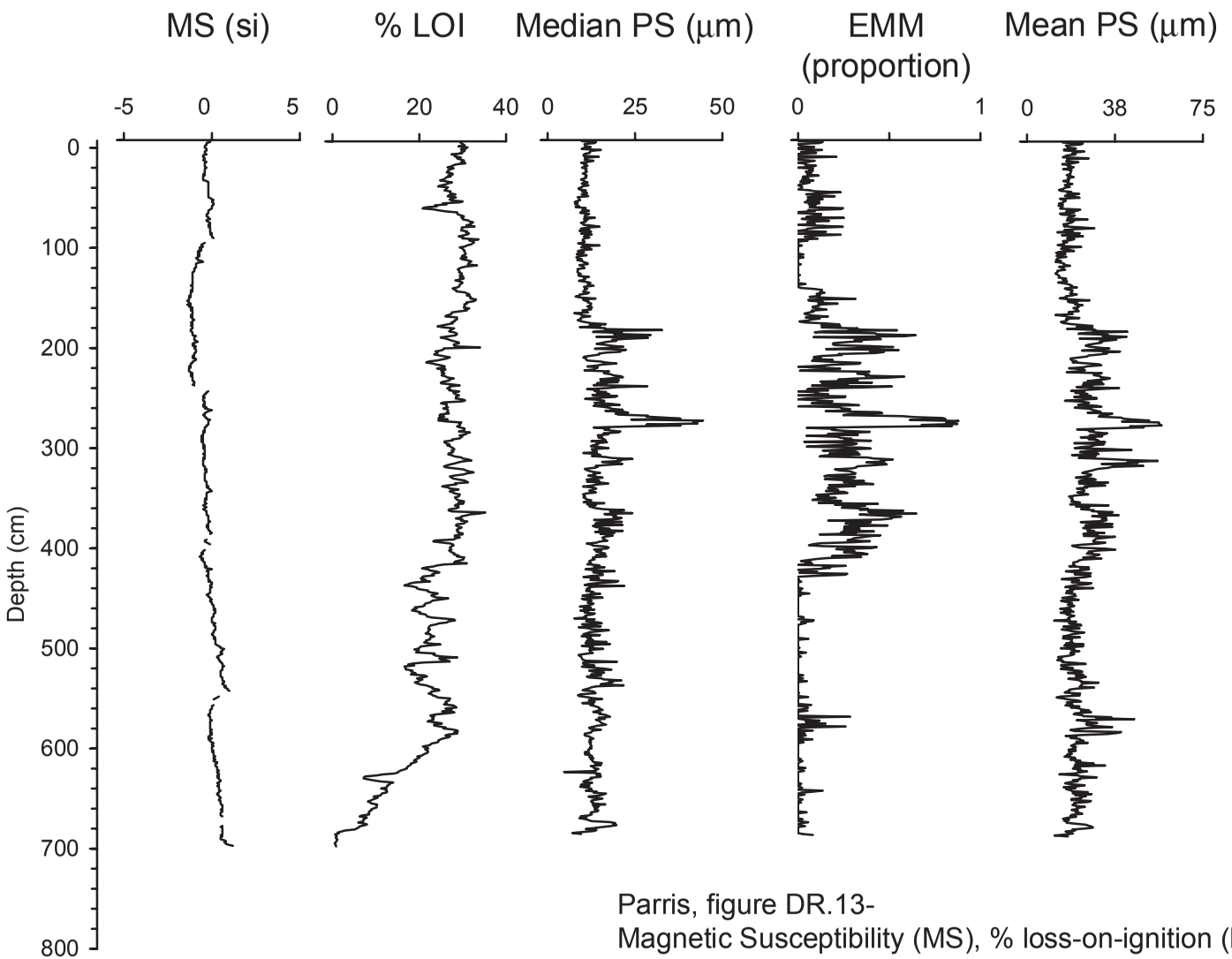

Parris, figure DR.13-
Magnetic Susceptibility (MS), % loss-on-ignition (LOI), mean and median particle size (PS), and proportion of coarsest EM results for the Crystal Lake core (CR).

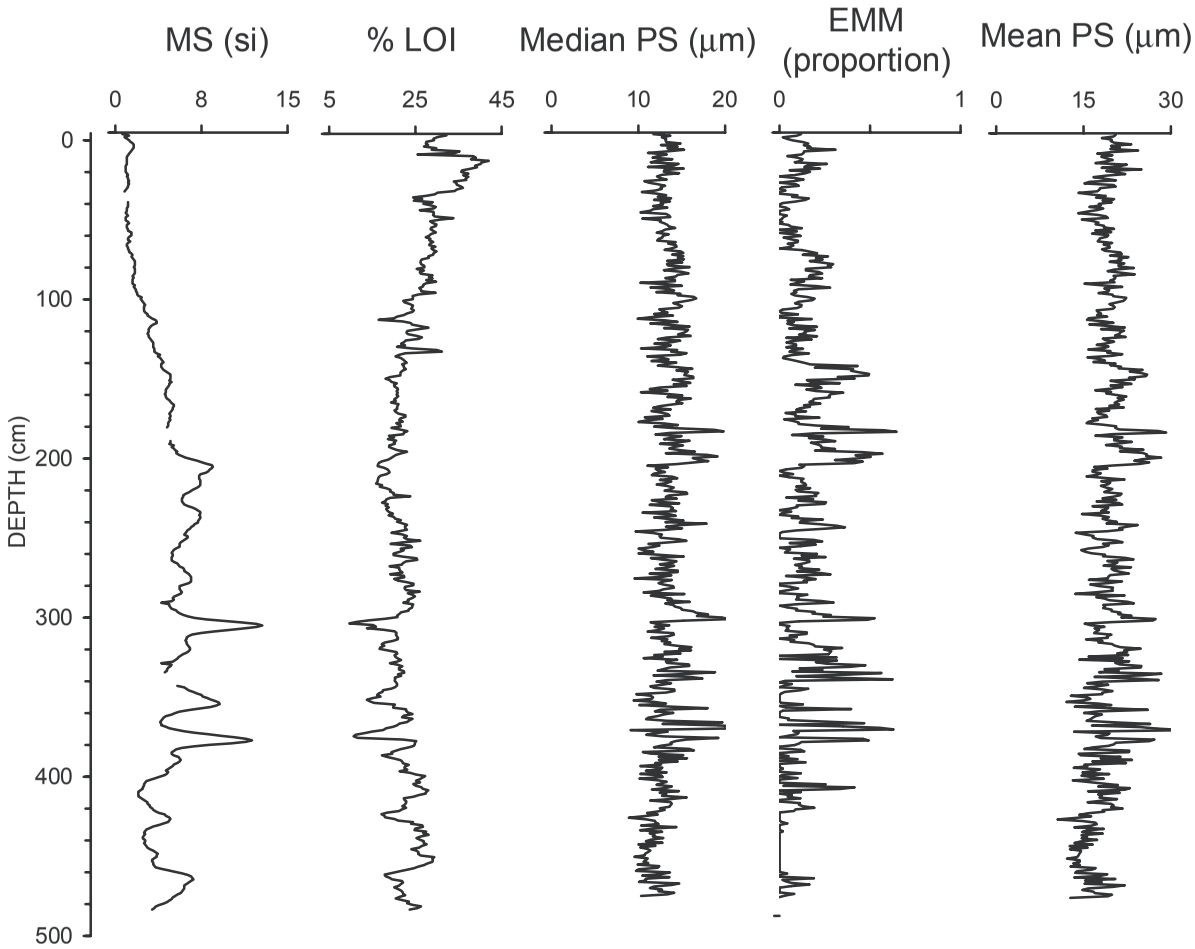

Parris, figure DR.14-
Magnetic Susceptibility (MS), % loss-on-ignition (LOI), mean and median particle size (PS), and the proportion of the coarsest EM result for the Ogontz Lake core (OG).

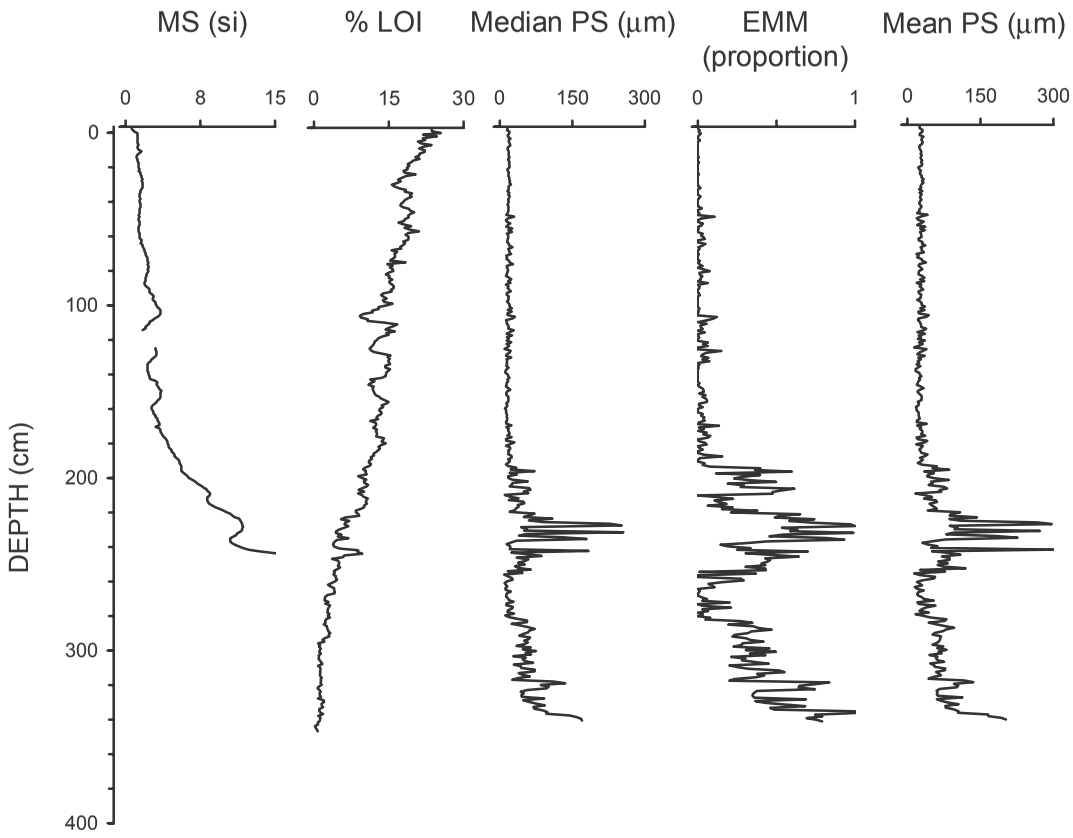

Parris, figure DR.15-
Magnetic Susceptibility (MS), % loss-on-ignition (LOI), mean and median particle size (PS), and the proportion of the coarsest EM results for the Stinson Lake core 1 (ST1).

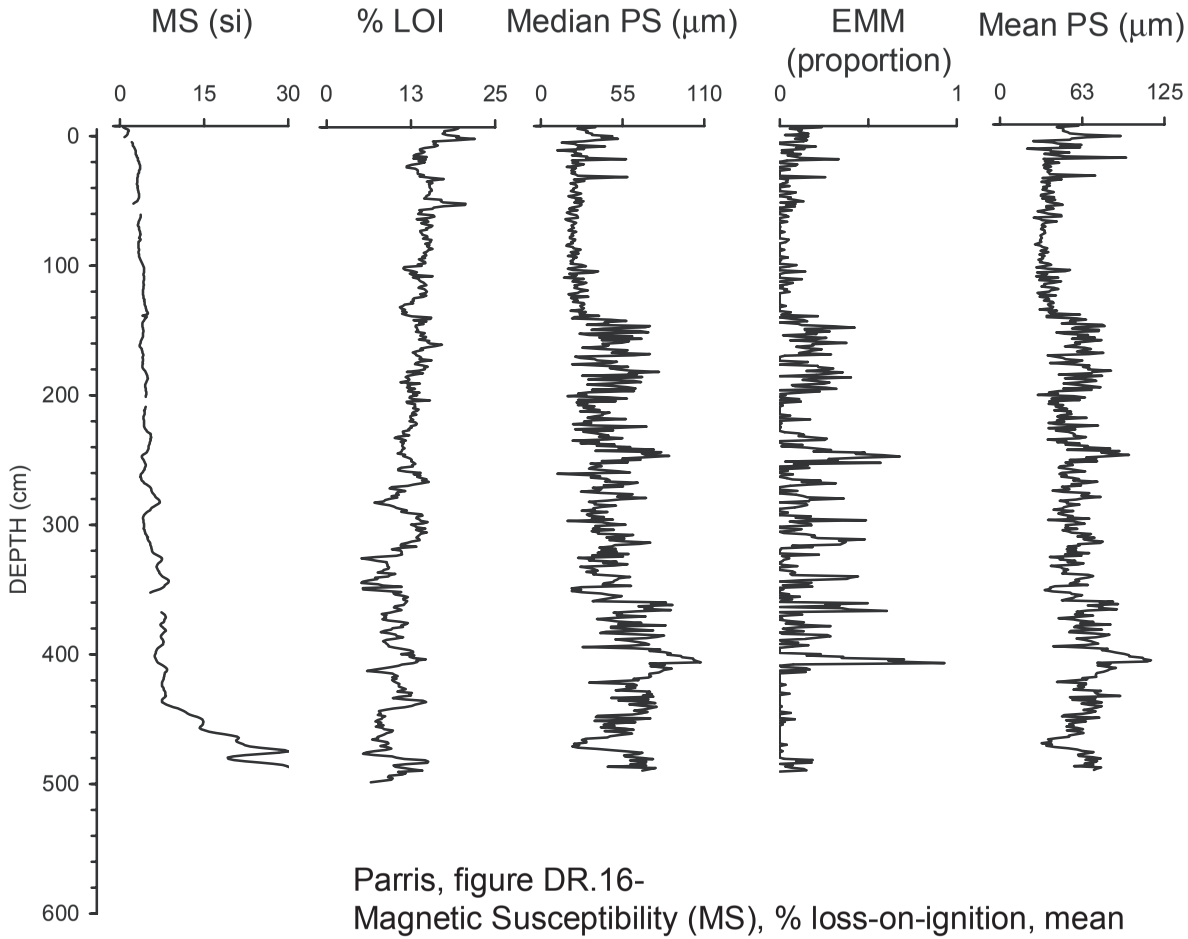

Parris, figure DR.16-
Magnetic Susceptibility (MS), % loss-on-ignition, mean and median particle size (PS), and proportion of the coarsest EM results for the Stinson Lake core (ST2).

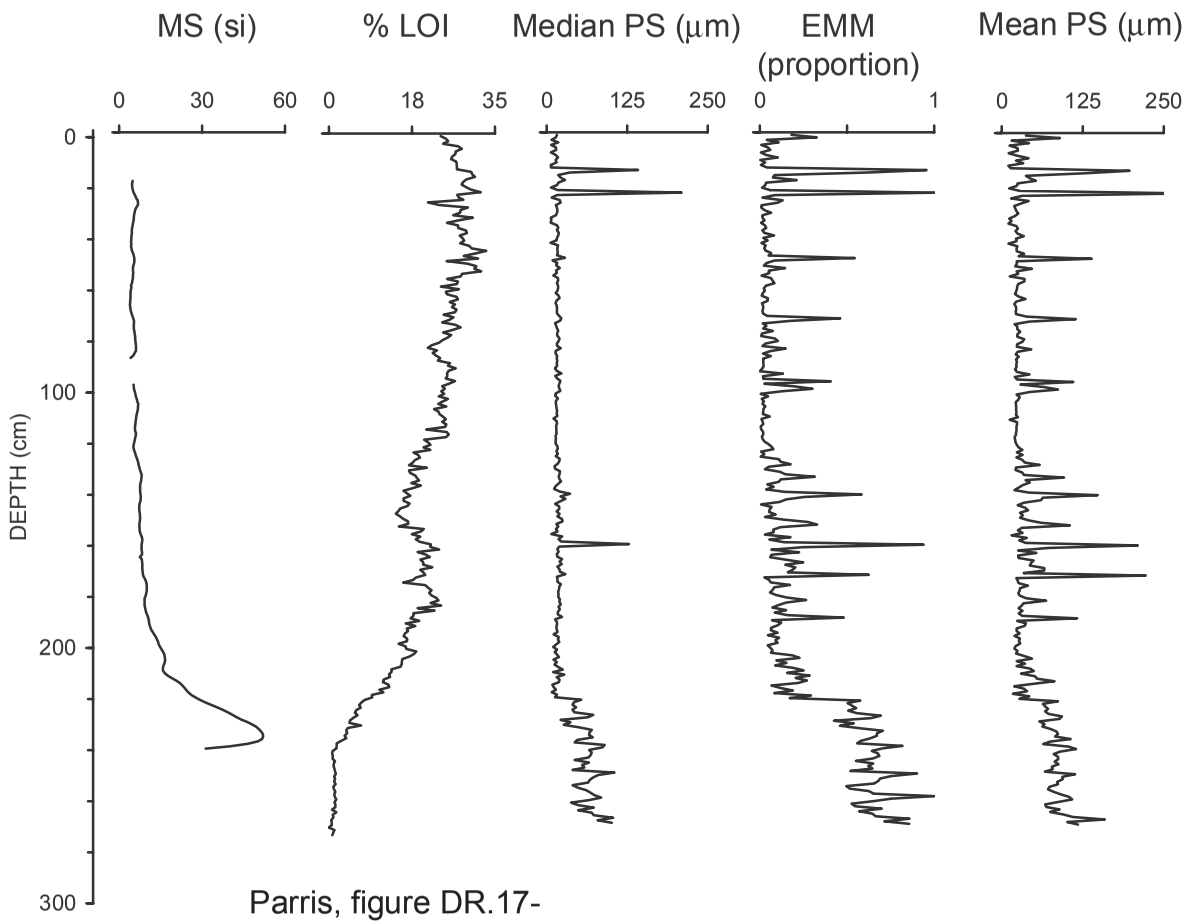

Parris, figure DR.17-
Magnetic Susceptibility (MS), % loss-on-ignition (LOI), mean and median particle size (PS), and proportion of the coarsest EM results for South Pond core 1 (SU1).

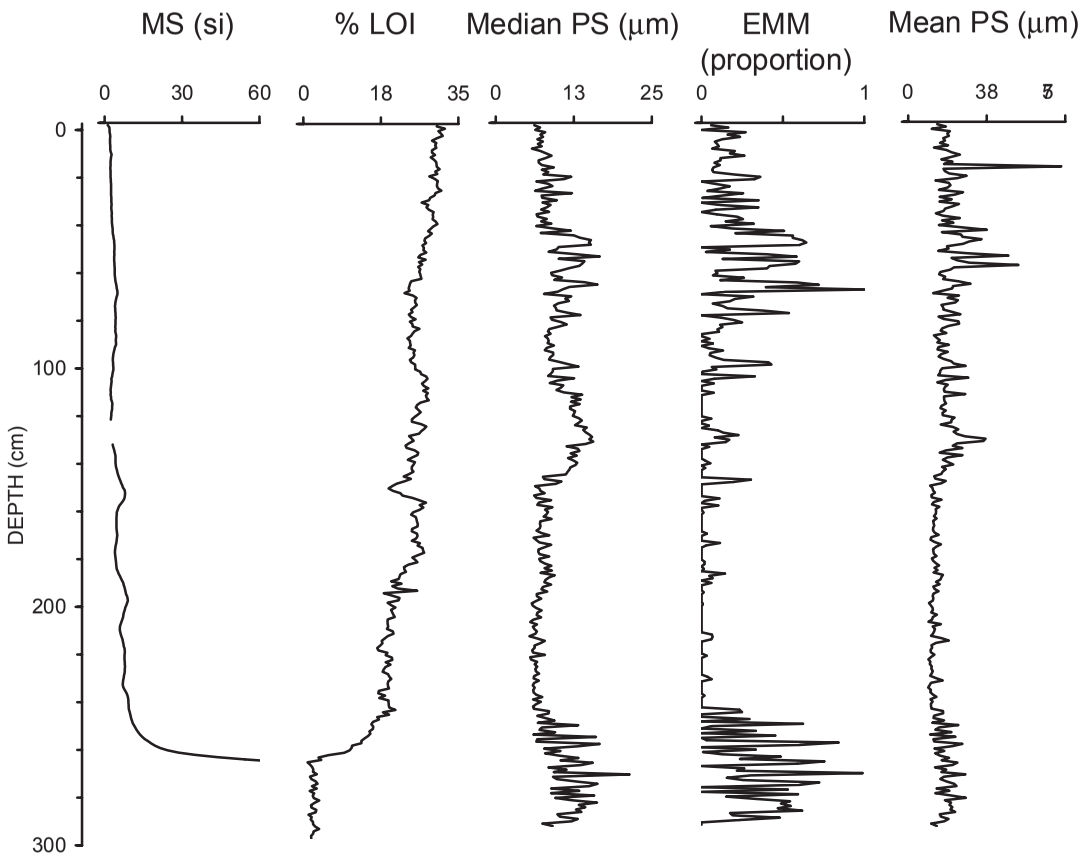

Parris, figure DR.18-
Magnetic Susceptibility (MS), % loss-on-ignition (LOI), mean and median particle size (PS), and proportion of the coarsest EM results for South Pond core 2 (SU2).

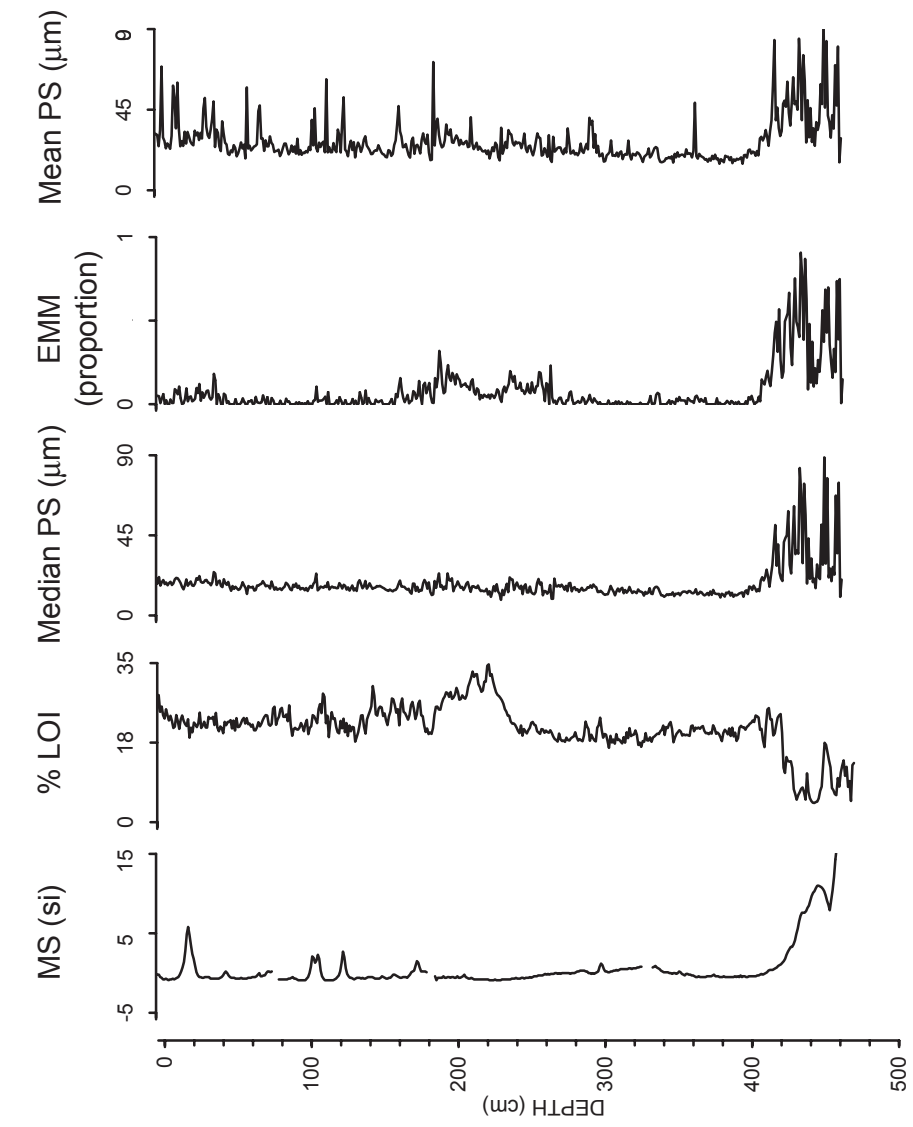

Parris, figure DR.19-
Magnetic Susceptibility (MS), % loss-on-ignition (LOI), mean and median particle size (PS), and proportion of the coarsest EM results for Sandy Pond core (SY).

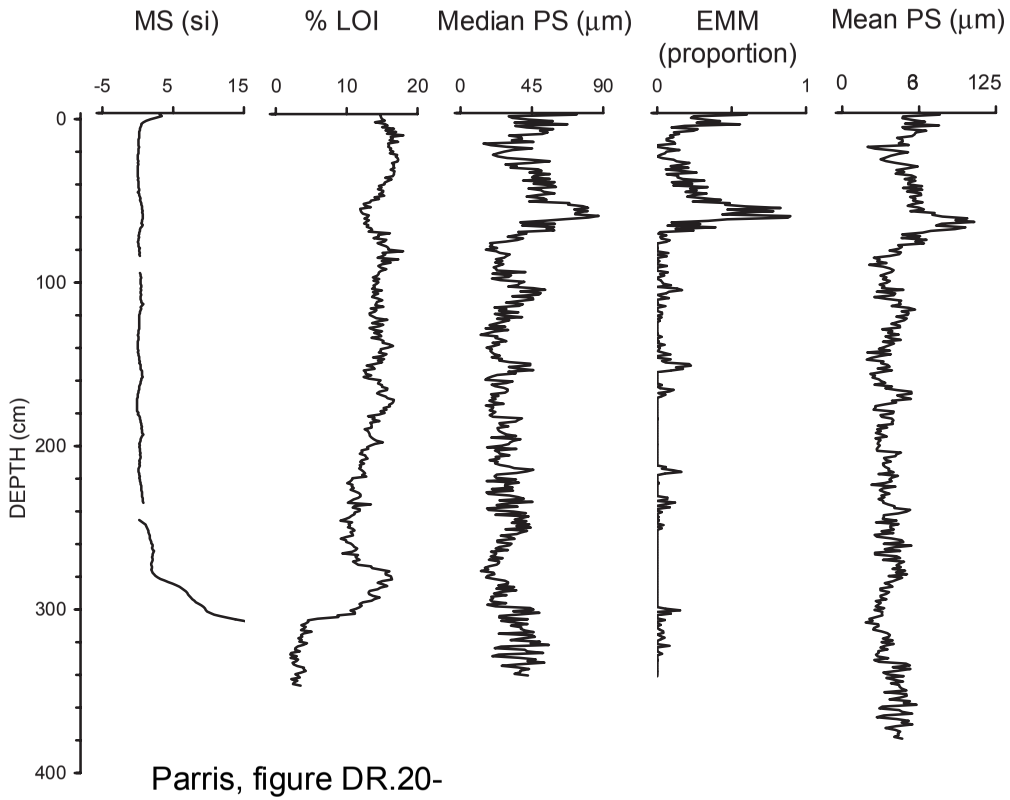

Parris, figure DR.20-
Magnetic Susceptibility (MS), % loss-on-ignition (LOI), mean and median particle size (PS), and proportion of the coarsest EM results for Worthley Pond core (WO).

CHAPTER 4

Paper for submission to *Geological Society of America Bulletin*

Particle size identification of Holocene paleofloods in the northeastern United States

Adam S. Parris† (aparris@zoo.uvm.edu), Paul R. Bierman† (pbierman@zoo.uvm.edu), Anders J. Noren†‡ (anoren@zoo.uvm.edu), Maarten Prins§ (prim@geo.vu.nl), Andrea Lini† (alini@zoo.uvm.edu)

†Geology Department
University of Vermont
Burlington, Vermont 05405 USA
(802) 656-4411 (voice)
(802) 656-0045 (fax)

‡Limnological Research Center
N.H. Winchell School of Earth Sciences
310 Pillsbury Drive SE
University of Minnesota
Minneapolis, MN 55455
(612) 626-7889 (voice)

§Faculty of Earth and Life Sciences
Department of Paleoecology and Paleoclimatology
Vrije Universiteit Amsterdam
De Boelelaan 1085
1081 HV Amsterdam The Netherlands
(+31) 020 4447327 (voice)
(+31) 020 6462457 (fax)

ABSTRACT

The frequency and timing of Holocene paleofloods in the hilly terrain of New Hampshire and Maine are identified clearly by high resolution (cm-by-cm) particle size analysis and ^{14}C analysis of sediment cores taken from six post-glacial ponds and lakes (~ 0.1- 1.4 km^2, surface area). Eight sediment cores (4.5- 6 m in length) were taken near the base of stream delta foreslopes, which contain sediment records ranging in age from historic to $\geq$ 14,500 cal yr B.P. In all eight cores, particle size data show clear signs of episodic, high energy deposition where proxy measurements such as loss-on-ignition (LOI) and magnetic susceptibility (MS) do not, emphasizing the utility of grain size analysis in paleoflood and paleostorm investigations made using lake sediment cores.

End-member modeling (EMM) of the particle size data from each core produces 3-5 representative size frequency distributions. Whole core changes in the proportion of each end-member distribution (EMD) represent changing depositional conditions. Concurrent increases in mean and median particle size, and in the relative abundance of the coarsest end-member(s), indicate episodic, increased transport capacity of inflowing tributaries (the result of rainstorms, rain on snow events, and/or snowmelt) and the resultant deposition of coarse, clastic sediment into lakes. The coarse EMDs are generally well sorted, and have modal particle sizes ranging from coarse silt to medium sand. The fine EMDs are generally poorly sorted, and have modal particle sizes ranging from fine to medium silt. The EMM results show grading of terrestrial flood layers, as well as an increase in intermediate sediment sizes over time, the result of delta progradation.

We find that flood frequency in NH and ME varied in regular cycles of ~1,300, ~600, and ~350 years. Terrestrial sediment delivery, grain size, and, by inference, flooding in this region peaked around 0.8, 1.4, 2.1, 3.0, 3.9, 6.8, 8.2, 11.5, and 13.3 cal kya, and appears to be presently increasing toward another peak. There is an increase in the number of floods that occurred after ~4,000 cal yr B.P. The timing and cyclicity of flooding are similar to the timing and recurrence interval of hurricanes inferred from salt marsh sediments sampled along the north Atlantic and Gulf of Mexico coast.

INTRODUCTION

Paleostorm and paleoflood research contribute to our understanding of long-term climate change and help define the severity and distribution of natural hazards over time frames longer than the written record (Hupp, 1988; Komar, 1988; Baker, 1988; Noren et al., 2002). Understanding the natural variability and cyclicity in such events is prerequisite to detecting changes in their frequency that may accompany the current increase in global temperatures caused, at least in part, by human emission of greenhouse gases (IPCC, 2001). Deciphering records of extreme precipitation and damaging floods preserved in geologic archives enables society to better understand and plan for floods of the future. For instance, in the heavily populated northeastern United States, historical floods caused by extreme rainstorms significantly changed the landscape and damaged infrastructure (Ludlum, 1963 & 1996). Existing paleostorm records suggest even larger floods occurred prior to European settlement of North America (Brown et al., 2000).

Paleoflood research was pioneered using slackwater deposits as a means of measuring the timing and stage of extreme flood events on rivers in the southwestern

United States (Kochel and Baker, 1982). Since then, geomorphologists have deciphered other paleohydrologic archives including floodplain deposits, as well as alluvial, debris, and overwash fans (Brakenridge, 1980; Bull, 1991; Bierman et al., 1997; Knox, 1999; Nott et al., 2001; Jennings et al., 2003). Such research extends short-duration, modern hydrologic records to longer temporal scales, providing a better indication of the natural patterns of extreme events prior to human impact on climate or the landscape. For example, prehistoric paleoflood records from mid-western North America suggest rapid changes in flood patterns in response to climate change through the Holocene (Knox, 1993; Knox, 2000); similar records from western North America detail the frequency of the El Nino-Southern Oscillation (ENSO) before modern times (Ely et al., 1993).

During exceptional floods, competent streams deposit terrestrial sediment into lakes interrupting the accumulation of fine-grained sediment (Page et al., 1994; Bierman et al., 1997; Rodbell et al., 1999; Brown et al., 2000; Lamoreaux, 2000; Nesje et al., 2001; Brown et al., 2002). Coarse, light colored, inorganic sediment layers observed and identified in lake sediment cores are interpreted as the result of increases in stream velocity and discharge linked temporally to major historical precipitation events (Page et al., 1994; Campbell, 1998; Thorndycraft et al., 1998; Lamoreaux, 2000; Nesje et al., 2001; Ambers, 2001). Terrestrial sediment layers in lake sediment cores have been used to construct paleostorm chronologies around the world including the United States, Europe, and New Zealand (Eden and Page, 1998; Rodbell et al., 1999; Brown et al., 2000; Lamoreaux, 2000; Nesje et al., 2001; Noren et al., 2002).

Regional periods of increased storminess (ca. 2.5, 6, 9 cal kya) in New England were identified by an increase in terrestrial sediment deposition identified in four sediment cores taken from Ritterbush Pond, in northern Vermont (Bierman et al., 1997; Brown et al., 2000 and 2002) and verified by dating contemporaneous periods of increased alluvial fan aggradation (Jennings et al., 2003). Periods of storminess (ca. 2.6, 5.8, 9.1, 11.9 cal kya) were identified from 13 lake sediment cores taken throughout Vermont and eastern New York (Noren et al., 2002). Frequency analysis of terrestrial flood layers in Noren et al.'s cores revealed 3000 year cycles of storms in this region throughout the Holocene, correlating with the period and phase of the GISP2 time series of aerosol deposition and with cooler temperatures in Europe.

Deciphering the history of extreme hydrologic events from the characteristics of lake sediment remains a new and somewhat uncertain endeavor. Only a few studies have used particle size analysis to identify and characterize coarse-grained, terrestrial flood layers in freshwater lake sediments (Campbell, 1998; Campbell et al., 1998; Brown et al., 2000; Beierle, 2002). Most paleohydrologic interpretations rely on proxy measurements, such as loss-on-ignition (LOI), to identify periods of increased terrestrial sediment transport into lakes indicating increased runoff events. Yet, as a direct indicator of the sediment transport capacity of inflowing tributaries, particle size analysis seems the ideal analytical method for identifying the physical landscape response to extreme hydrologic events (Campbell, 1998). Paleo-oceangraphic and paleoclimatic studies of marine cores widely employ particle size analysis to detect coarse-grained, terrestrial sediment layers, high-energy depositional events indicative of flooding caused, in some cases, by

increased precipitation (Brown et al., 1999; Prins et al., 2000; Syvitski et al., 1999; Drake, 1999).

Changes in depositional conditions are usually inferred from general, down-core statistics such as mean and median particle size (Beierle, 2002). Folk and Ward (1957) illustrated the need to characterize particle-size distributions on the basis of depositional process, but noted the difficulty in achieving this goal due to mixing of different sizes during deposition. Particle size samples often produce polymodal size distributions with separate modes indicating a large volume of both fine and coarse particles. For instance, particle size analysis of a lake sediment core from Alberta, Canada, suggests that, at any given core depth, terrestrial sediment is a combination of many particle sizes, all of which indicate different depositional conditions (Campbell, 1998). A wide variety of statistical methods have been employed to "unmix" such samples into representative particle sizes or distributions so as to better define depositional processes (for summaries see Syvitski, 1991; Prins & Weltje, 1999).

Recently, end member modeling (EMM) was developed to interpret particle size distributions based on depositional processes (Weltje, 1997; Prins et al., 1999, 2002). EMM utilizes all the particle size distributions from a core to create discrete end-member distributions (EMDs) (Weltje, 1997; Prins et al., 1999, 2002). Each sample can then be defined as the weighted sum of multiple EMDs. Changes in the relative contribution of each EMD down each core indicate changes in depositional conditions.

In this study, we present a regional paleoflood record for six freshwater lakes in New Hampshire and one in western Maine, based primarily on high resolution (cm by

cm) analysis of siliclastic grain size in ~3,500 sediment samples taken from 8 cores (Figure 1, Table 1). We find that high resolution grain size analysis is a more sensitive and direct method of identifying terrestrial flood layers in freshwater lake sediments than other commonly employed analytical techniques. Such sensitivity allows identification of previously unrecognized paleohydrologic events, which increases the resolution of paleoflood frequency analysis. End-member modeling of particle size data (Weltje, 1997; Prins et al., 1999) allows us to interpret particle size distributions in terms of depositional process, including high energy flood events, and to speculate about temporal connections between our data and the record of paleohurricanes along the Atlantic coast.

[1]FIELD METHODS & LAKE SETTING

A total of 9 cores (~4.5- 6 m long) were collected from the 6 study lakes using a modified Reasoner percussion piston coring device without a core catcher (Reasoner, 1993; Brown et al., 2002; Figure 1 and Table 1). Two of these cores (CR 1 & CR 2) were taken from the same location and combined to form one sediment record[1], hereafter referred to as CR. Cores were cut into 1.5 m sections in the field, and then stored at 4^{o}C. The topmost 2-62 centimeters of the sediment record is not captured by the Reasoner device because the piston does not immediately begin to move up the core as it is pounded into the sediment and because it is difficult to judge accurately the depth of the sediment-water interface. Field reconnaissance for all six of the study lakes was performed in the summer and fall of 2001.

[1] GSA Data Repository item XXXXX data showing the match between CR & CR2, using Magnetic Susceptibility, loss-on-ignition, particle size, and ^{14}C data, and a detailed explanation of Field and Lab methods.

While the lakes all have similar geomorphic characteristics, they vary in size and extent (Table 1). All of the lakes in this study are relatively small (0.1- 1.4 km^2), but of variable depth (~12- 28 m). Drainage basin areas also vary (~1- 23 km^2); relief ranges from 226 to 655 m. Although it is the smallest, most shallow lake with the lowest relief, Sandy Pond (SY) drains a steep catchement as reflected by a relief ratio (drainage basin relief/drainage basin area) of 205 m/km^2, which is larger than those of the remaining lakes, 17- 58 m/km^2. Stinson Lake (ST), the largest lake (1.4 km^2) with the biggest basin (23 km^2) and the highest relief (655 m), lies at the highest elevation of ~396 m, whereas Crystal Lake (CR) lies at the lowest elevation, ~146 m.

The study area is bordered to the north by South Pond (SU), and to the south by Sandy Pond (SY), which is also the westernmost lake (Figure 1). The two eastern lakes, Crystal Lake (CR) and Worthley Pond (WO), are both only ~65 km from the Atlantic Ocean. In contrast to previous paleostorm records inferred from lake sediment in New York and Vermont (Brown et al., 2000; Noren et al., 2002), the lakes in this study are much closer to the North Atlantic coast, and thus, the path of many more tropical storms and nor'easters (Boose et al., 2001; Donnelly et al., 2001).

Lakes in this study have low aquatic productivity (Lord, 2002), and thus, they differ from those previously studied in Vermont and New York (Brown, 2000; Noren, 2002). The bedrock in all the basins is granite or granodiorite except for Crystal Lake (CR) and Ogontz Lake (OG) which have metamorphic bedrock in the basins (quartzite and schist, respectively). All of the basins are covered by thick surficial deposits, comprised mostly of glacial till, but also fluvio-glacial deposits, and by a mixture of

deciduous and coniferous forest. At least one competent stream flows down each high relief basin, incising surficial material and, in some cases, exposing bedrock in the channel.

These streams deposit abundant sand and gravel on the lake margin and create sandy deltas (Brown et al., 2000; Noren et al., 2002). Observations of these streams made during reconnaissance of each lake in the summer and fall of 2001 suggest that each stream changes abruptly from a transport-limited, fine-grained channel at the lake margin to a supply-limited, coarse-grained channel higher in the basin. These observations suggest that coarse grains are transported to the lake margin, and then, as Brown (2000) suggested, the terrestrial sediment layers are formed as sand on or near the lake margin is eroded and deposited in the lake during floods. During reconnaissance of the Crystal Lake (CR) basin, a thunderstorm dropped significant amounts of rain (~2.5 cm) in 30- 45 minutes, and signs of bank and bed scour were evident at the mouth of the channel on the lake margin.

LAB METHODS

Using a Bartington Magnetic Susceptibility Meter (model MS2) mounted on an automated track, we measured MS at 1 cm intervals soon after returning each core to the lab. Each core section was then split, and half of each section was retained as an archive. The other half was photographed immediately with a high-resolution digital camera. To construct a visual log, we examined the cores at 0.5 cm resolution for changes in color, texture, and the abundance and location of terrestrial macrofossils. We sampled the cores at 1 cm intervals, collecting macrofossils wherever present. All samples were freeze dried

for at least 48 hours. LOI was performed by combusting ~250 mg of each sample at 450^0C for ~2.5 hours.

Dates were obtained for 80 individual macrofossils (~8- 10 per core) using accelerator mass spectrometeric (AMS) analysis of radiocarbon (^{14}C) at Lawrence Livermore National Laboratory (Table 2). Samples were prepared using standard techniques and calibrated using CALIB v4.2 (Stuiver and Reimer, 1993; Stuiver et al., 1998). Single calibrated ages were determined in the same fashion as Noren et al. (2002).

Inorganic grain size samples were prepared for laser diffraction using a three-treatment technique [1]. First, we used 30% H_2O_2 to remove organic sediment from each 300 mg sample. The samples were then treated with 10 mL of 1M NaOH to remove biogenic silica. Both of these treatments took place while the samples were in a sonicating hot bath (70^oC). Finally, several mL of dispersant (25 g of sodium metaphosphate dissolved in 500 mL of de-ionized water) were added to each sample. Grain size analysis was performed on a Coulter LS 230 small volume module at Middlebury College. A 50 cm section of the Ogontz Lake core (OG) was replicated to test reproducibility in our preparation techniques (Data Repository Figure DR.9), and a 35 μm garnet powder standard obtained from Coulter was run before each use of the laser diffraction unit (Figure DR10).

DATA ANALYSIS

End member modeling

The EMM utilizes an inversion algorithm applied separately to each particle-size distribution from each core to create a set of estimated output values (% volume) for each

size class in a distribution (samples per core= 275-718; Weltje, 1997). These values are used to form the representative, end-member size frequency distributions (EMDs), which together are used to de-convolve polymodal, particle size distributions measured for each sample. The number of end-members created by the algorithm must be chosen in advance based on goodness-of-fit statistics (coefficient of determination, r^2) between the input and the output values for each size class (Prins and Weltje, 1999; Prins et al., 2002). The goal of this choice is to minimize the number of EMDs needed to model the data set without simply recreating it (Weltje, 1997).

The EMM of the SU1 core is explained here to illustrate the selection of the number of end-members for each core. Goodness-of-fit statistics (median r^2 values) across individual size classes for different numbers of end-members suggest that two size ranges (15-84 μm, ≥213 μm) are poorly reproduced by a two end member model (Figure 3A). The range ≥213 μm is not considered important for most cores because this size range represents a very small portion of the mass of the samples. However, the finer size range (15- 84 μm) is considered much more important because it comprises a large portion of the mass of the sample. Median coefficients of determination across particle sizes increase as the number of end members used in the model increase (Figure 3B). The median coefficient of determination for a five-end-member model of the SU1 core is 0.96, i.e. 96% of the variance in each particle size class is reproduced. Goodness-of-fit statistics (r^2) statistics do not improve drastically if more EMDs are used in the de-convolution. Therefore, a five-end-member model is the optimal choice (Figure 3C and 3D).

We used the relative proportion of the coarsest EMDs down core to examine trends in high energy terrestrial sediment deposition through the Holocene (Table 3). We used only those coarse EMDs with median proportions < 0.2 (or 20%) in the whole core for this method. Thus, for the SU1 and ST1 core, we summed the relative proportion of the two coarsest EMDs. Sediment described by intermediate EMDs with a median abundance of > 0.2 is considered to be the result of normal depositional conditions and sediment sources.

Time Series Filter

Significant peaks in the down-core abundance of the coarsest end-member(s), as well as mean and median particle size, were identified by filtering the data with singular spectrum analysis (SSA, Broomhead and King, 1986; Vautard and Ghil, 1989), using a 20-point window to identify the first principal component. The linear trend of this filter was removed and added back to the mean of the original data set to define the background. We examined peaks greater than one or two standard deviation(s) from this background in order to determine paleohydrologic events (Table 4 and Figure 8). For the LOI records, we performed the same analysis using one or two standard deviation(s) greater and less than the background to identify significant troughs, as well as peaks, which were found, in the visual stratigraphic log, to occur along the same depth as large macrofossils in coarse, terrestrial sediment layers.

Age Modeling

Because the terrestrial flood layers are deposited rapidly and the remaining parts of each core result from slow deposition of fine-grained material (Bierman et al., 1997),

we mathematically compress the composite sediment record by removing the rapidly deposited terrestrial flood layers from the stratigraphy (Brown et al., 2000; Noren, 2002; Noren et al., 2002; Brown et al., 2002). This systematic compression removed from ~4 to 19 percent of the core sediment. Non-inverted ^{14}C ages were used to construct age models for each core, for which we assumed linear sedimentation rates between successive ages. Comparing these age models to the compressed core stratigraphy yields age estimates for each inferred terrestrial flood layer in each core. The age estimates for terrestrial flood layers found in individual cores taken adjacent to different deltas in the same lake (ST1 and ST2 (Stinson Lake); SU1 and SU2 (South Pond)) were combined into individual histograms for each core to compare hydrologic events within the basin (Figure 8A). Regional flood frequency was analyzed by combining all flood ages from all cores into a single histogram (Figure 8B). Each 100 year bin of the summary histogram is weighted for the number of sediment records that span that time interval.

Spectral Analysis

We used spectral analysis to determine whether significant periodicities exist in our data. Using the Analyseries v 1.2 (Paillard et al., 1996) and SSA-MTM Toolkit v4.1 (Mann and Lees, 1996) software packages, we removed the linear trend of the frequency time series and analyzed the data with the multitaper, Blackman-Tukey, and maximum entropy methods (c.f., Noren et al., 2002). We performed these analyses on our data interpolated to several intervals ranging from 50 to 200 years, all with similar results (Table 5 and Figure 10).

RESULTS

Magnetic Susceptibility

Magnetic Susceptibility (MS) provided rapid evaluation of the cores by confirming the presence of only the most significant terrestrial sediment layers. However, the MS2 integrates measurements over ~5 cm intervals, and therefore, MS records are low resolution (Figure DR.4). Median MS values for the cores ranged from -0.40- 119.6 (SI units). Slightly negative values of MS were obtained for cores CR, SY, and WO. We attribute those values to instrument error where sediments contained no appreciable magnetic mineral content. In several cases (CR, ST1, ST2, SU1, SU2, WO), the bottom of the cores contained long (~1-1.5 m) sections of inorganic sediment with exceptionally high MS values (~100- 350 SI units). These sections contained inorganic rhythmites with alternating layers of gray clay and sand or silt. Peaks in MS in these sections correspond to sand and silt layers (~2- 10 cm thick), and troughs indicate more clay-rich layers of sediment. We restrict our paleoflood analysis of the sediment cores to the gyttja-dominated sections, where coarser grained, terrestrial sediment layers can be interpreted more confidently as the result of floods. A sharp decrease in MS marks the transition between inorganic sediment low in the core and organic-rich mud (gytta). Gyttja-dominated, upper sections of the core have much lower MS values (~0- 15 SI), and contain few significant peaks indicative of terrestrial sediment layers (Figure DR4).

Loss-on-ignition

Whole core median LOI values range from 12.5- 25.6 % illustrating the oligotrophic nature of these lakes (Figure 4). LOI values gradually increase from 0- 2 %

in the early-Holocene core bottoms to ~ 15- 35 % at the top of the cores. Because cores in this study contain a lower percentage of organic material than cores taken from lakes in Vermont and New York (Brown et al., 2000; Noren et al., 2002), sharp troughs in LOI, indicative of terrestrial flood layers, are not as pronounced. These troughs are difficult to distinguish from the varying baseline of LOI values down depth in the cores, and illustrate the difficulty of using LOI as a means of detecting terrestrial flood layers. Sharp peaks in LOI occur along the same depths as large or abundant macrofossils found in the visual stratigraphic log, and are often surrounded by coarse-grained, terrestrial sediment. Baseline LOI values of 0- 1 % correlate with sections of the core containing gray, inorganic rhythmites identified in the visual log and by MS. Gradual, and sometimes pronounced increases in LOI from these low baselines correspond to depths with diffuse or sharp stratigraphic boundaries between brown, organic-rich mud and the gray rhythmites. These boundaries indicate the onset of primary productivity in the lakes and the establishment of ecosystems in these basins (Lord, 2002). Because ecosystem establishment signifies more stable, vegetated hillslopes, these boundaries also provide useful markers to determine the depth above which we interpret terrestrial sediment layers as the result of floods.

Radiocarbon Dating

Radiocarbon dates for 80 terrestrial macrofossils vary from 845 to 12,345 ^{14}C years (Table 2). Radiocarbon uncertainties range from 35 to 330 ^{14}C years, with a median of 45 ^{14}C years. Median calibrated ^{14}C age uncertainty is ± 240 years, and varies from ± 15 to ± 730 years. In some of the study lakes (CR, ST2, SU1, SY, WO), the topmost

radiocarbon date indicated that the assumed linear sedimentation rate would not extrapolate to modern [1]. In age modeling of these cores, we used only the sediment record below the depth of the topmost radiocarbon age.

Particle Size Records

All of the cores are comprised dominantly of fine-grained material with a mean for all cores of 14 % sand, 69 % silt and 17% clay (Table 3 and Figure 5). Four cores (ST1, ST2, SU1, WO) contain more abundant coarse sediment, $\geq$ 17 % sand (Table 3). The remaining cores (CR, OG, SU2, SY) contain less coarse sediment, $\leq$ 8 % sand (Table 3). Fine-grained sediment samples generally have unimodal size distributions (Figure 6). Coarser layers, interpreted as terrestrially derived flood sediment, are comprised of both poorly-sorted and well-sorted coarse sediments with polymodal and unimodal distributions (Figure 6).

Traditional summary statistics (mean, median, mode, skewness, kurtosis, standard deviation) do not describe polymodal size distributions well (Beierle, 2002). We find terrestrial sediment layers with poor sorting and polymodal size distributions are most clearly identified by increases in mean particle size and standard deviation, less so by median particle size, and poorly by mode, skewness, or kurtosis (Figures 5 & 6A). Although some trends in mode, skewness, and kurtosis are related to the presence of terrestrial sediment layers, these statistics are not directly related to an increase in volume of coarse particles (Figure 6A). Particle size statistics most related to terrestrial sediment inputs in marine and lacustrine sediment cores are mean and median (Campbell, 1998;

Brown et al., 1999; Brown et al., 2000; Beierle, 2002). Of those two, coarse terrestrial sediment is most clearly identified by mean particle size in our cores.

Mean particle size maxima are on average 33 μm greater than median particle size maxima, and are sometimes present where median particle size maxima are not (Figure 5). The coarsest maxima for mean and median particle size records (301 and 255 μm, respectively) were both in the ST1 core. The finest maximum in the mean particle size record (32 μm) was in the OG core, whereas the finest maximum in the median particle size record (21 μm) was in the SU2 core. Mean particle size varies by an average 27 μm in the coarsest cores (ST1, ST2, SU1, WO) and by an average 7 μm in the finest cores (CR, OG, SU2, SY). ST2 is the coarsest core overall with a whole-core mean particle size of 54 μm and a whole core median particle size of 43 μm. SU2 is the finest core overall with a whole-core mean particle size of 17 μm and a whole-core median particle size of 9 μm. An overall increase in mean and median grain size occurs near the bottom of some cores (ST1, SU1, SU2), marking the transition from organic-rich mud to inorganic rhythmites with a coarse matrix (Figure 5). These transitions occur at similar depths as increases in MS and decreases in LOI, which mark the same stratigraphic boundaries.

End Member Model Distributions

The r^2 statistics indicate that the sediments in this study are adequately described as mixtures of three to five end-member distributions (EMDs) all of which are unimodal (Table 3 & Figure 3). In the SU1 core for example, the particle size distribution of end member 1 (EMD1) is somewhat poorly sorted with a dominant mode of ~373 μm (medium sand) (Figure 3C). The second end-member (EMD2) is fairly well sorted with a

dominant mode of 122 μm (very fine sand), and the third end-member (EMD3) is somewhat poorly sorted with a mode of 53 μm (coarse silt) (Figure 3C). EMD 4 displays the best sorting and has a mode of 19 μm (medium silt) (Figure 3C). EMD5 is poorly sorted with a mode of 6 μm (very fine silt) (Figure 3C).

Cores with a high, overall volume of sand (ST1, ST2, SU1, WO) are modeled using four or five EMDs; cores with a lower overall volume of sand (CR, OG, SU2, SY) are modeled using three EMDs (Table 3). All of the cores have one or two coarse EMDs with modes ranging from 40 μm (coarse silt) to 373 μm (medium sand), and a fine EMD with modes ranging from 6 μm (very fine silt) to 26 μm (medium silt) (Table 3). Intermediate EMDs have modes between the two extremes.

Because the mode of each EMD represents the dominant particle size, the median proportions of each EMD for an entire core reflects the amount of sediment in that size range (Table 3). High median proportions show that the finest and intermediate EMDs represent the dominant particle sizes in the cores (Table 3). Similar to the whole core mean and median particle size records, median proportions of all EMDs show that ST2 is the coarsest core overall and that SU2 is the finest core overall.

Discreet peaks in the proportion of the coarsest EMD(s) identify coarse-grained layers in all of the cores (Figure 6 &7). In the SU1 and SY cores, the proportion of the intermediate EMDs gradually increase from the early Holocene at the bottom of the core to the late Holocene at the top, whereas the finest EMDs decrease slightly in proportion over the same interval likely the result of delta progradation (Figure 3). Increases in the proportion of the coarsest EMD(s) of the ST1, SU1, and SU2 cores coincide with

increases in mean and median particle size, MS, and LOI, delineating the boundary between overlying organic mud and inorganic, basal rhythmites with a coarse matrix (Figure 7).

DISCUSSION

Holocene floods, caused either by storms or rain-on-snow events, in tributaries flowing in lake basins in New Hampshire and Maine, produce a physical sedimentological response that is detected in the sediment record more clearly by particle size analysis than by other more, traditional proxy analyses. In the basins we studied, hydrologic events occurred from 13,340 cal yr BP until the present day, and are detected more frequently by the particle size records than LOI records. Climatic trends inferred from the particle size records are consistent with dated geomorphic records of hurricane landfalls on the Atlantic and Gulf of Mexico coast, but do not show strong cycles of storminess, such as those inferred from previous studies of lake sediment in New England (Brown et al., 2000; Noren et al., 2002).

Interpreting the particle size record

Particle size, as interpreted by traditional statistics and by end-member models, may be related to two different sedimentological processes: 1. mixing of sediment, which is transported by different mechanisms and/or supplied from different sources; or 2. selective sorting during unidirectional transport and deposition, producing sediments whose particle size changes systematically with distance from a common source (Prins et al., 2000). Previous researchers have shown that terrestrial sediment layers in lake sediment cores increase in thickness and in particle size with proximity to the delta, in

this case, the terrestrial sediment source (Eden and Page, 1998; Brown, 2000; Brown et al., 2000; Bosley et al., 2001; Parris et al., 2001).

The mode, sorting, and proportion of the EMDs in two cores taken near two different deltas in South Pond reflect a similar sediment source, varying distance from their respective delta, and the physical transport capacity of the inflowing tributaries feeding each delta. SU1 was collected in shallower water than SU2, and SU1 was collected directly on the toeslope, nearer to the foreslope, of its respective delta (Figure 2). Similarity between the mode and sorting of fine and intermediate EMDs in both of the South Pond cores (SU1, SU2) suggest a common sediment source for both cores. The fine EMDs (SU2= EMD3, SU1= EMD5) in both cores are almost identical in mode and sorting, and one intermediate EMD in SU1 (EMD2) and the intermediate EMD in SU2 (EMD2) are also nearly identical in mode and sorting. The volume of sand, number of EMDs, and the mode of the coarse EMDs are all greater in the SU1 core (Table 3), and the thickest of the terrestrial sediment layers was higher in SU1 (8 cm) than SU2 (5 cm).

Grading of terrestrial sediment layers in cores from Ritterbush Pond, in northern Vermont, and in turbidite deposits in cores from the Makran continental slope suggest selective sorting of sediment during deposition by a decelerating current of denser, sediment-laden river water in less dense lake water (Brown et al., 2000; Prins et al., 2000). Such grading of the coarse-grained terrestrial sediment layers in both South Pond cores is evident as sharp peaks in the proportion of the coarsest EMDs are followed by a gradual decrease in the proportion of the intermediate EMD from the bottom of each layer to the top (Figure 6B, 6C, 6D). Grading is identified less clearly in traditional

particle size statistics such as mean, median, standard deviation, skewness, and kurtosis and not at all in the visual stratigraphic log (Figure 6A), which emphasizes the benefit of using the EMM approach. The depositional mechanism need not be a turbidity current, but may be a density current which still undergoes selective suspension fallout during emplacement (Boggs, 1995).

Increased mode and proportion of the coarse EMDs, then, should reflect increases in the transport capacity of the inflowing tributaries, and therefore, hydrologic events. Such increases also can reflect different processes: wave erosion at the lake margin; slumping of lake marginal or delta foreset sediment to deeper water; or increased proximity to sediment source due to lake level lowering (Campbell, 1998). Wave erosion is considered a minimal influence on the amount coarse particles in small, deep lakes with weak inlet streams, and therefore, fewer within-lake currents (Campbell, 1998). Slumping and subsequent deposition of coarse sediment from shallow to deep water produces clearly identifiable turbidites or coarse packages of sediment (Campbell, 1998). Examination of the visual stratigraphy in our cores did not reveal such clearly identifiable units in the sections dominated by organic rich mud, and lake level is considered a minimal influence in open lakes in humid climates where perimeter bathymetry is steep and where the level is controlled by an outlet sill (Campbell et al., 1994; Campbell, 1998; Brown et al., 2000; Noren et al., 2002).

Overall, our cores display slow sedimentation rates, and ^{14}C analysis of terrestrial sediment layers suggest rapid, episodic deposition (Bierman et al., 1997; Brown et al., 2000). Therefore, we suggest that the density currents which deposited the terrestrial

sediment layers in our cores were caused by an increase in the physical sediment transport capacity of inflowing tributaries, owing to increases in stream velocity and discharge. Sharp, distinct peaks in the proportion of the coarsest EMDs reflect such hydrologic events. Previous paleostorm studies using lake sediment cores from New England suggest that such hydrologic events are dominantly caused by storms (including rain-on-snow), as opposed to earthquakes, blight or disease of vegetation, or wildfires, all of which can cause increased terrestrial sediment deposition into lakes (Bierman et al., 1997; Brown et al., 2000; Brown et al., 2002; Noren et al., 2002). Studies of lake sediment cores from the Canadian Arctic suggest that snowmelt floods do not transport enough sediment to produce significant terrestrial sediment layers (Lamoreaux, 2000).

Campbell (1998) postulated that an increase in transport capacity caused deposition of coarse particles in Pine Lake (Alberta, Canada) which has physical characteristics similar to our lakes. She suggested that the strength of the particle size record as a paleoclimate signal is dependent on the noise produced by the strength or the influence of other processes. The latter suggestion further demonstrates the benefit of the EMM, as it can "unmix" sediment populations and thus reduce noise associated with other processes, such as delta progradation, which are unrelated to paleostorminess (Figure 3; Prins et al., 2002).

Filtering out hydrologic events from "noise"

The number of hydrologic events detected varies between different data sets, such as LOI, mean and median particle size, and EMM, and varies depending on whether we apply 1 or 2 σ time series filters (Table 4 and Figure 8). LOI detected 70 and 32 events

for the 1 and 2 σ time series filters, respectively, on ST2, the core with the highest volume of sand (Table 4). Mean particle size was the most sensitive of the traditional particle size statistics for all the cores, detecting an average of 39 and 20 events for the 1 and 2 σ filters, respectively (Table 4). Median particle size was the most sensitive if we consider cores individually, with maximum event detection reaching 88 and 52 events for the 1 and 2 σ filters, respectively, on OG (Table 4). This same core, one of the fine-grained cores with low volumes of sand, contained the most events detected by all of the particle size records, (mean and median particle size, and EMM records; Table 4).

The large difference between the mean number of events identified by 1 and 2 σ filters (31 and 8, respectively) on the raw LOI data results from a lack of significant troughs in the LOI records and from sensitivity of the 1 σ filter to the local background (Figure 8 and Table 4). For example, the 1 σ filter on SU1 LOI data identifies flood events in the LOI record where the local background changes as little as ~1-2 % (Figure 8), most likely negligible shifts in the data. The 2 σ filter on LOI data does not resolve this problem as it detects very few events, especially in comparison to particle size records (Table 4). Troughs in LOI data are lesser in magnitude than those found in Brown et al. (2000) and Noren et al.'s (2002) cores because our cores contain less organic material overall.

The 1 σ filter on LOI data identifies events, where no events are identified in any of the particle size records. For example, at a depth of ~125 cm in the SU1 record, two events are detected solely by a 1 σ filter on LOI (Figure 8). Terrestrial sediment must be delivered to the lake to create significant troughs in the LOI data, such as those found at

~125 cm in SU1. One possible reason for such discrepancies between LOI and particle size records is that the source sediment for inflowing tributaries could change to finer-grained sediment. However, increases in the proportion of the coarsest EMD in SU1 occur through the Holocene, suggesting that a lack of available coarse grains was not the case (Figure 8). Another possible reason for the discrepancy between the different analytical methods is that events defined solely by LOI reflect terrestrial sediment delivered to the entire lake, by other tributaries. In such a case, particle size would not reflect the transport capacity of the primary tributary supplying the delta adjacent to which the core was taken. In all the cores, the 2 σ filter was not sensitive to such events in the LOI record, and the 1 σ filter is problematic for its sensitivity to the local background data. Thus, LOI records were not a robust means for event frequency analysis.

The 1 σ time series filter of all mean and median particle size records also was sensitive to changes in the local background. For example, ~ 3-7 events in SU1 were identified from by small increases in mean and median particle size (~ 10 μm; Figure 8). 2 σ events, therefore, are a more robust reflection of flood layers in the mean and median particle size records. The coarsest EMD records are sensitive to polymodal size distributions (Figures 6, 7 and 8). Thus, we were able to identify more events in all the cores with a 1 σ filter of EM records (mean= 29) than with a 2 σ filter of mean and median particle size records (mean= 20 and 18, respectively; Table 4). The background data in the EMD records are flat, and the EMD records already reflect a coarse estimate of the terrestrially-derived sediment layers. Therefore, the 1 σ filter accurately avoids

detection of events where smaller shifts in the data may not indicate hydrologic event deposition, such as those found in LOI, and mean and median particle size records (Figure 8).

Hydrologic event chronologies

Contemporaneous deposition of terrestrial sediment layers does occur in basins where we collected multiple cores, as revealed by the South Pond (SU1 and SU2) and Stinson Lake (ST1 and ST2) chronologies (Figure 9A). There is some agreement between the SU1 and SU2 chronologies in the mid-Holocene (4- 6.5 cal kya; Figure 9A), and there is agreement between the ST1 and ST2 chronologies in the mid- Holocene (6- 8 cal kya; Figure 9A). The ST2 record contains more events in the late Holocene (<6 cal kya) than ST1, however the opposite is true for the rest of the Holocene (>6 cal kya). Differences in the hydrologic event chronologies of cores taken from different deltas within the same lake may reflect the differing sensitivities of individual drainage basins to orographic effects on rainfall, the availability of erodible sediment in the catchment, varying antecedent soil moisture levels, or other factors of landscape conditioning (Rodbell et al., 1999; Noren et al., 2002). Noren et al. (2002) noted that the lack of agreement between chronologies from different lake basins suggested localized, convective thunderstorms as the mechanism for floods that caused terrestrial sediment deposition; to overcome this effect, they compiled all modeled storm layer ages to form a regional event record.

Compiling the data from our 6 lakes, we found that the regional chronology of hydrologic events in NH and ME is both similar and different from the Vermont and New

York records (Brown et al., 2000; Noren et al., 2002; Figures 9B and 9C). During the Holocene, peaks in hydrologic events recorded by the EMM occurred ~ 0.8, 1.4, 2.1, 3.0, 3.9, 6.8, and 11.5 cal kya (Figure 9B). Smaller event peaks occurred ~8.2 and 13.3 cal kya (Figure 9B). There is a notable lack of agreement between our event chronology and Noren et al.'s (2002) chronology in the mid to early Holocene (4- 10 cal kya; Figure 9B). However, late Holocene events in our records and in Noren et al.'s (2002) records peak at similar times (0-3.5 cal kya; Figure 9B).

Climate patterns in the United States during the Holocene

Noren et al. (2002) suggested that the lake sediment record for VT and NY, inferred from LOI and other proxies, reflected periods of storm-induced erosion and deposition of terrestrial sediment, in part, because their record showed some correlation with periods of increased alluvial fan aggradation (Noren et al., 2002; Jennings et al., 2003). Our event chronology, compiled from EMM records, corresponds fairly well with periods of increased alluvial fan aggradation in VT and NY (Bierman et al., 1997; Jennings et al., 2003), including times when Noren et al.'s (2002) chronology does not correspond to fan records (1.5- 2, 4, 4.8, 7.7, 8.3 cal kya). Although the time series filtering of our LOI records was less certain, an event chronology compiled from our LOI records shows very little agreement to any of the records for hydrologic events, and by inference storminess (Figure 9).

The timing of the late Holocene event peaks in the EMM record corresponds to other geologic records of flooding and storminess in North America (Figure 9). Most notably, intense hurricane strikes in Florida and Alabama, recorded by overwash events,

increased around 4,000 cal yr BP, and peaked ca. 0.8, 1.4, 2.2, 2.6, and 3.0-3.2 kya (Liu and Fearn, 1993 and 2000). Both the overall increase in the number of hurricanes and the peaks in hurricane activity correspond to the EMM event chronology which shows storms increasing about 4,000 cal yr BP and peaking ~ 0.8, 1.4, 2.1, 3.0 cal kya (Figure 9). These peaks in the EMM event chronology also correspond to an increase in the number of floods in the north-central United States (Knox, 1999) and megafloods on the Mississippi river (Brown et al., 1999; Figure 9). Mid-Holocene peaks in EMM event chronology also correspond to increases in flooding in the north-central United States (Knox, 1999; Figure 9).

Liu and Fearn (2000) postulated that the increase in overwash events on the Gulf of Mexico coast was related to a shift in the jet stream ~ 3,000 ^{14}C yr BP, which altered the path of hurricanes that strike on the Gulf coast and moved across the central United States. They cite the contemporaneous increase in the number of floods in the north central US and the Mississippi basin as evidence for this change in the path of the hurricanes (Figure 9). The predominant path of hurricanes prior to this shift, ca. 6,000 ^{14}C yr BP, was up the Atlantic coast (Liu and Fearn, 2000). The EMM event chronology shows a prominent peak ca. 6,800 cal yr. BP (Figure 9B).

Noren et al. (2002) suggest convective thunderstorms as the mechanism for generating the terrestrial sediment layers in their record, suggesting that the regional influence of tropical cyclones, such as hurricanes, would cause centennial clustering of events and thus more terrestrial sediment deposition in the lakes they studied. Our EMM chronology shows more frequent periods of increased hydrologic events, and particularly

during the late Holocene, contains some centennial clustering. The timing and clustering of the EMM chronology, compiled from lakes which are closer to the Atlantic coast, suggest a stronger connection to hurricane patterns than previous, more continentally derived paleostorm chronologies (Brown et al., 2000; Noren et al., 2002; Figure 9).

The 3,000 year cycle in Noren et al.'s (2002) record was thought to reflect large scale climatic patterns. Specifically, Thompson and Wallace (2001) and Noren et al. (2002) suggest that the low phase of the Artic Oscillation produces conditions favorable for extreme storms in the northeastern United States. Our data show no strong millennial scale cycles such as those found in Noren et al.'s record, with the exception of ~5,000-6,000 year cycles which are uncertain because our record is only 13 ky long (Figure 10). In contrast, raw spectrums from all our records have more power at the centennial scale, but none of the centennial cycles are strong enough or consistent enough between different particle size spectrums to suggest one dominant cycle (Table 5 and Figure 10).

Noren et al. (2002) were able to compile two storminess records, one composed solely by LOI and one composed from all proxy records, to produce similar spectral signals with a dominant, 3,000 yr cycle. Particle size records, including EMM, are more sensitive to terrestrial sediment layer detection. This sensitivity may have interfered with our ability to find a dominant cycle. Discrepancies between the two records may reflect a combination of differences in analytical methods, the type of storms causing terrestrial sediment deposition, the geographic distribution of lakes in the study area, and the differing sensitivities of individual lake basins to factors influencing terrestrial sediment deposition.

CONCLUSIONS

High resolution particle size analysis of lake sediment from NH and ME demonstrates the utility of this approach for paleolimnological studies, particularly those concerned with elucidating storm and flood patterns of the past. When analyzed in sediment cores taken in locations proximal to the terrestrial sediment source, particle size data clearly define the flux of terrestrial sediment in the lake, associated with increases in the discharge of inflowing tributaries. Traditional particle size statistics or end-member models of particle size distributions can be used for time series analysis, revealing more frequent terrestrial sediment deposition than other proxies, such as MS and LOI. Radiocarbon analysis and particle size data can be combined to provide important records of climate changing over time, specifically the frequency of paleohydrologic events (Campbell et al., 1998). In New England, such analyses suggest that centennial and millenial scale cycles of storminess exist, and that periods of storminess in NH and ME correlate with hurricane frequency through the later Holocene.

REFERENCES CITED

Ambers, R. K., 2001, Using the sediment record in a western Oregon flood-control reservoir to assess the influence of storm history and logging on sediment yield: Journal of Hydrology, v. 244, no. 3-4, p. 181-200.

Baker, V. R., 1988, Flood erosion, in Baker, V. R., Kochel, R. C., and Patton, P. C., eds., Flood Processes: Flood Geomorphology: New York, John Wiley and Sons, p. 81-96.

Beierle, B. D., Lamoureux, S. F., Cockburn, J. M. H., and Spooner, I., 2002, A new method for visualizing particle size distributions: Journal of Paleolimnology, v. 27, no. 2, p. 279-283.

Bierman, P., Lini, A., Zehfuss, P., Church, A., Davis, P. T., Southon, J., and Baldwin, L., 1997, Postglacial ponds and alluvial fans: Recorders of Holocene landscape history: GSA Today, v. 7, no. 10, p. 1-8.

Boggs, S. J., 1995, Principles of Sedimentology and Stratigraphy: New Jersey, Prentice Hall, Inc., 774 p.

Boose, E. R., Chamberlin, K. E., and Foster, D. R., 2001, Landscape and regional impacts of hurricanes in New England: Ecological Monographs, v. 71, no. 1, p. 27-48.

Bosley, A. C., Bierman, P. R., Noren, A., and Galster, J., 2001, Identification of paleoclimatic cycles during the Holocene using grain size analysis of sediments cored from Lake Morey in Fairlee, VT, in Geological Society of America, Northeastern Section, 36th annual meeting, p. 85.

Broomhead, D. S., and King, G. P., 1986, Extracting qualitative dynamics from experimental data: Physica D, v. 20, p. 217-236.

Brown, P., Kennett, J. P., and Ingram, B. L., 1999, Marine evidence for episodic Holocene megafloods in North America and the northern Gulf of Mexico: Paleoceanography, v. 14, no. 4, p. 498-510.

Brown, S. L., Bierman, P. R., Lini, A., and Southon, J., 2000, 10 000 yr record of extreme hydrologic events: Geology, v. 28, no. 4, p. 335-338.

Brown, S., Bierman, P., Lini, A., Southon, J., and Davis, P. T., 2002, Lake cores as archives of Holocene watershed erosion events: Journal of Paleolimnology, v. 28, p. 219-236.

Bull, W. B., 1991, Geomorphic responses to climate change: New York, Oxford University Press, 326 p.

Campbell, I. D., Campbell, C., Apps, M. J., Rutter, N. W., and Bush, A. B. G., 1998, Late Holocene ~1500 yr climatic periodicities and their implications: Geology, v. 26, no. 5, p. 471-473.

Campbell, I. D., Last, W. M., Campbell, C., Clare, S., and McAndrews, J. H., 2000, The late-Holocene paleohydrology of Pine Lake, Alberta: a multiproxy investigation: Journal of Paleolimnology, v. 24, p. 427-441.

Collins, E. S., Scott, D. B., and Gayes, P. T., 1999, Hurricane records on the South Carolina coast: Can they be detected in the sediment record?: Quaternary International, v. 56, p. 15-26.

Donnelly, J. P., Bryant, S. S., Butler, J., Dowling, J., Fan, L., Hausmann, N., Newby, P. E., Shuman, B. N., Stern, J., Westover, K., and Webb III, T., 2001a, 700 yr. sedimentary record of intense hurricane landfalls in southern New England: Geological Society of America Bulletin, v. 113, no. 6, p. 714-727.

Donnelly, J. P., Roll, S., Wengren, M., Butler, J., Lederer, R., and Webb III, T., 2001b, Sedimentary evidence of intense hurricane strikes from New Jersey: Geology, v. 7, p. 615-618.

Drake, E. D., 1999, Temporal and Spatial Variability of the sediment grain-size distribution on the Eel shelf: the flood layer of 1995: Marine Geology, v. 154, p. 169-182.

Eden, D. N., and Page, M. J., 1998, Palaeoclimatic implications of a storm erosion record from late Holocene lake sediments, North Island, New Zealand: Palaeogeography, Palaeoclimatology, Palaeoecology, v. 139, p. 37-58.

Ely, L. L., Enzel, Y., Baker, V. R., and Cayan, D., 1993, A 5,000-Year Record of Extreme Floods and Climate Change in the Southwestern United States: Science, v. 262, p. 410-412.

Folk, R. L., and Ward, W. C., 1957, Brazos River bar: a study in the significance of grain size parameters: Journal of Sedimentary Petrology, v. 27, p. 3-26.

Grove, J. M., 1988, The Little Ice Age: London, Methuen, 498 p.

Hass, H. C., 1993, Depositional processes under changing climate: upper SubAtlantic granulometric records from the Skagerrak (NE-North Sea): Marine Geology, v. 111, p. 361-378.

Hupp, C. R., 1988, Plant ecological aspects of flood geomorphology and paleoflood history, in Baker, V. R., Kochel, R. C., and Patton, P. C., eds., Flood Processes: Flood Geomorphology: New York, John Wiley and Sons, p. 335-356.

I, I. W. G., 2001, Climate Change 2001: The Scientific Basis, in Intergovernmental Panel on Climate Change, Geneva, Switzerland.

Jackson, S. T., and Whitehead, D. R., 1991, Holocene vegetation patterns in the Adirondack Mountains: Ecology, v. 72, no. 2, p. 641-653.

Jennings, K. L., Bierman, P., and Southon, J., 2003, Timing and style of deposition on humid-temperate fans, Vermont, USA: Geological Society of America Bulletin, v. 115, no. 2, p. 182-199.

Keim, B., Mayewski, P. A., Zielinski, G. A., Wake, C., Carpenter, K., Cox, J., Souney, J., Sanborn, P., and Rodgers, M., 1998, New England's Changing Climate, Weather and Air Qualitry: Durham, Hew Hampshire, University of New Hampshire, 48 p.

Knox, J. C., 1993, Large increases in flood magnitude in reponse to modest changes in climate: Nature, v. 361, no. 6411, p. 430-432.

Knox, J.C., 1999, Sensitivity of modern and Holocene floods to climate change: Quaternary Science Reviews, v. 19, p. 439-457.

Kochel, R. C., and Baker, V. R., 1982, Paleoflood hydrology: Science, v. 215, no. 4531, p. 353-361.

Komar, P. D., 1988, Sediment transport by floods, in Baker, V. R., Kochel, R. C., and Patton, P. C., eds., Flood Processes: Flood Geomorphology: New York, John Wiley and Sons, p. 97-112.

Lamb, H. H., 1979, Variation and changes in the wind and ocean circulation: the Little Ice Age in the northeast Atlantic: Quaternary Research, v. 11, p. 1-20.

Lamoureux, S. F., 2000, Five centuries fo interannual sediment yield and rainfall-induced erosion in the Canadian High Arctic recorded in lacustrine varves: Water Resources Research, v. 36, p. 309-318.

Liu, K., and Fearn, M. L., 1993, Lake-sediment record of late Holocene hurricane activities from coastal Alabama: Geology, v. 21, p. 793-796.

Liu, K., and Fearn, M., L., 2000, Reconstruction of Prehistoric Landfall Frequencies of Catastrophic Hurricanes in Northwestern Florida from Lake Sediment Records: Quaternary Research, v. 54, p. 238-245.

Lord, A. M., 2003, Evolution rates of post-glacial lake ecosystems in northern New England: A Geochemical Study using Lake Sediments [Master's thesis]: University of Vermont, 111 p.

Ludlum, D., 1963, Early American Hurricanes: Boston, American Meteorological Society, 198 p.

Ludlum, D., 1996, The Vermont Weather Book: Montpelier, VT, Vermont Historical Society, 302 p.

Mann, M. E., and Lees, J. M., 1996, Robust estimation of background noise and signal detection in climatic time series: Climatic Change, v. 33, p. 409-445.

McCave, I. N., Manighetti, B., and Robinson, S. G., 1995, Sortable silt and fine sediment size/composition slicing; parameters for paleocurrent speed and paleooceanography: Paleoceanography, v. 10, p. 593-610.

Meeks, H. A., 1986, Vermont's land and resources: Shelburne, VT, New England Press, 332 p.

Nesje, A., Dahl, S. O., Matthews, J. A., and Berrisford, M. S., 2001, A ~4,500-yr record of river floods obtained from a sediment core in Lake Atnsjfen, eastern Norway: Journal of Paleolimnology, v. 25, no. 3, p. 329-342.

Newby, P. E., Killoran, P., Waldorf, M. R., Shuman, B. N., Webb, R. S., and Webb III, T., 2000, 14,000 years of sediment, vegetation, and water-level changes at the Makepeace Cedar Swamp, southeastern Massachusetts: Quaternary Research, v. 53, p. 352-368.

Noren, A., Bierman, P. R., Steig, E. J., Lini, A., and Southon, J., 2002, Millennial-scale storminess variability in the northeastern United States during the Holocene epoch: Nature, v. 419, no. 6909, p. 821-824.

Noren, A., 2002, A 13,000-Year Regional Record of Holocene Storms in the Northeastern United States [Master's thesis]: University of Vermont, 170 p.

Nott, J., and Hayne, M., 2001, High frequency of 'super-cyclones' along the Great Barrier Reef over the past 5,000 years: Nature, v. 413, p. 508-512.

O'Brien, S. R., Mayewski, P. A., Meeker, L. D., Meese, D. A., Twickler, M. S., and Whitlow, S. I., 1995, Complexity of Holocene climate as reconstructed from a Greenland ice core: Science, v. 270, p. 1962-1964.

Ouellet, M., 1997, Lake sediments and Holocene seismic hazard assessment within the St. Lawrence Valley, Quebec: Geological Society of America Bulletin, v. 109, p. 631-642.

Page, M. J., Trustrum, N. A., and DeRose, R. C., 1994, A high-resolution record of storm-induced erosion from lake sediments, New Zealand: Journal of Paleolimnology, v. 11, p. 333-348.

Paillard, D., Labeyrie, L., and Yiou, P., 1996, Macintosh program performs time-series analysis: Eos, transactions, v. 77, p. 379.

Parris, A., Bosley, A., Bierman, P., Lini, A., Noren, A., Lord, A., Conlan, A., and Morgan, L., 2001, Grain by grain; Holocene storms and hillslope erosion in New England, in Geological Society of America Abstracts with Programs, p. 314.

Prins, M. A., 1999, Pelagic, hemipelagic and trubidite deposition in the Arabian Sea during the late Quaternary: unravelling the signals of eolian and fluvial sediment supply as functions of tectonics, sea-level and climate change by means of end-member modelling of siliclastic grain-size distributions [Ph.D thesis]: Utrecht University, 192 p.

Prins, M. A., and Weltje, G. J., 1999, End-member modelling of siliclastic grain-size distributions: The late Quaternary record of eolian and fluvial sediment supply to the Arabian Sea and its paleoclimatic signficance, in Numerical Experiments in Stratigraphy: Recent Advances in Stratigraphic and Sedimentologic Computer Simulations, p. 91-111.

Prins, M. A., Postma, G., and Weltje, G. J., 2000, Controls on terrigenous sediment supply to the Arabian Sea during the late Quaternary: the Makran continental slope: Marine Geology, v. 169, p. 351-371.

Prins, M. A., Bouwer, L. M., Beets, C. J., Simon, R. T., Weltje, G. J., Kruk, R. W., Kujipers, A., and Vroon, P. Z., 2002, Ocean circulation and iceberg discharge in the glacial North Atlantic: Inferences from unmixing of sediment size distributions: Geology, v. 30, no. 6, p. 555-558.

Reasoner, M. A., 1993, Equipment and procedure improvements for a lightweight, inexpensive, percussion core sampling system: Journal of Paleolimnology, v. 8, p. 273-281.

Rodbell, D. T., Seltzer, G. O., Anderson, D. M., Abbott, M. B., Enfield, D. B., and Newman, J. H., 1999, A ~15,000-year record of El Nino-Driven alluviation in southwestern Ecuador: Science, v. 283, no. 5401, p. 516-520.

Shuman, B. N., Bravo, J., Kaye, J., Lynch, J. A., Newby, P. E., and Webb III, T., 2001, Late Quaternary Water-Level Variations and Vegetation History at Crooked Pond, Southeastern Massachusetts: Quaternary Research, v. 56, p. 401-410.

Spear, R., Davis, M. B., and Shane, L. C., 1994, Late Quaternary history of low- and mid-elevation vegetation in the White Mountains of New Hampshire: Ecological Monographs, v. 64, p. 85-109.

Stuiver, M., and Reimer, P. J., 1993, Extended 14C Data Base and Revised CALIB 3.0 14C Age Calibration Program: Radiocarbon, v. 35, p. 215-230.

Syvitski, J. P. M., 1991, Principles, methods, and application of particle-size analysis: Cambridge, Cambridge University Press, 368 p.

Thomson, D. J., 1982, Spectrum estimation and harmonic analysis: Proc. IEEE, v. 70, p. 1055-1096.

Thorndycraft, V., Hu, Y., Oldfield, F., Crooks, P. R. J., and Appleby, P. G., 1998, Individual flood events detected in the recent sediments of Petit Lac d'Annecy, eastern France: The Holocene, v. 8, no. 6, p. 741-746.

Vautard, R., and Ghil, M., 1989, Singular spectrum analysis in non-linear dynamics, with applications to paleoclimatic time series: Physica D, v. 35, p. 395-424.

Webb, R. S., Anderson, K. H., and Webb III, T., 1993, Pollen Response-Surface Estimates of Late-Quaternary Changes in the Moisture Balance of the Northeastern United States: Quaternary Research, v. 40, p. 213-227.

Webb III, T., Bartlein, P. J., Harrison, S. P., and Anderson, K. J., 1993, Vegetation, lake levels, and climate in eastern North America for the past 18,000 years, in Wright, H. E., Kutzbach, J. E., Street-Perrot, F. A., Bartlein, P. J., Ruddiman, W. F., and Webb III, T., eds., Global climates since the last glacial maximum: Minneapolis, University of Minnesota, p. 415-467.

Weltje, G. J., 1997, End-member modelling of compositional data: numerical-statistical algorithms for solving the explicit mixing problem: Journal of Mathematical Geology, v. 29, p. 503-549.

Zong, Y., and Tooley, M. J., 1999, Evidence of mid-Holocene storm-surge deposits from Morecambe Bay, northwest England: A biostratigraphical approach: Quaternary International, v. 55, p. 43-50.

Figure captions

Figure 1. Map showing location of study area in the northeastern United States (inset, shaded) and lakes from which we collected and analyzed sediment cores. SU= South Pond, OG=Ogontz Lake, WO=Worthley Pond, CR=Crystal Lake, ST=Stinson Lake, SY=Sandy Pond.

Figure 2. South Pond (SU) watershed, Stark, New Hampshire (NH). Dots indicate core locations. Dashed line is watershed boundary. Bathymetric contour interval, 6 m; topographic contour interval, 30 m. Adapted from U.S. Geological Survey quadrangle maps. USU= Upper South Pond; RP= Rocky Pond

Figure 3. End-member model results of South Pond core 1 (SU1). A. Median r^2 for all size classes in a particle size distribution for the different number of end-members in a model. Increasing the number of end-members past five does not improve the r^2; therefore, a five end-member model was chosen for the SU1 core. B. r^2 values for the individual size classes for end-member models with 3, 4, and 5 end-member models. Two size ranges (15-84 μm, ≥213 μm) are explained poorly by the 3 and 4 end-member models. C. End-member size distributions for the SU1 core. The first end member distribution has the coarsest mode, and the remaining four distributions have progressively finer modes. D. Whole core trends in the relative proportion of each end-member distribution for the SU1 core. The proportion of the first two end member distributions was summed to examine trends in terrestrial sediment deposition.

Figure 4. Whole-core percent mass loss-on-ignition values (1 cm sample interval). Core ID letters correspond to lakes in Table 1 and Fig.1

Figure 5. Traditional particle size parameters for the SU1 core (1 cm sample interval).

Figure 6. Sediment layers inferred to have been caused by flooding. A. Traditional particle size statistics and size distributions for a sediment layer in the SU1 core with a polymodal size distribution. B. End-member model statistics and size distributions for the same terrestrial sediment layer as A. C. End-member statistics and size distributions for a terrestrial sediment layer from the SU1 core with a unimodal distribution. D. End-member statistics and size distributions for terrestrial sediment layer in the SU2 core with less pronounced shift in the volume of coarse silt, typical of polymodal size distributions. PS= Particle size; EM= End-member distribution

Figure 7. Coarse end-member records from each core. Core ID letters correspond to lakes in Table 1 and Fig. 1. Note the flat background and discreet peaks, which are ideal for time series filtering identification of terrestrial sediment layers. *Records were compiled by summing the relative abundance (cm-by-cm) of the first two end-members for the whole core.

Figure 8. Comparison of event detection by time series filtering of LOI, mean and median particle size, and end-member records for part of the SU1 record (0-200 cm). The top (0- 26 cm) of the SU1 record is above uppermost ^{14}C date and so not considered. Time series filter superimposed on all raw data curves. For LOI, only +/- one and two σ lines are shown. For mean and median particle size and the end-member record, the reconstructed baseline is shown in light gray and the +1 and +2 σ lines are shown in progressively darker tones. The dark bands on the bar graphs indicate fine grained mud,

not indicative of sediment delivery during floods, and the white bands are the locations of the flood sediment layers defined by 1 and 2 σ.

Figure 9. Inferred hydrologic events in the northeastern United States and relevant climate records. A. Individual terrestrial sediment layer ages defined by EMM of sediment records from study lakes. B. Histogram of terrestrial sedimentation events (100 yr bins) defined by EMM records. Histogram values are weighted by the inverse of the number of chronologies that cover each time interval. C. Other relevant climate records. Storminess as follows. 1. Three periods of increased storminess inferred from terrestrial sediment deposition in lakes from Vermont and New York (Brown et al., 2000; Noren et al., 2002), 2. Storm-related aggradational events on alluvial fans in Vermont (Bierman et al., 1997; Jennings et al., 2003), 3A. Little Ice Age historical evidence (Lamb, 1979), 3B. High frequency of hurricane landfalls along the northern Gulf of Mexico coast and Florida panhandle (Liu and Fearn, 1993 and 2000), 3B. Occurrence of storm surge deposits on the northwestern coast of England (Zong and Tooley, 1999). Floods as follows 4. Increased magnitude of 1.58 yr. recurrence interval floods in the north-central United States (NCUS; Knox, 1999), 5. Increased magnitude of the largest floods in the NCUS (Knox, 1999), 6. Highest frequency of megafloods on the Mississippi River (Brown et al., 1999). D. Histogram of terrestrial sedimentation events (100 yr bins) defined by LOI records. Histogram values are weighted by the inverse of the number of chronologies that cover each time interval.

Figure 10. Multitaper spectral analysis (three tapers) of hydrologic events defined by 1 and 2 σ filters on A. EMM, B. mean particle size, C. median particle size, and D.

LOI time series, interpolated with a 100-yr interval and with linear trend removed (Thompson, 1982). CI= Confidence interval. Confidence intervals are relative to red noise estimated from lag-1 autocorrelation with a median averaging filter (Mann and Lees, 1996). The two σ time series were rescaled such that the confidence intervals apply to both power

TABLE 1. GEOMORPHIC CHARACTERISTICS OF CORED LAKES

Core	Lake	Location	Surface area (km^2)	Maximum depth (m)	Elevation (m)	Drainage basin area (km^2)	Drainage basin relief (m)	Relief ratio† (m km^{-2})	Latitude	Longitude
CR	Crystal Lake	Eaton Center, NH	0.4	18	146	15	353	24	N43°54’	W71°05’
OG	Ogontz Lake	Lisbon, NH	0.3	22	202	23.6	408	17	N44°15’	W71°54’
ST1, ST2	Stinson Lake	Rumney, NH	1.4	22	396	20.7	655	32	N43°52’	W71°48’
SU1, SU2	South Pond	Stark, NH	0.7	27.9	340	7.4	427	58	N44°36’	W71°22’
SY	Sandy Pond	Richmond, NH	0.1	12	288	1.1	226	205	N42°46’	W72°17’
WO	Worthley Pond	Peru, ME	1.4	15	174	13.5	344	25	N44°24’	W70°26’

† Drainage basin relief (m)/Drainage basin area (km^2)

TABLE 2. RADIOCARBON AGES OF MACROFOSSILS

CAMS number†	Lake	Core	Depth (cm)	Age (^{14}C yr BP)	Age (cal yr BP)‡	1σ cal age range
90546	Crystal	1	17	845 ± 40	740	788-701
90547	Crystal	1	53	1490 ± 45	1370	1411-1313
82778	Crystal	1	80	1900 ± 40	1840	1894-1742
82779	Crystal	1	133	2210 ± 60	2230	2312-2152
78252	Crystal	1	205	2980 ± 40	3150	3238-3079
82780	Crystal	1	338	4980 ± 40	5700	5737-5656
78253	Crystal	1	442	7390 ± 60	8220	8325-8063
82781	Crystal	1	525	8655 ± 40	9600	9664-9548
82782	Crystal	1	535	8700 ± 60	9640	9734-9552
82783	Crystal	2	110	8820 ± 90	9890	10146-9705
82784	Crystal	2	128	9050 ± 60	10200	10244-10154
78254§	Crystal	2	146	9040 ± 190	10170	10474-9894
78255	Crystal	2	238	11350 ± 330	13350	13801-12996
78210	Ogontz	1	112	1070 ± 50	980	1049-933
78211	Ogontz	1	210	1870 ± 40	1800	1886-1737
78212	Ogontz	1	316	2510 ± 40	2580	2732-2492
78213	Ogontz	1	423	3490 ± 70	3750	3836-3644
78214	Ogontz	1	488	4370 ± 50	4930	5023-4863
78220	Stinson	1	35	1640 ± 40	1540	1606-1426
82790	Stinson	1	70	2665 ± 35	2770	2784-2749
78221	Stinson	1	105	3570 ± 90	3860	3976-3722
78222	Stinson	1	151	4430 ± 40	5010	5220-4877
78223	Stinson	1	200	5890 ± 70	6710	6793-6635
82791	Stinson	1	230	7275 ± 40	8100	8158-8022
78224	Stinson	1	279	8160 ± 110	9150	9393-9001
90552#	Stinson	1	368	12180 ± 270	14380	15121-13826
82792#	Stinson	1	408	12345 ± 45	14500	15021-14123
82793	Stinson	2	34	950 ± 35	860	922-796
82794	Stinson	2	109	1945 ± 40	1890	1930-1830
82795	Stinson	2	196	2860 ± 40	2970	3059-2886
78294	Stinson	2	272	3690 ± 40	4030	4086-3979
78295	Stinson	2	341	4400 ± 50	4950	5037-4871
82796	Stinson	2	420	5865 ± 40	6690	6727-6641
85472	Stinson	2	462	7150 ± 40	7950	8004-7878
78296	Stinson	2	496	9170 ± 90	10320	10419-10230
78297	Stinson	2	506	9940 ± 50	11330	11543-11230

82797	South	1	26	3150 ± 190	3350	3628-3079
82798	South	1	50	3890 ± 70	4320	4415-4185
78203	South	1	76	4430 ± 110	5060	5277-4870
82799	South	1	114	6090 ± 70	6950	7149-6803
78204	South	1	153	7840 ± 60	8640	8925-8482
78205	South	1	186	8870 ± 40	10030	10149-9893
78206	South	1	243	10070 ± 40	11520	11692-11343
78207#	South	1	284	10160 ± 40	11800	11947-11583
82800§	South	1	330	9410 ± 40	9410	9467-9358
78208#	South	1	370	10300 ± 80	12120	12564-11767
78209#	South	1	388	10560 ± 60	12570	12828-12353
82801	South	2	36	1680 ± 90	1600	1708-1422
78268	South	2	70	2530 ± 40	2600	2741-2494
82802	South	2	114	3900 ± 120	4320	4511-4149
78290	South	2	154	5170 ± 70	5900	6164-5756
78291	South	2	161	5250 ± 110	6040	6173-5912
78292	South	2	199	6930 ± 40	7730	7787-7690
78293	South	2	246	8660 ± 240	9770	10143-9474
90550#	South	2	326	11100 ± 45	13080	13155-12998
90551#	South	2	343	11825 ± 40	13870	14040-13614
82807§	Sandy	1	19	3300 ± 90	3540	3634-3416
85474§	Sandy	1	29	3470 ± 190	3730	3969-3478
90549	Sandy	1	62	2265 ± 40	2260	2341-2162
82808	Sandy	1	103	2550 ± 120	2610	2761-2466
78256	Sandy	1	141	3510 ± 120	3790	3961-3636
82809	Sandy	1	175	4470 ± 110	5130	5289-4974
82810	Sandy	1	192	5060 ± 40	5820	5887-5748
82811	Sandy	1	253	6955 ± 45	7760	7821-7698
78257	Sandy	1	330	8270 ± 50	9280	9400-9136
82812	Sandy	1	426	9920 ± 40	11280	11334-11228
78258	Sandy	1	464	11440 ± 50	13340	13475-13188
78259	Sandy	1	470	11660 ± 40	13590	13807-13481
90548	Worthley	1	2	1310 ± 40	1240	1286-1183
82785	Worthley	1	21	2140 ± 40	2140	2293-2055
78215	Worthley	1	59	3570 ± 40	3870	3954-3779
82786	Worthley	1	116	4955 ± 40	5680	5724-5621
78216	Worthley	1	161	6020 ± 180	6870	7157-6661
82787	Worthley	1	220	7815 ± 40	8590	8633-8540
78217	Worthley	1	291	9360 ± 40	10570	10661-10504
78218	Worthley	1	321	10380 ± 50	12350	12612-11981

78219#	Worthley	1	366	11620 ± 40	13600	13809-13454
82788#	Worthley	1	375	11885 ± 40	13950	14062-13816
82789#	Worthley	1	385	12280 ± 60	14460	15026-14100

† Center for Accelerator Mass Spectrometry, Lawrence Livermore National Laboratory
‡ Calibrated using CALIB version 4.2 (Stuiver et al., 1998)
§ inverted dates not used
# dates not used because they were in gray rhythmite sections, not used in analysis

TABLE 3. SUMMARY OF END MEMBER MODELING RESULTS

Core	Samples analyzed	Median r^2	Number of end members (EMs)	Mean %sand	Mean %silt	Mean %clay	EM1 MA†	EM2 MA	EM3 MA	EM4 MA	EM5 MA	EM1 mode (μm)	EM2 mode (μm)	EM3 mode (μm)	EM4 mode (μm)	EM5 mode (μm)
CR	718	0.73	3	6	71	23	0.05	0.29	0.59	NA	NA	48	33	13	NA	NA
OG	488	0.73	3	3	82	15	0.10	0.71	0.18	NA	NA	40	16	7	NA	NA
ST1‡	350	0.90	4	21	63	15	0.05	0.12	0.25	0.58	NA	213	121	57	19	NA
ST2	506	0.94	4	32	58	10	0.09	0.33	0.25	0.33	NA	121	84	33	16	NA
SU1	275	0.96	5	17	66	17	0.00	0.07	0.20	0.37	0.19	373	121	58	19	6
SU2‡	299	0.76	3	4	66	31	0.05	0.29	0.57	NA	NA	40	19	6	NA	NA
SYR	475	0.88	3	8	74	18	0.02	0.43	0.51	NA	NA	84	22	15	NA	NA
WO	350	0.88	4	21	68	11	0.07	0.35	0.29	0.30	NA	84	70	27	26	NA

NA- Not applicable because only 3 or 4 end members in model
† Whole core median abundance
‡ Volumes do not add to zero due to rounding error

TABLE 4. NUMBER OF EVENTS DETECTED BY DIFFERENT TECHNIQUES AND FILTERS

	LOI (1σ)	LOI (2 σ)	Mean PS (1 σ)	Mean PS (2 σ)	Median PS (1 σ)	Median PS (2 σ)	Coarse EMDs (1 σ)	Coarse EMDs (2 σ)
CR	15	2	44	15	44	14	40	10
OG	25	6	81	45	88	52	57	31
ST1	40	12	11	7	12	8	14	10
ST2	70	32	59	24	63	30	45	29
SU1	23	2	27	21	25	17	21	15
SU2	31	5	33	19	14	6	24	15
SY	17	2	27	17	13	6	14	8
WO	31	3	34	12	40	16	20	7
Mean	31	8	39	20	37	18	29	15
Median	28	4	33	18	32	15	22	12
Min	15	2	11	7	12	6	14	7
Max	70	32	81	45	88	52	57	31

LOI- Loss-on-ignition
PS- Particle size
EMDs- End-member distributions
1 σ, 2 σ- One and two standard deviation time series filters

TABLE 5. CYCLES DEFINED BY SPECTRAL ANALYSIS

	LOI 1 σ	LOI 2 σ	Mean 1 σ	Mean 2 σ	Median 1 σ	Median 2 σ	Coarse EMDs 1 σ	Coarse EMDs 2 σ
50† yr- 95% CI	496, 482, 415, 387	NA	6387, 387	482	6387	690, 655	5677, 1022, 946, 630, 313	5110, 982, 429, 402, 331
50 yr- 99% CI	NA	350	267	4645	433, 375	5677	NA	NA
100† yr- 95% CI	486, 415, 390, 385	486, 448, 280	587, 363	4645, 454	6387, 375, 315	404, 320	5677, 630, 278	415, 319
100 yr- 99% CI	NA	351	6011, 267	NA	442	5677, 685, 623	311	4866
200† yr- 95% CI	824, 487, 469	757, 446	589	4985, 771	625, 482	5677, 657, 632, 483	924, 615, 521	530, 413
200 yr- 99% CI	NA	485, 466	5677	NA	NA	400	NA	400

LOI- Loss-on-ignition
PS- Particle Size
EMDs- End-member distributions
CI- Confidence interval
NA- Not applicable; power spectrum did not have any peaks above this CI
† Sampling interval used for spectral analysis; corresponds to bin interval for the histogram time series used for individual spectral analyses

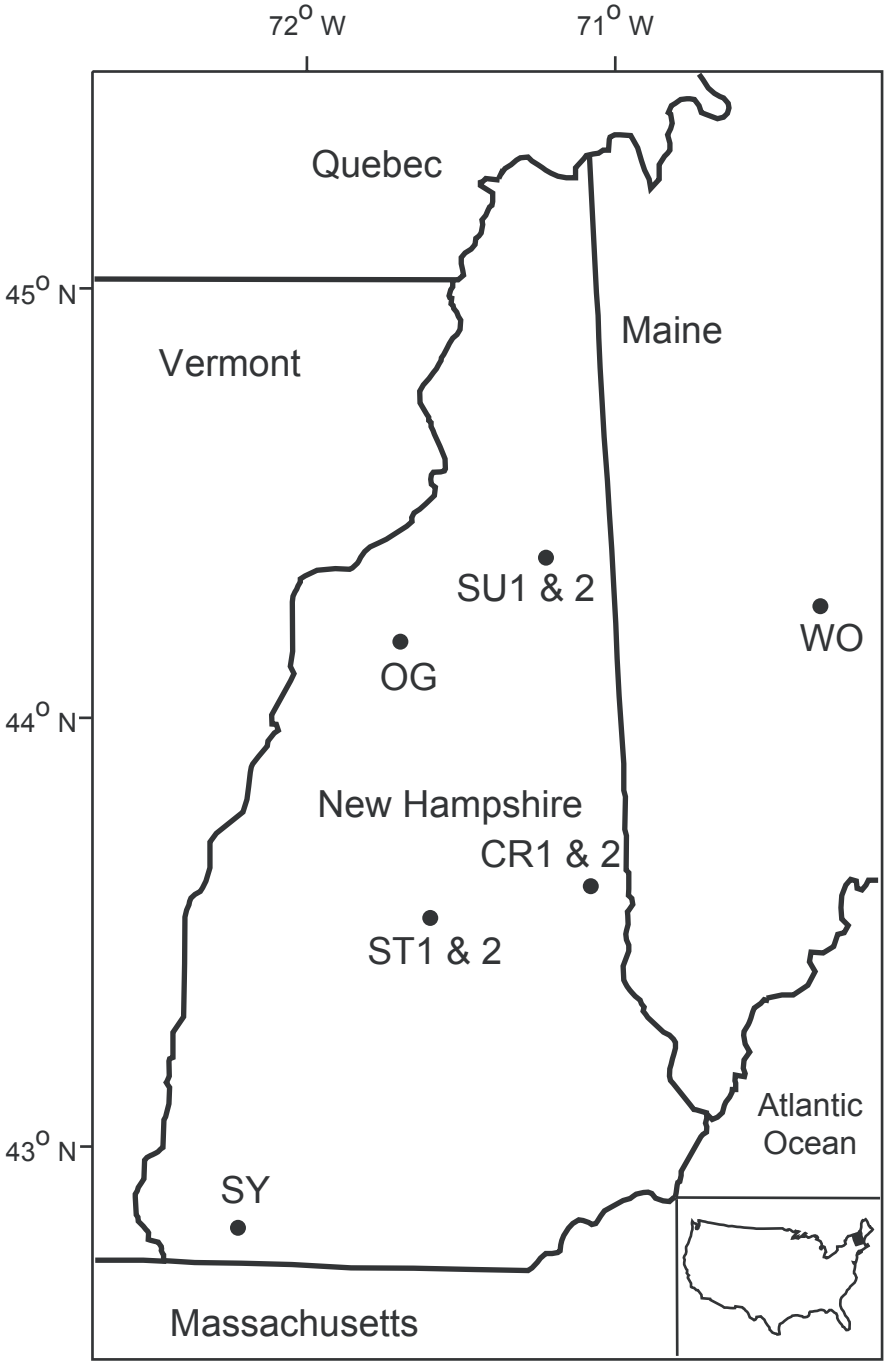

Parris, figure 1

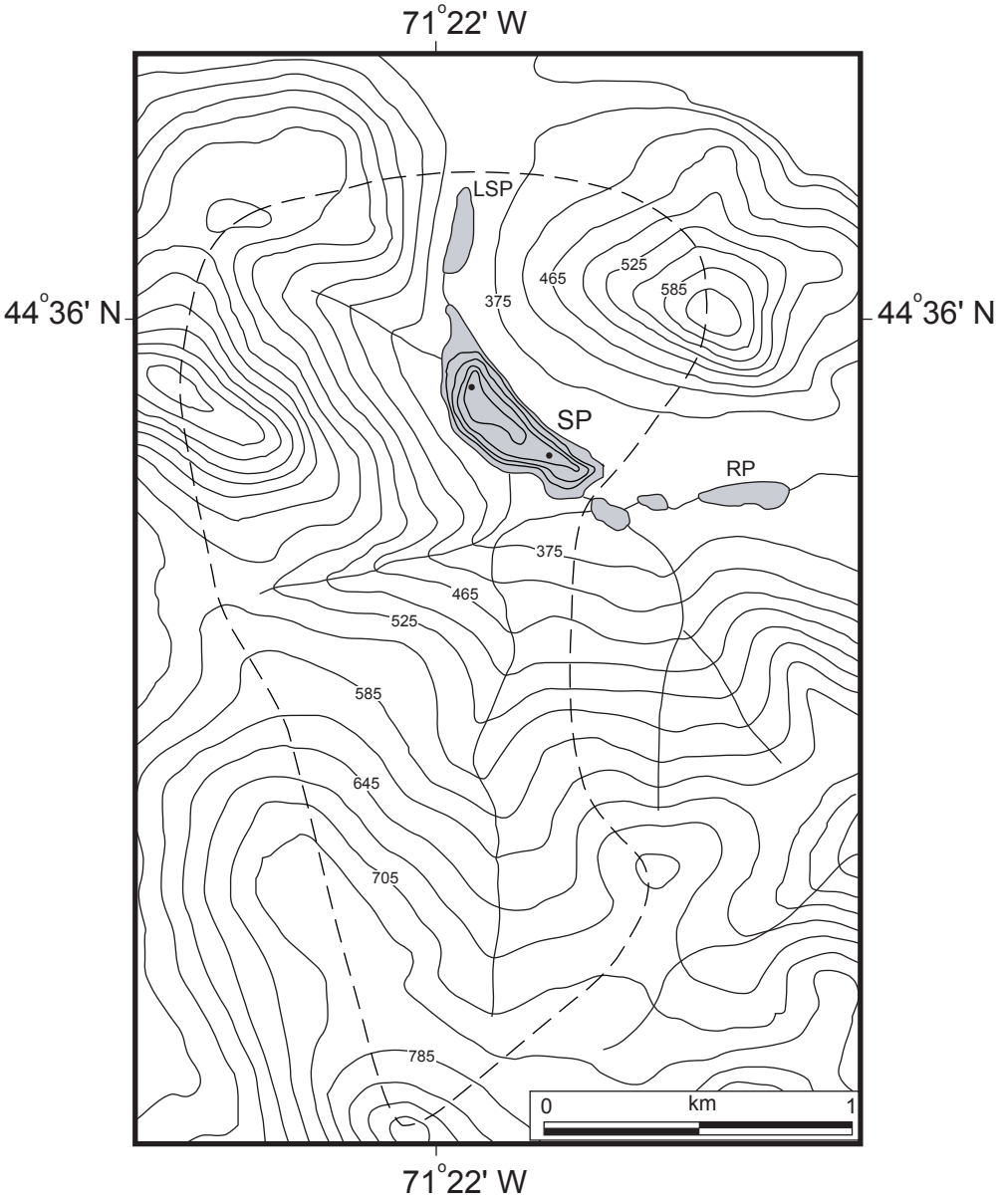

Parris, figure 2

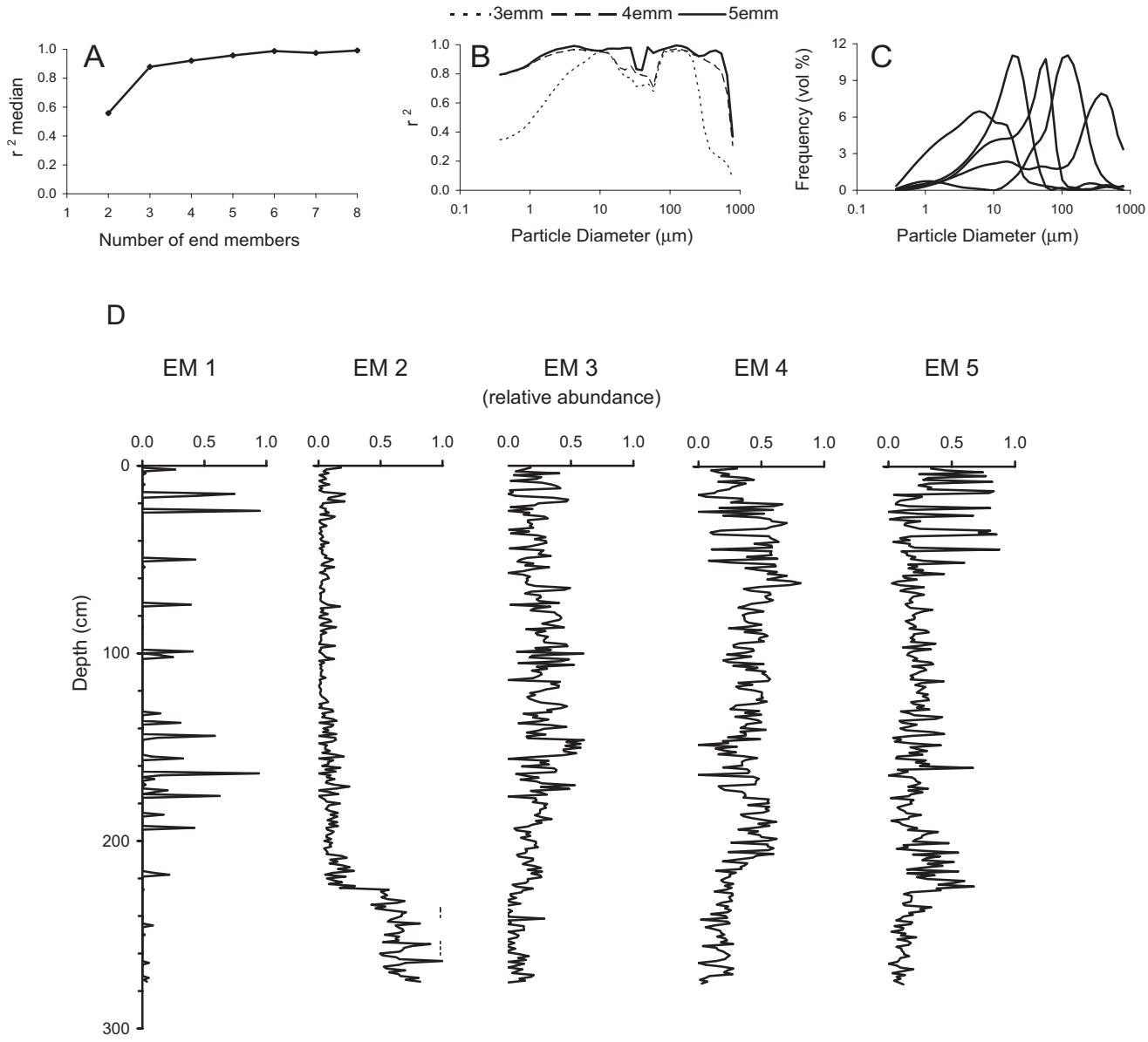

Parris, Figure 3

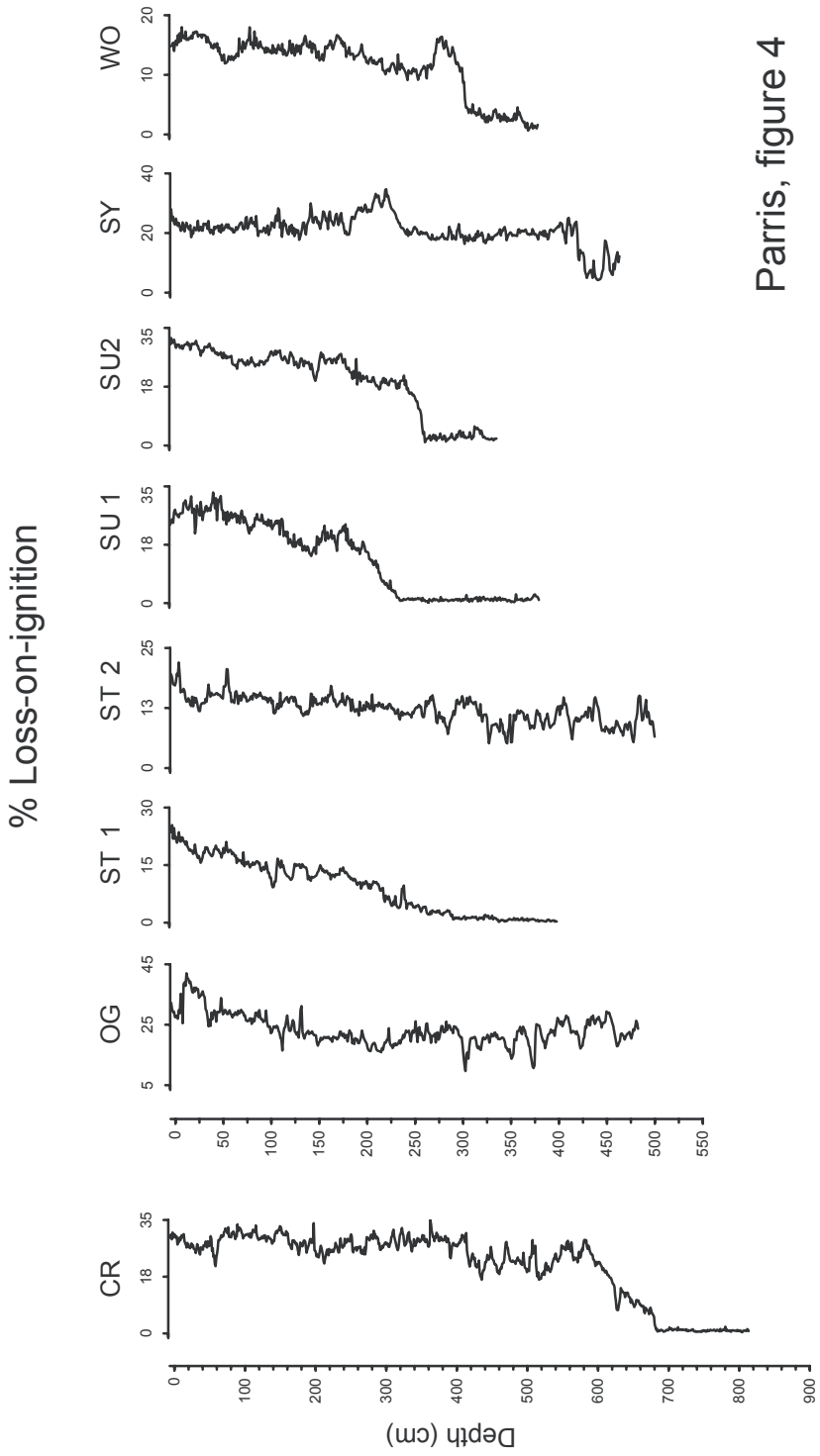

Parris, figure 4

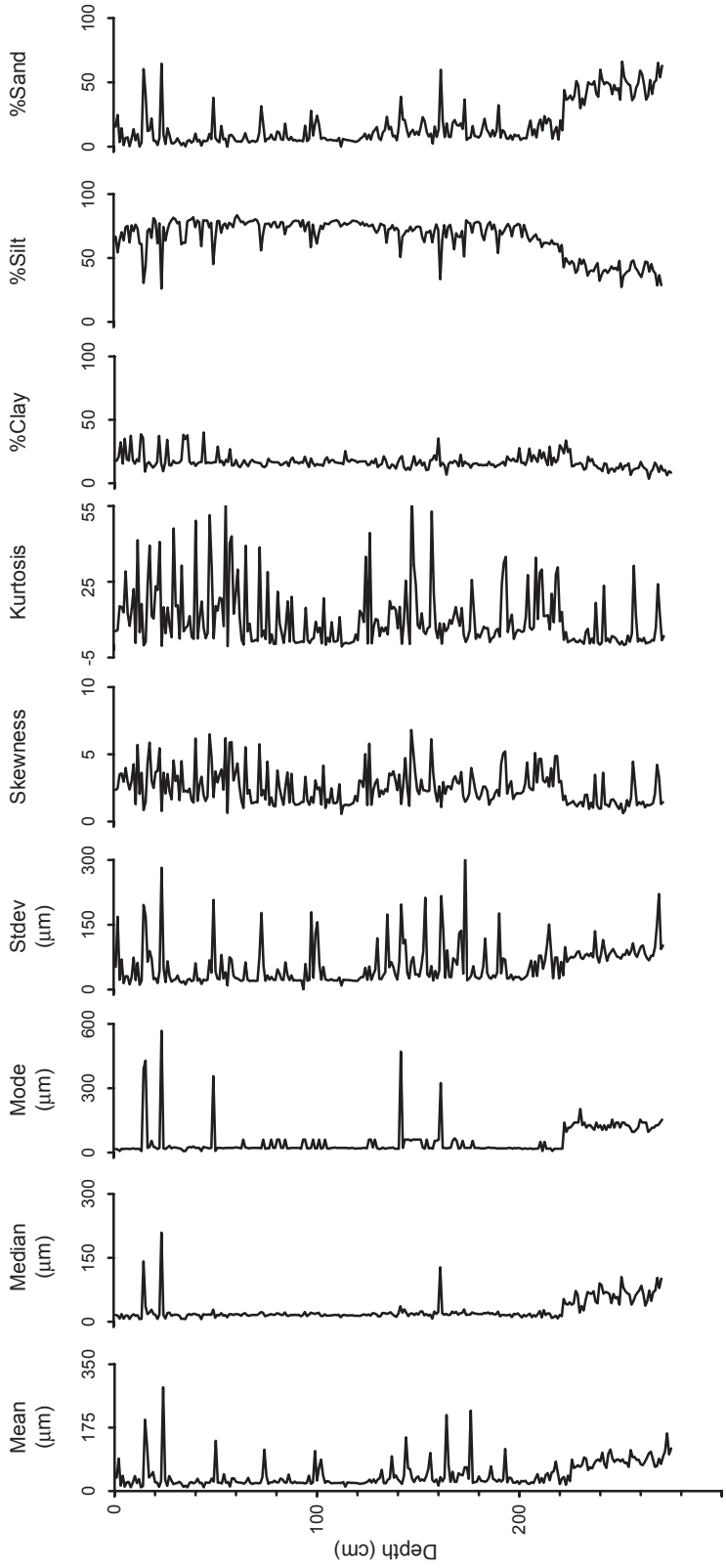

Parris, Figure 5

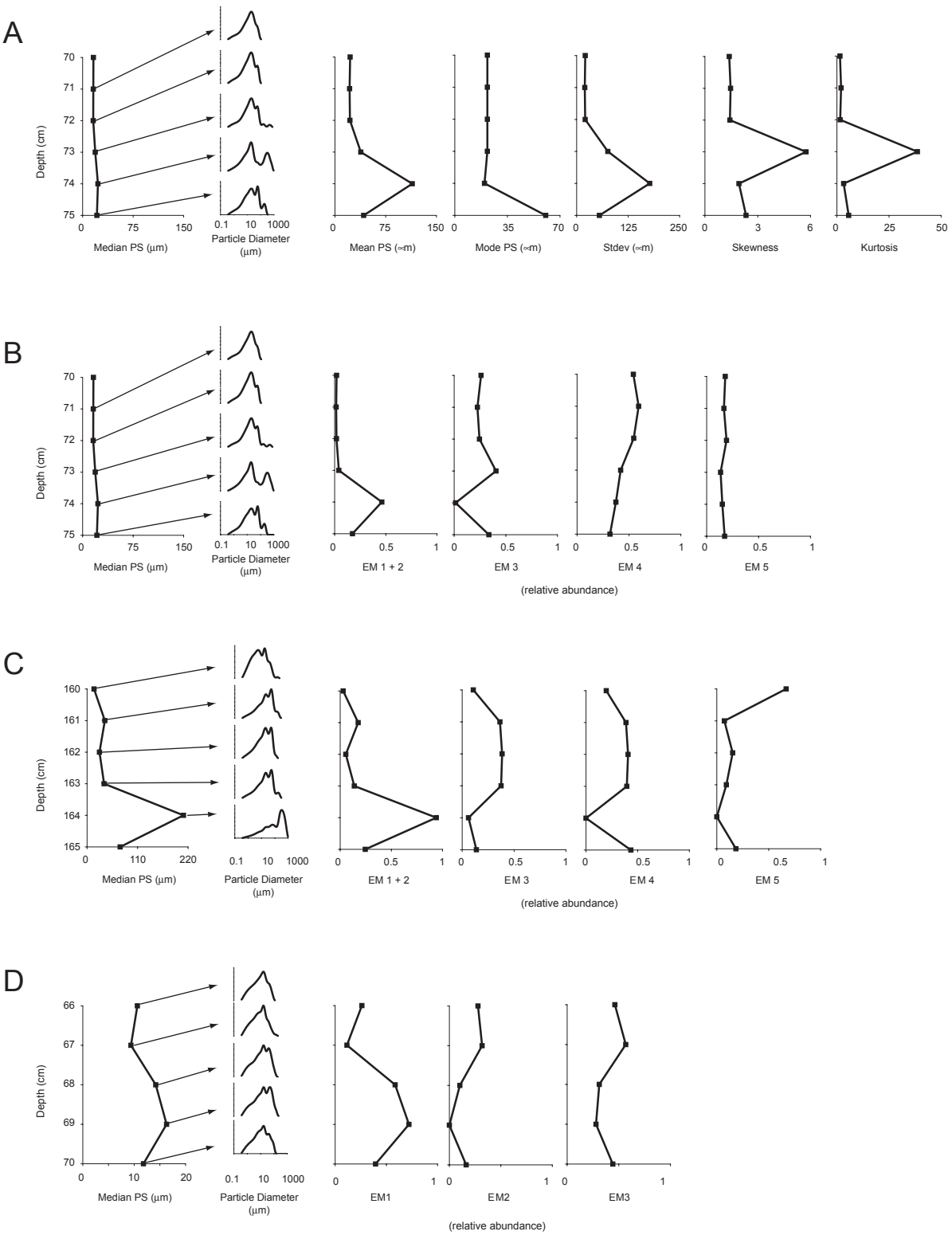

Parris, figure 6

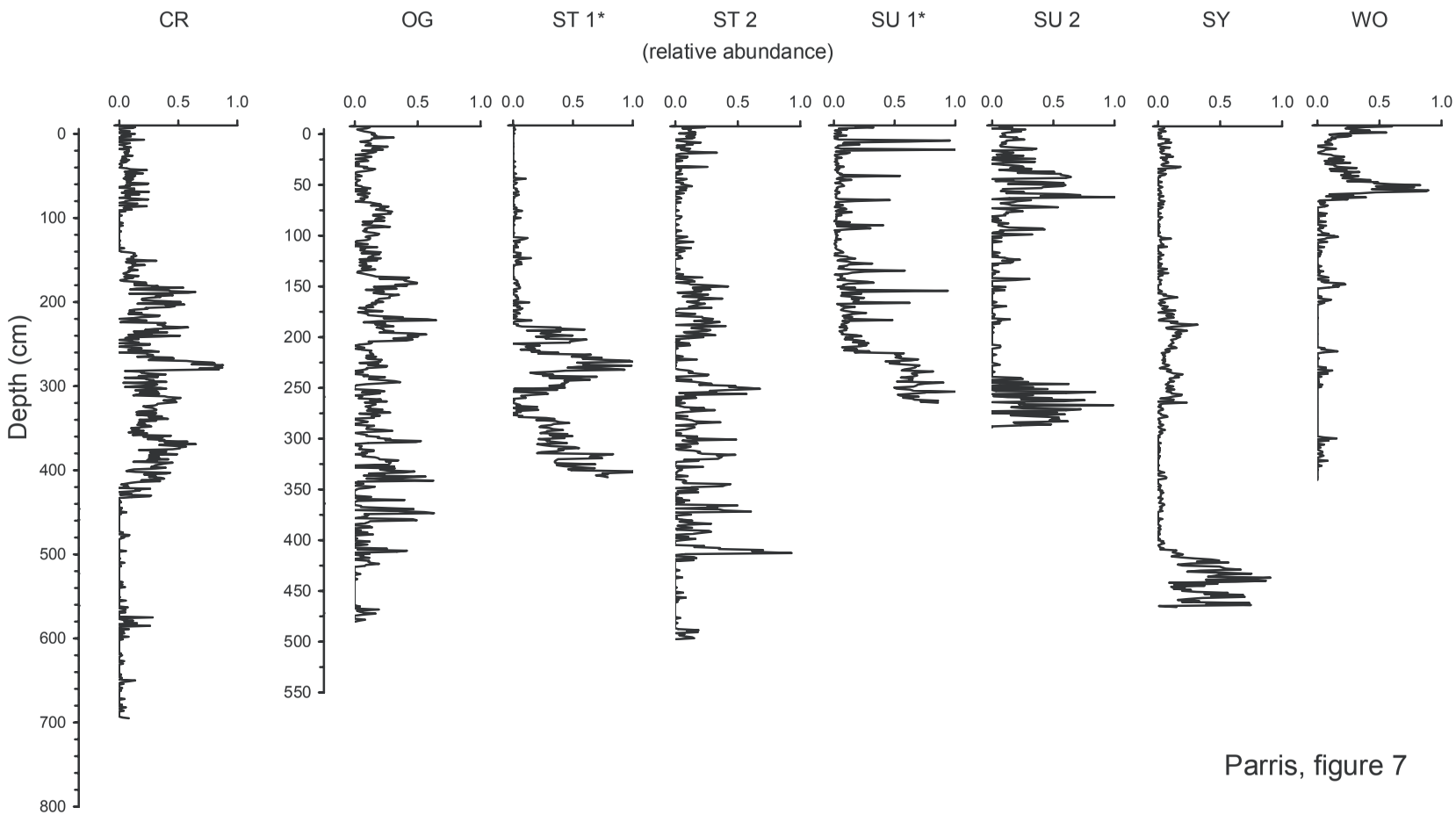

Parris, figure 7

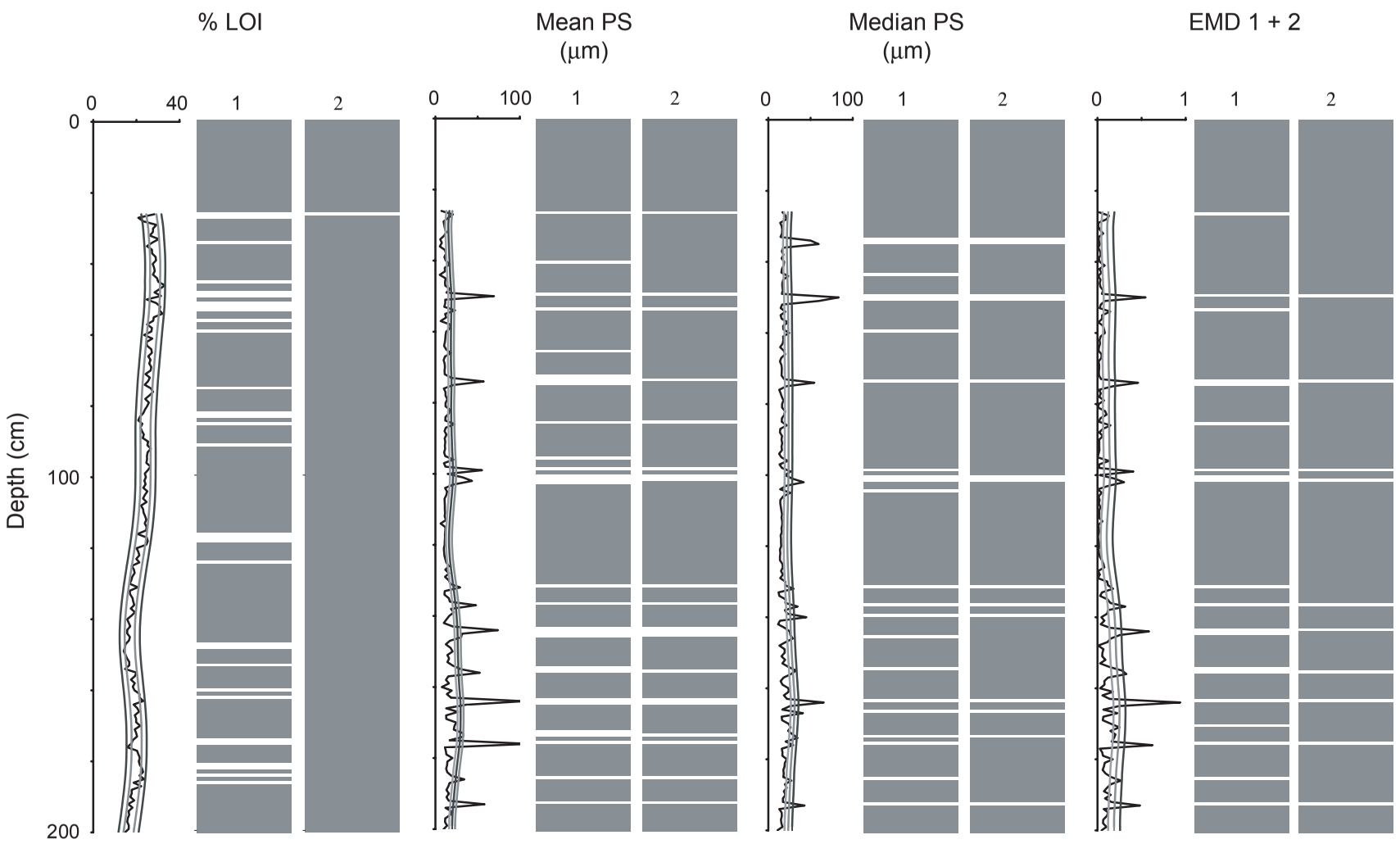

Parris, figure 8

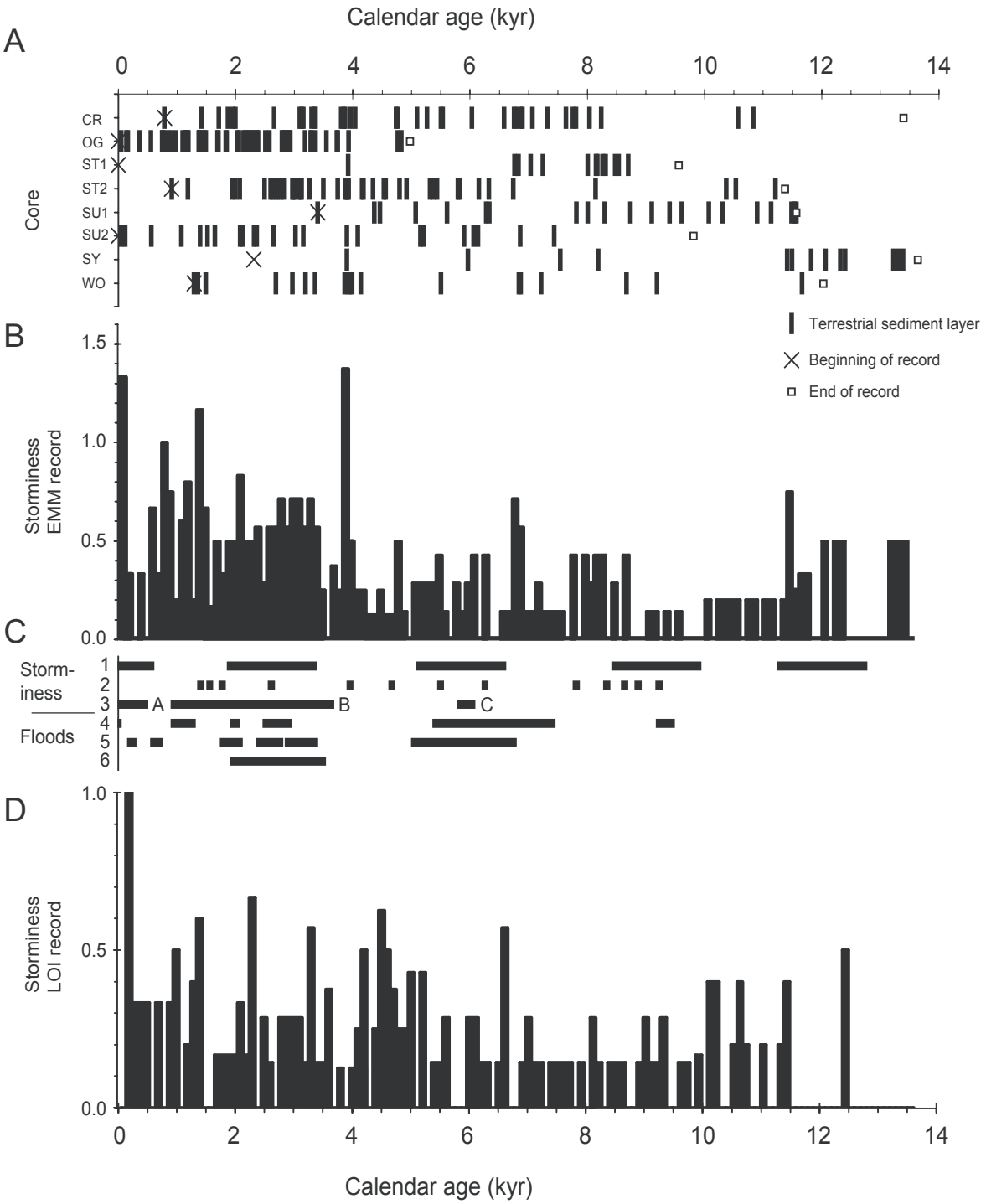

Parris, figure 9

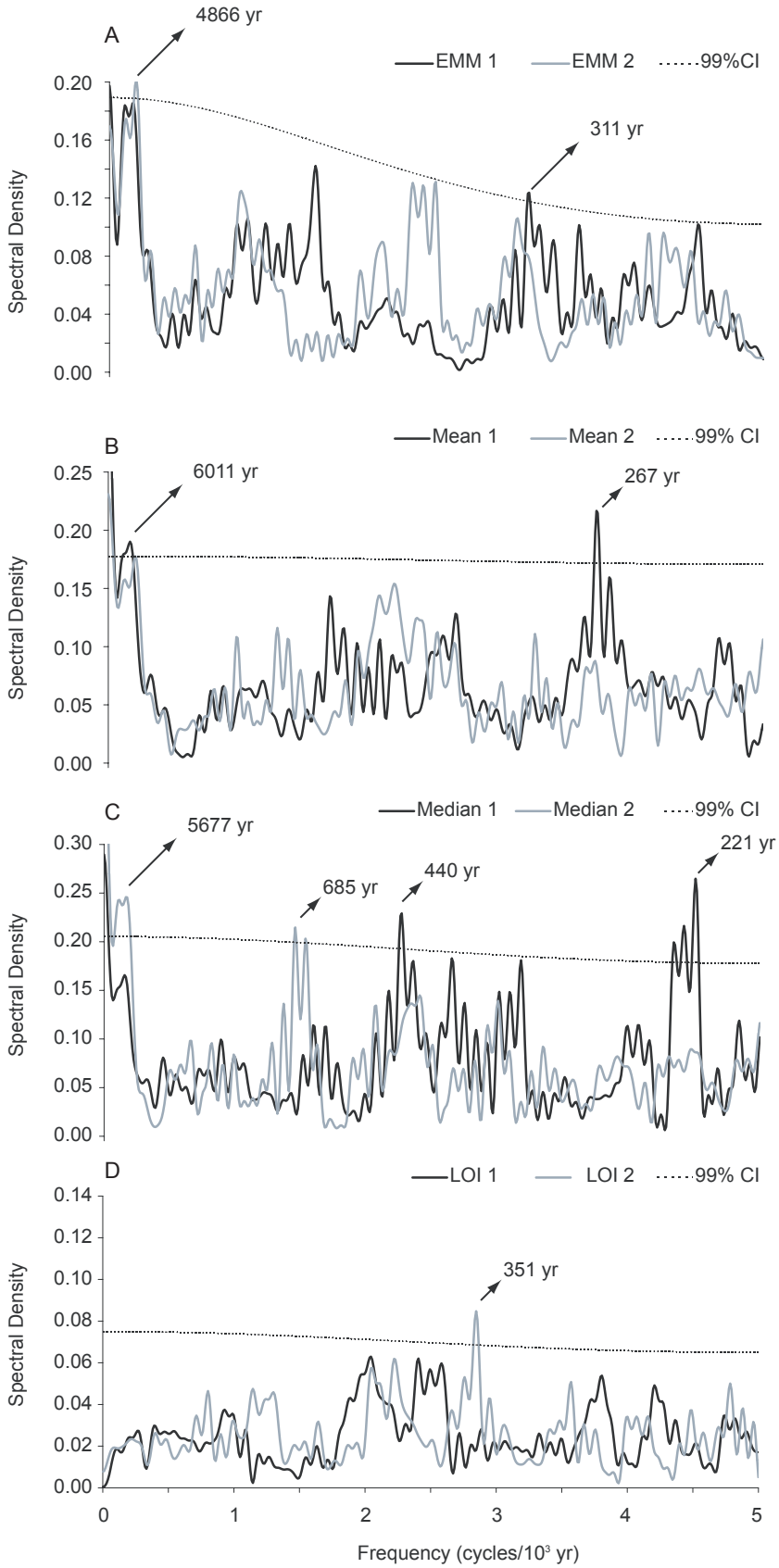

Parris, figure 10

CHAPTER 5

The use of particle size analysis for revealing storm and flood patterns in New England lake sediment was a great success. This approach to analyzing lake sediment is a sensitive, illustrative means to quantify the physical process of terrestrial sediment delivery. It reveals a high resolution pattern of storms and floods in New Hampshire and Maine. It also promises to provide a great deal of insight to future paleostorm studies in New England.

Summary of Findings

1. Although terrestrially-derived sediment layers are often lighter than the surrounding gytta in sediment cores, many of the layers in cores were not visible with the naked eye. Magnetic susceptibility (MS), loss-on-ignition (LOI), and particle size analysis do reveal discreet terrestrial sediment layers, though, and particle size analysis reveals an upward fining of terrestrially-derived sediment layers.
2. Particle size analysis is the most sensitive method for revealing terrestrially-derived sediment layers related to storm-induced erosion and deposition in lake sediment cores. Particle size data reveal more of these paleohydrologic events than other proxy methods, such as MS and LOI. End-member modeling of particle size distributions reveals a detailed record of deposition in lakes, as far back in time as the length of the sediment record.
3. A delicate balance must be struck with coring location, as those cores taken nearest to the delta foreslope have the most terrestrial sediment layers, which

also are more easily identifiable by thicker layers with sand-sized particles, as opposed to thin layers of coarse silt in more distal cores.

4. Basinwide hydrologic events do occur as indicated by contemporaneous terrestrially-derived flood layers in cores near different deltas within the same lake. However, disparate ages for terrestrially-derived flood layers between the same cores reveal that some hydrologic events do not cause basinwide deposition. Furthermore, a disparity between the ages of terrestrially-derived flood layers also exists between core records from different basins throughout New England. Such a lack of direct correlation is likely influenced both by mechanism (i.e. convective thunderstorms vs. large scale synoptic storms) and by factors influencing landscape response to storms or flood mechanisms within individual and separate basins.

5. Combining the ages of events reveals periods of storminess in NH and ME centered around ~ 0.8, 1.4, 2.1, 3.0, 3.9, 6.8, 8.2, 11.5, and 13.3 cal kya. This chronology of storms is most similar to geologic records of hurricanes on the Atlantic and northern Gulf of Mexico coast, as well as floods in the mid-western United States. However, the NH and ME chronology of storms is significantly different than other paleostorm patterns as measured by proxy methods in lake sediment studies from Vermont and New York (Brown et al., 2000; Noren et al., 2002). In comparison to these studies, there are no strong millennial scale cycles, rather there appears to be more strength in centennial

scale spectra. This difference may be related to climatic forcing, (i.e. more dominant influence of hurricane activity), methodological differences, or both.

Suggestions for future research

1. **Short and box core collection combined with Pb-210 dating.** Short cores preserve the historic sediment record and can be dated using Pb-210 for the purpose of matching terrestrially-derived sediment layers to written and measured records of precipitation in historic times. Such correlation between the sediment record and the precipitation record is necessary to determine the characteristic response and process of storm-induced deposition. As seen by my results, terrestrially-derived sediment layers are not always deposited uniformly, rather they vary with proximity to source, and also seen by my results, basinwide deposition does not always occur due to differing hydrologic events and to differing landscape conditions. Because short cores also are considerably shorter in length than Reasoner cores, they can be collected all over the delta and in the stream channel adjacent to the lake. Particle size analysis of short cores taken throughout deltas on the Gulf of Mexico coast successfully tracked deposition in all directions from the adjacent channel supplying these deltas to offshore locations (Okazaki et al., 2001). Such directional transport analysis, when paired with the temporal analysis provided by Pb-210, is crucial to developing any measurement of the magnitude of storms throughout the past. This analysis is best done on a lake for which a Reasoner core already has been analyzed for MS, LOI, and particle size. The particle size populations then can be examined throughout

the entire Holocene, and most importantly, the effect of land use on depositional patterns in the historic sediment record can be separated better from the storm-induced patterns.

2. **Isotopic and compositional analysis of short cores.** Isotopic analysis of short cores can help reveal the effect of agricultural runoff in the historic sediment record (Lord, 2002). Compositional analysis, paired with particle size analysis, of sediment cores taken in the Arabian Sea aided the interpretation of sediment source and path of deposition (Prins et al., 2000). Along with the short core analyses mentioned above, such compositional and particle size analysis could aid in the determination of sediment source and path of deposition. Furthermore, some machines are capable of simultaneously providing particle size and compositional data, such as SEM, which would provide two independent means of measuring particle size, laser diffraction and image analysis, to check results. Such compositional data also aids particle size analysis as it may help determine the origin and fate of aggregate particles, or at the very least, if pretreatment techniques need be altered, and if there is minerologic influence on laser diffraction, such as the presence of micas.
3. **Particle size analysis of Noren et al.'s (2002) cores.** Significant differences in the climate patterns suggested by my data and Noren et al.'s (2002) data will never be resolved until particle size analysis is done on their cores. Large scale climate patterns for all of New England may be hiding in such data. Also, such a

combined data set could aid analysis of the geographic distribution of storms in New England.

COMPREHENSIVE BIBLIOGRAPHY

Alley, R. B., Mayewski, P. A., Sowers, T., Stuiver, M., Taylor, K. C., and Clark, P. U., 1997, Holocene climatic instability: A prominent, widespread event 8,200 yr. ago: Geology, v. 25, no. 6, p. 483-486.

Ambers, R. K., 2001, Using the sediment record in a western Oregon flood-control reservoir to assess the influence of storm history and logging on sediment yield: Journal of Hydrology, v. 244, no. 3-4, p. 181-200.

Antevs, E., 1922, The recession of the last ice sheet in New England, American Geographical Society Research Series, 120 p.

Baker, V. R., 1988, Flood erosion, in Baker, V. R., Kochel, R. C., and Patton, P. C., eds., Flood Processes: Flood Geomorphology: New York, John Wiley and Sons, p. 81-96.
Barth, H. G., 1984, Modern Methods of Particle Size Analysis: New York, John Wiley and Sons, 309 p.

Beierle, B. D., Lamoureux, S. F., Cockburn, J. M. H., and Spooner, I., 2002, A new method for visualizing particle size distributions: Journal of Paleolimnology, v. 27, no. 2, p. 279-283.

Benn, D. I., and Evans, D. J. A., 1998, Glaciers and Glaciation: London, Arnold Publishers, 734 p.

Bengtsson, L., and Enell, M., 1986, Chemical analysis, in B.E. Berglund, ed., Handbook of Holocene Palaeoecology and Palaeohydrology: New York, Wiley and Sons, p. 423-454.

Bierman, P., Lini, A., Zehfuss, P., Church, A., Davis, P. T., Southon, J., and Baldwin, L., 1997, Postglacial ponds and alluvial fans: Recorders of Holocene landscape history: GSA Today, v. 7, no. 10, p. 1-8.

Boggs, S. J., 1995, Principles of Sedimentology and Stratigraphy: New Jersey, Prentice Hall, Inc., 774 p.

Bond, G. C., Showers, W., Cheseby, M., Lotti, R., Almasi, P., deMenocal, P., Priore, P., Cullen, H., Hajdas, I., and Bonani, G., 1997, A Pervasive Millenial-Scale Cycle in North Atlantic Holocene and Glacial Climates: Science, v. 278, no. 5341, p. 1257-1266.

Boose, E. R., Chamberlin, K. E., and Foster, D. R., 2001, Landscape and regional impacts of hurricanes in New England: Ecological Monographs, v. 71, no. 1, p. 27-48.

Bosley, A. C., Bierman, P. R., Noren, A., and Galster, J., 2001, Identification of paleoclimatic cycles during the Holocene using grain size analysis of sediments cored from Lake Morey in Fairlee, VT, in Geological Society of America, Northeastern Section, 36th annual meeting, p. 85.

Brakenridge, G. R., 1980, Widespread episodes of stream erosion during the Holocene and their climatic cause: Nature, v. 283, p. 655-656.

Broomhead, D. S., and King, G. P., 1986, Extracting qualitative dynamics from experimental data: Physica D, v. 20, p. 217-236.

Brown, P., Kennett, J. P., and Ingram, B. L., 1999, Marine evidence for episodic Holocene megafloods in North America and the northern Gulf of Mexico: Paleoceanography, v. 14, no. 4, p. 498-510.

Brown, S., 1999, Terrestrial Sediment Deposition in Ritterbush Pond: Implications for Holocene Storm Frequency in norther Vermont [Master's thesis]: University of Vermont, 170 p.

Brown, S. L., Bierman, P. R., Lini, A., and Southon, J., 2000, 10 000 yr record of extreme hydrologic events: Geology, v. 28, no. 4, p. 335-338.

Brown, S., Bierman, P., Lini, A., Southon, J., and Davis, P. T., 2002, Lake cores as archives of Holocene watershed erosion events: Journal of Paleolimnology, v. 28, p. 219-236.

Bull, W. B., 1991, Geomorphic responses to climate change: New York, Oxford University Press, 326 p.

Campbell, C., 1998, Late Holocene Lake Sedimentology and Climate Change in Southern Alberta, Canada: Quaternary Research, v. 49, p. 96-101.

Campbell, I. D., Campbell, C., Apps, M. J., Rutter, N. W., and Bush, A. B. G., 1998, Late Holocene ~1500 yr climatic periodicities and their implications: Geology, v. 26, no. 5, p. 471-473.

Campbell, I. D., Last, W. M., Campbell, C., Clare, S., and McAndrews, J. H., 2000, The late-Holocene paleohydrology of Pine Lake, Alberta: a multiproxy investigation: Journal of Paleolimnology, v. 24, p. 427-441.

Collins, E. S., Scott, D. B., and Gayes, P. T., 1999, Hurricane records on the South Carolina coast: Can they be detected in the sediment record?: Quaternary International, v. 56, p. 15-26.

Conkey, L. E., 1986, Red spruce tree-ring width and densities in eastern North America as indicators of past climate: Quaternary Research, v. 26, p. 232-243.

Conlan, A., 2001, Spatial extent of sediment pulses in Lake Morey, Fairlee, VT, in Vermont Geological Society Spring Meeting, Norwich University, Norwich, VT.

Cronin, T., Willard, D., Karlsen, A., Ishman, S., Verardo, S., McGeehin, J., Kerhin, R., Holmes, C., Colman, S., and Zimmerman, A., 2000, Climatic variability in the eastern United States over the past millenium from Chesapeake Bay sediments: Geology, v. 28, no. 1, p. 3-6.

Dansgaard, W., Johnsen, S. J., Clausen, H. B., Dahl-Jensen, D., Gundestrup, N., Hammer, C. U., and Oeschger, H., 1984, North Atlantic climatic oscillations revealed by deep Greenland ice cores, in Hansen, J. E., and Takahashi, T., eds., Climate processes and climate sensitivity: Washington, D.C., American Geophysical Union, p. 288-306.
Davis, M. B., Spear, R., and Shane, L. C., 1980, Holocene Climate of New England: Quaternary Research, v. 14, p. 240-250.

Davis, R. B., and Jacobson, G. L., Jr, 1985, Late glacial and early Holocene landscapes in northern New England and adjacent areas of Canada: Quaternary Research, v. 23, p. 341-368.

Digerfeldt, G., 1986, Studies on past lake-level fluctuations, in Berglund, B. E., ed., Handbook of Holocene Palaeoecology and Palaeohydrology: New York, John Wiley and Sons, p. 127-143.

Donnelly, J. P., Bryant, S. S., Butler, J., Dowling, J., Fan, L., Hausmann, N., Newby, P. E., Shuman, B. N., Stern, J., Westover, K., and Webb III, T., 2001a, 700 yr. sedimentary record of intense hurricane landfalls in southern New England: Geological Society of America Bulletin, v. 113, no. 6, p. 714-727.

Donnelly, J. P., Roll, S., Wengren, M., Butler, J., Lederer, R., and Webb III, T., 2001b, Sedimentary evidence of intense hurricane strikes from New Jersey: Geology, v. 7, p. 615-618.

Dott, R. H., Jr., 1983, 1982 SEPM Presidential Address: Episodic Sedimentation- How normal is average? How rare is rare? Does it matter?: Journal of Sedimentary Petrology, v. 53, no. 1, p. 5-23.

Drake, E. D., 1999, Temporal and Spatial Variability of the sediment grain-size distribution on the Eel shelf: the flood layer of 1995: Marine Geology, v. 154, p. 169-182.

Dunne, T. B., and Leopold, L. B., 1978, Water in Environmental Planning: San Francisco, W.H.Freeman, 818 p.

Easterling, D. R., Meehl, G. A., Parmesan, C., Changnon, S. A., Karl, T. R., and Mearns, L. O., 2000, Climate Extremes: Observations, Modeling, and Impacts: Science, v. 289, no. 5487, p. 2068-2074.

Eden, D. N., and Page, M. J., 1998, Palaeoclimatic implications of a storm erosion record from late Holocene lake sediments, North Island, New Zealand: Palaeogeography, Palaeoclimatology, Palaeoecology, v. 139, p. 37-58.

Edwards, B. D., 2002, Variations in sediment texture on the northern Monterey Bay National Marine Sanctuary continental shelf: Marine Geology, v. 181, p. 83-100.

Ely, L. L., Enzel, Y., Baker, V. R., and Cayan, D., 1993, A 5,000-Year Record of Extreme Floods and Climate Change in the Southwestern United States: Science, v. 262, p. 410-412.

Enzel, Y., Cayan, D., Balling, R. C., Jr., Wells, S. G., Anderson, R. Y., and Brown, W. J., 1988, Large-scale "anomalous" Northern Pacific storm patterns recorded in the Mojave River hydrologic system, American Geophysical Union, 1988 fall meeting, American Geophysical Union, p. 1220.

Folk, R. L., and Ward, W. C., 1957, Brazos River bar: a study in the significance of grain size parameters: Journal of Sedimentary Petrology, v. 27, p. 3-26.

Gran, S. E., Bierman, P., and Nichols, K. K., 1999, Teaching winter geohydrology using frozen lakes and snowy mountains: Journal of Geoscience Education, v. 47, no. 5, p. 420-447.

Gremillion, P. T., and Rodbell, D. T., 1998, Overturn history of an iron-rich meromictic lake as an indicator of extreme meteorological events, in Geological Society of America, annual meeting, p. 114.

Grove, J. M., 1988, The Little Ice Age: London, Methuen, 498 p.

Hass, H. C., 1993, Depositional processes under changing climate: upper SubAtlantic granulometric records from the Skagerrak (NE-North Sea): Marine Geology, v. 111, p. 361-378.

Hayne, M., and Chappell, J., 2001, Cyclone frequency during the last 5,000 years at Curacoa Island, north Queensland, Australia: Palaeogeography, Palaeoclimatology, Palaeoecology, v. 168, no. 3-4, p. 207-219.

Hupp, C. R., 1988, Plant ecological aspects of flood geomorphology and paleoflood history, in Baker, V. R., Kochel, R. C., and Patton, P. C., eds., Flood Processes: Flood Geomorphology: New York, John Wiley and Sons, p. 335-356.

I, I. W. G., 2001, Climate Change 2001: The Scientific Basis, in Intergovernmental Panel on Climate Change, Geneva, Switzerland.

Jackson, S. T., and Whitehead, D. R., 1991, Holocene vegetation patterns in the Adirondack Mountains: Ecology, v. 72, no. 2, p. 641-653.

Jennings, K. L., Fredriksen, G., Noren, A. J., and Bierman, P. R., 1999, Characterizing alluvial fan deposits in Vermont and eastern New York, in Geological Society of America, annual meeting, p. 50-51.

Jennings, K. L., 2001, Depositional Histories of Vermont Alluvial Fans [Master's thesis]: University of Vermont, 265 p.

Jennings, K. L., Bierman, P., and Southon, J., 2003, Timing and style of deposition on humid-temperate fans, Vermont, USA: Geological Society of America Bulletin, v. 115, no. 2, p. 182-199.

Keim, B., Mayewski, P. A., Zielinski, G. A., Wake, C., Carpenter, K., Cox, J., Souney, J., Sanborn, P., and Rodgers, M., 1998, New England's Changing Climate, Weather and Air Qualitry: Durham, Hew Hampshire, University of New Hampshire, 48 p.

Knox, J. C., 1993, Large increases in flood magnitude in reponse to modest changes in climate: Nature, v. 361, no. 6411, p. 430-432.

-, 1999, Sensitivity of modern and Holocene floods to climate change: Quaternary Science Reviews, v. 19, p. 439-457.

Kochel, R. C., and Baker, V. R., 1982, Paleoflood hydrology: Science, v. 215, no. 4531, p. 353-361.

Komar, P. D., 1988, Sediment transport by floods, in Baker, V. R., Kochel, R. C., and Patton, P. C., eds., Flood Processes: Flood Geomorphology: New York, John Wiley and Sons, p. 97-112.

Kutzbach, J. E., 1987, Model simulations of the climatic patterns during the deglaciation of North America, in Ruddiman, W. F., and Wright, H. E., eds., North America and adjacent oceans during the last deglaciation: Boulder, CO, Geological Society of America, p. 425-446.

Laird, L. D., and Campbell, I. D., 2000, High resolution palaeofire signals from Christina Lake, Alberta: A comparison of the charcoal signals extracted by two different methods: Palaeogeography, Palaeoclimatology, Palaeoecology, v. 164, p. 111-123.

Lamb, H. H., 1979, Variation and changes in the wind and ocean circulation: the Little Ice Age in the northeast Atlantic: Quaternary Research, v. 11, p. 1-20.

Lamoureux, S. F., 2000, Five centuries fo interannual sediment yield and rainfall-induced erosion in the Canadian High Arctic recorded in lacustrine varves: Water Resources Research, v. 36, p. 309-318.

Lamoureux, S. F., England, J. H., Sharp, M. J., and Bush, A. B. G., 2001, A varve record of increased 'Little Ice Age' rainfall with volcanic acitivity, Arctic Archipelago, Canada: The Holocene, v. 11, no. 2, p. 243-249.

Lavkulich, L. M., and Wiens, J. H., 1970, Comparison of Organic Matter Destruction by Hydrogen Peroxide and Sodium Hypochlorite and Its Effects on Selected Mineral Constituents, in Soil Science Society of America Proceedings, p. 755-758.

Lin, L., 1996, Environmental changes inferred from pollen analysis and 14C ages of pond sediments, Green Mountains, Vermont [Master's thesis]: University of Vermont, 125 p.

Liu, K., and Fearn, M. L., 1993, Lake-sediment record of late Holocene hurricane activities from coastal Alabama: Geology, v. 21, p. 793-796.
-, 2000, Reconstruction of Prehistoric Landfall Frequencies of Catastrophic Hurricanes in Northwestern Florida from Lake Sediment Records: Quaternary Research, v. 54, p. 238-245.

Lord, A., Lini, A., Toke, N., Parris, A., and Bierman, P., 2001, Post-glacial evolution of northern New England lakes, Geological Society of America, 2001 annual meeting, Geological Society of America (GSA), p. 314.

Lord, A. M., 2003, Evolution rates of post-glacial lake ecosystems in northern New England: A Geochemical Study using Lake Sediments [Master's thesis]: University of Vermont, 111 p.

Ludlum, D., 1963, Early American Hurricanes: Boston, American Meteorological Society, 198 p.
-, 1996, The Vermont Weather Book: Montpelier, VT, Vermont Historical Society, 302 p.

Mann, M. E., and Lees, J. M., 1996, Robust estimation of background noise and signal detection in climatic time series: Climatic Change, v. 33, p. 409-445.

Matthews, M. D., 1991, The effect of pretreatment on size analysis, in Syvitski, J. P. M., ed., Principles, methods, and application of particle size analysis: Cambridge, Cambridge University Press, p. 34-42.

McCave, I. N., Manighetti, B., and Robinson, S. G., 1995, Sortable silt and fine sediment size/composition slicing; parameters for paleocurrent speed and paleooceanography: Paleoceanography, v. 10, p. 593-610.

Meeks, H. A., 1986, Vermont's land and resources: Shelburne, VT, New England Press, 332 p.

Montgomery, D. R., and Buffington, J. M., 1997, Channel-reach morphology in mountain drainage basins: Geological Society of America Bulletin, v. 109, no. 5, p. 596-611.

Mullins, H. T., 1998, Environmental change controls of lacustrine carbonate, Cayuga Lake, New York: Geology, v. 26, no. 5, p. 443-446.

Meyers, P.A., and Ishiwatari, R., 1995, Organic matter accumulation records in lake sediments, in A Lerman, and Gat, J., eds., Physics and Chemistry of Lakes: New York, Springer – Verlag p. 279- 290.

Nesje, A., Dahl, S. O., Matthews, J. A., and Berrisford, M. S., 2001, A ~4,500-yr record of river floods obtained from a sediment core in Lake Atnsjfen, eastern Norway: Journal of Paleolimnology, v. 25, no. 3, p. 329-342.

Newby, P. E., Killoran, P., Waldorf, M. R., Shuman, B. N., Webb, R. S., and Webb III, T., 2000, 14,000 years of sediment, vegetation, and water-level changes at the Makepeace Cedar Swamp, southeastern Massachusetts: Quaternary Research, v. 53, p. 352-368.

Nittrouer, C. A., 1999, STRATAFORM: Overview of its design and synthesis of its results: Marine Geology, v. 154, no. 1-4, p. 3-12.

Noren, A. J., Bierman, P. R., Galster, J. C., Lini, A., Jennings, K. L., and Janukajtis, F. A., 1999, A regional record of Holocene storms from terrigenous lake sediment, northern New England, in Geological Society of America, annual meeting, p. 51.

Noren, A. J., Bierman, P. R., and Galster, J. C., 2001, A 13,000-year regional record of Holocene storms from terrigenous lake sediment, northeastern USA, in Geological Society of America, Northeastern Section, 36th annual meeting, p. 57.

Noren, A. J., Bierman, P. R., Steig, E. J., Lini, A., and Southon, J., 2002, Millennial-scale storminess variability in the northeastern United States during the Holocene epoch: Nature (London), v. 419, no. 6909, p. 821-824.

Noren, A., 2002, A 13,000-Year Regional Record of Holocene Storms in the Northeastern United States [Master's thesis]: University of Vermont, 170 p.

Nott, J., and Hayne, M., 2001, High frequency of 'super-cyclones' along the Great Barrier Reef over the past 5,000 years: Nature, v. 413, p. 508-512.

O'Brien, S. R., Mayewski, P. A., Meeker, L. D., Meese, D. A., Twickler, M. S., and Whitlow, S. I., 1995, Complexity of Holocene climate as reconstructed from a Greenland ice coe: Science, v. 270, p. 1962-1964.

Okazaki, H., Stanley, J., and Wright, E. E., 2001, Tecolutla and Nautla Deltas, Veracruz, Mexico: Texture to Evaluate Sediment Entrapment on Deltaic Plains and Bypassing onto the Gulf of Mexico Margin: Journal of Coastal Research, v. 17, no. 3, p. 755-761.

Ouellet, M., 1997, Lake sediments and Holocene seismic hazard assessment within the St. Lawrence Valley, Quebec: Geological Society of America Bulletin, v. 109, p. 631-642.

Page, M. J., Trustrum, N. A., and DeRose, R. C., 1994, A high-resolution record of storm-induced erosion from lake sediments, New Zealand: Journal of Paleolimnology, v. 11, p. 333-348.

Paillard, D., Labeyrie, L., and Yiou, P., 1996, Macintosh program performs time-series analysis: Eos, transactions, v. 77, p. 379.

Parris, A., Bosley, A., Bierman, P., Lini, A., Noren, A., Lord, A., Conlan, A., and Morgan, L., 2001, Grain by grain; Holocene storms and hillslope erosion in New England, in Geological Society of America Abstracts with Programs, p. 314.

Parris, A., Bosley, A., Noren, A., Bierman, P., Lini, A., and Ryan, P., 2002, Holocene flood frequency in New England: Large, episodic events in the sediment record, in GSA annual meeting, Denver, CO, p. 314.

Peteet, D. M., Nickmann, R. J., Heusser, L. E., Vogel, J. S., Nelson, D. E., and Southon, J., 1990, Younger Dryas climatic reversal in northeastern USA? AMS ages for an old problem: Quaternary Research, v. 33, p. 219-230.

Prins, M. A., 1999, Pelagic, hemipelagic and trubidite deposition in the Arabian Sea during the late Quaternary: unravelling the signals of eolian and fluvial sediment supply as functions of tectonics, sea-level and climate change by means of end-member modelling of siliclastic grain-size distributions [Ph.D thesis]: Utrecht University, 192 p.

Prins, M. A., and Weltje, G. J., 1999, End-member modelling of siliclastic grain-size distributions: The late Quaternary record of eolian and fluvial sediment supply to the Arabian Sea and its paleoclimatic signficance, in Numerical Experiments in Stratigraphy: Recent Advances in Stratigraphic and Sedimentologic Computer Simulations, p. 91-111.

Prins, M. A., Postma, G., and Weltje, G. J., 2000, Controls on terrigenous sedimen supply to the Arabian Sea during the late Quaternary: the Makran continental slope: Marine Geology, v. 169, p. 351-371.

Prins, M. A., Bouwer, L. M., Beets, C. J., Simon, R. T., Weltje, G. J., Kruk, R. W., Kujipers, A., and Vroon, P. Z., 2002, Ocean circulation and iceberg discharge in the glacial North Atlantic: Inferences from unmixing of sediment size distributions: Geology, v. 30, no. 6, p. 555-558.

Reasoner, M. A., 1993, Equipment and procedure improvements for a lightweight, inexpensive, percussion core sampling system: Journal of Paleolimnology, v. 8, p. 273-281.

Ridge, J. C., Besonen, M. R., Brochu, M., Brown, S., Callahan, J. W., Cook, G. J., Nicholoson, R. S., and Toll, N. J., 1999, Varve paleomagnetic, and 14C chronologies for late Pleistocene events in New Hampshire and Vermont (USA): Geographie physique et Quaternaire, v. 53, no. 1, p. 79-106.

Robbins, J. A., and Edgington, D. N., 1975, Determination of recent sedimentation rates in Lake Michigan using Pb-210 and Cs-137: Geochimica et Cosmochimica Acta, v. 39, p. 289-304.

Rodbell, D. T., Seltzer, G. O., Anderson, D. M., Abbott, M. B., Enfield, D. B., and Newman, J. H., 1999, A ~15,000-year record of El Nino-Driven alluviation in southwestern Ecuador: Science, v. 283, no. 5401, p. 516-520.

Shuman, B. N., Bravo, J., Kaye, J., Lynch, J. A., Newby, P. E., and Webb III, T., 2001, Late Quaternary Water-Level Variations and Vegetation History at Crooked Pond, Southeastern Massachusetts: Quaternary Research, v. 56, p. 401-410.

Spear, R., Davis, M. B., and Shane, L. C., 1994, Late Quaternary history of low- and mid-elevation vegetation in the White Mountains of New Hampshire: Ecological Monographs, v. 64, p. 85-109.

Stuiver, M., and Reimer, P. J., 1993, Extended 14C Data Base and Revised CALIB 3.0 14C Age Calibration Program: Radiocarbon, v. 35, p. 215-230.

Stuiver, M. G., P.M., and Braziunas, T. F., 1995, The GISP2 d18O Climate Record of the Past 16,500 Years and the Role of the Sun, Ocean, and Volcanoes: Quaternary Research, v. 44, p. 341-354.

Syvitski, J. P. M., 1991, Principles, methods, and application of particle-size analysis: Cambridge, Cambridge University Press, 368 p.

Syvitski, J. P. M., and McCave, I. N., 1991, Principles and methods of geological particle size analysis, in Syvitski, J. P. M., ed., Principles, methods, and application of particle size analysis: Cambridge, Cambridge University Press, p. 3-21.

Thompson, W. B., 1999, History of research on glaciation in the White Mountains, New Hampshire (USA): Geographie physique et Quaternaire, v. 53, p. 7-24.

Thompson, W. B., Fowler, B. K., and Dorion, C. C., 1999, Deglaciation of the northwestern White Mountains, New Hampshire: Geographie physique et Quaternaire, v. 53, p. 59-77.

Thompson, L. G., Yao, T., Mosley-Thompson, E., Davis, M. E., Henderson, K. A., and Lin, P. N., 2000, A High-Resolution Millenial Record of the South Asian Monsoon from Himalayan Ice Cores: Science, v. 289, no. 5486, p. 1916-1919.

Thompson, D. W. J., and Wallace, J. M., 2001, Regional Climate Impacts of the Northern Hemisphere Annular Mode: Science, v. 293, no. 5527, p. 85-89.

Thompson, W. B., 2001, Deglaciation of western Maine, in Weddle, T. K., and Retelle, M. J., eds., Deglaciation History and Relative Sea-Level Changes, Northern New England and Adjacent Canada: Boulder, CO, Geological Society of America, p. 109-123.

Thomson, D. J., 1982, Spectrum estimation and harmonic analysis: Proc. IEEE, v. 70, p. 1055-1096.

Thorndycraft, V., Hu, Y., Oldfield, F., Crooks, P. R. J., and Appleby, P. G., 1998, Individual flood events detected in the recent sediments of Petit Lac d'Annecy, eastern France: The Holocene, v. 8, no. 6, p. 741-746.

Vautard, R., and Ghil, M., 1989, Singular spectrum analysis in non-linear dynamics, with applications to paleoclimatic time series: Physica D, v. 35, p. 395-424.

Webb, R. S., Anderson, K. H., and Webb III, T., 1993, Pollen Response-Surface Estimates of Late-Quaternary Changes in the Moisture Balance of the Northeastern United States: Quaternary Research, v. 40, p. 213-227.

Webb III, T., Bartlein, P. J., Harrison, S. P., and Anderson, K. J., 1993, Vegetation, lake levels, and climate in eastern North America for the past 18,000 years, in Wright, H. E., Kutzbach, J. E., Street-Perrot, F. A., Bartlein, P. J., Ruddiman, W. F., and Webb III, T., eds., Global climates since the last glacial maximum: Minneapolis, University of Minnesota, p. 415-467.

Weltje, G. J., 1997, End-member modelling of compositional data: numerical-statistical algorithms for solving the explicit mixing problem: Journal of Mathematical Geology, v. 29, p. 503-549.

Wheatcroft, R. A., 1990, Preservation of potential sedimentary event layers: Geology, v. 18, p. 843-845.

Winkler, M. G., 1985a, A 12,000-year history of vegetation and climate for Cape Cod, Massachusetts: Quaternary Research, v. 23, p. 301-312.
-, 1985b, Charcoal analysis for paleoenvironmental interpretation: a chemical assay: Quaternary Research, v. 23, p. 313-326.

Zong, Y., and Tooley, M. J., 1999, Evidence of mid-Holocene storm-surge deposits from Morecambe Bay, northwest England: A biostratigraphical approach: Quaternary International, v. 55, p. 43-50.

APPENDIX B: CD-ROM OUTLINE

I. Grain size data

- A. CR
- B. CR2
- C. CR Rerun
- D. MO 1
- E. MO 2
- F. OG
- G. OG Reruns
- H. ST 1
- I. ST 2
- J. ST 2 N
- K. ST 2 Rerun
- L. Standards
- M. SU 1
- N. SU 1 Rerun
- O. SU 2
- P. SU 2 Rerun
- Q. SY
- R. SY Rerun
- S. WO

II. Reconnaissance Pictures

A. Crystal

B. South

C. Stinson

D. Worthley

III. Loss-on-ignition

A. Crystal 1

B. Crystal 2

C. Ogontz

D. Sandy

E. South 1

F. South 2

G. Stinson 1

H. Stinson 2

I. Worthley

IV. Magnetic Susceptibility Data

A. Adam's summaries

B. Figure data

C. Raw data- "magfiles"

V. AMS- radiocarbon data